69

08/485070

1995 1995

AI T

OPTICAL DISC SYSTEM

CROSS REFERENCE TO RELATED APPLICATIONS.

This is a continuation-in-part of Ser. No. 08/376,882, filed , Now U.S. Palent No. 5, 129, 5//
January 20, 1995, which is a continuation-in-part of Ser. No.

08/105,866, filed August 11, 1993, which is a continuation of

Ser. No. 07/657,155, now U.S. Patent No. 5,265,079, filed

February 15, 1991.

BACKGROUND OF THE INVENTION

. Field of the Invention.

The present invention relates to data storage systems of the type that include a housing having an opening for receipt of a removable disc cartridge in which an information recording medium is mounted for protection. More particularly, it relates to a system for rapidly encoding and writing information onto optical disks in a high density format, and for reading and decoding the information written thereon.

2. Description of the Related Art

20 Overview.

15

25

The demand for mass data storage continues to increase with expanding use of data processing systems and personal computers.

Optical data storage systems are becoming an increasingly popular means for meeting this expanding demand. These optical data systems provide large volumes of relatively low-cost storage that may be quickly accessed.

1

In optical disc systems, coded video signals, audio signals, or other information signals are recorded on a disc in the form of information tracks on one or both planar surfaces of the disc. At the heart of an optical storage system is at least one laser (or other light source). In a first operating mode, the laser generates a high-intensity laser beam that is focused on a small spot on an information track of a rotating storage disc. high-intensity laser beam raises the temperature of the recording surface of the material above its Curie Point -- the point at which the material loses its magnetization and accepts the magnetization of the magnetic field in which the disc is placed. Thus, by controlling or biasing this surrounding magnetic field, and allowing the disc to cool below its Curie Point in a controlled magnetic environment, information may be recorded on the disc in the form of magnetic domains referred to as "pits" on the recording medium.

5

10

15

20

25

Subsequently, when the operator desired to reproduce or read the previously recorded information, the laser enters a second operating mode. In this mode, the laser generates a low-intensity laser beam that is again focused on the tracks of the rotating disc. This lower intensity laser beam does not heat the disc above its Curie Point. The laser beam is, however, reflected from the disc surface in a manner indicative of the previously recorded information due to the presence of the previously formed pits, and the previously recorded information may thereby be reproduced. Since the laser may be tightly

focused, an information processing system of this type has advantages of high recording density and accurate reproduction of the recorded information.

The components of a typical optical system include a housing with an insertion port through which the user inserts the recording media into the drive. This housing accommodates, among other items, the mechanical and electrical subsystems for loading, reading from, writing to, and unloading an optical disc. The operation of these mechanical and electrical subsystems are typically within the exclusive control of the data processing system to which the drive is connected.

5

10

15

20

25

Within the housing of a conventional system that uses disc cartridges, a turntable for rotating a disc thereon is typically mounted on the system baseplate. The turntable may comprise a spindle having a magnet upon which a disc hub is mounted for use. The magnet attracts the disc hub, thereby holding the disc in a desired position for rotation.

In optical disc systems, as discussed above, it is necessary to magnetically bias the disc during a writing operation by applying a desired magnetic field to at least the portion of the disc being heated by the laser during the writing (recording or erasing) operation. Thus, it is necessary to mount a magnetic field biasing device where it may be conveniently placed in close proximity to the disc surface when the disc is held in position by the magnet associated with the spindle.

A variety of media or disc types are used in optical data



storage systems for storing digital information. For example, standard optical disc systems may use 5 ¼ inch disks, and these optical disks may or may not be mounted in a protective case or cartridge. If the optical disc is not fixedly mounted in a protective cartridge, an operator manually removes the disc from the protective case. The operator would then manually load the disc onto a loading mechanism, using care to prevent damage to the recording surface.

Alternatively, for purposes of convenience and protection, a disc may be mounted within an enclosure or a cartridge that is itself inserted into the insertion port of the drive and is then conveyed to a predetermined position. These disc cartridges are well known in the computer arts. The disc cartridge comprises a cartridge housing containing a disc upon which data may be recorded.

Cartridge Loading.

5

10

15

20

25

To protect the disc when the cartridge is external from the drive, the disc cartridge typically includes at least one door or shutter that is normally closed. The cartridge shutter may have one or more locking tabs associated with it. The corresponding disc drive includes a mechanism for opening the door or shutter on the cartridge as the cartridge is pushed into the system.

Such a mechanism may comprise a door link that makes contact with a locking tab, thereby unlocking the shutter. As the cartridge is inserted further into the drive, the shutter is opened to partially expose the information recording medium contained

therein. This permits a disc hub to be loaded onto a spindle of a motor or other drive mechanism, and permits entry of a readwrite head and a bias magnetic into the protective cartridge. The disc, when rotated by the drive mechanism, permits the readwrite head to access all portions of the disc media.

5

10

15

20

25

To conserve space in optical storage systems, it is desirable to minimize the size required by the apparatus that loads a disc onto and unloads the disc from a spindle. Conventional loading and unloading devices vary depending upon the type of disc being used. A conventional disc loading and unloading system that uses disc cartridges is typically capable of automatically transporting a disc cartridge from a receiving port onto the spindle. When the disc is no longer required, a conventional disc loading and unloading system automatically unloads the disc from the spindle. A loading device for performing this loading and unloading of the disc is generally constructed so that during disc loading (i.e., when the disc is moved from an ejected position into the player and onto the spindle), the disc is moved horizontally, parallel to the baseplate and turntable, towards the turntable. When the disc has been positioned above the turntable, the disc is lowered vertically, perpendicular to the face of the turntable, onto the spindle. Once on the turntable, a spindle magnet attracts the disc hub fixed to the center of the media, thereby clamping the disc in a rotatable condition for read-write operations.

When an operator is finished using the disc, the operator

initiates an eject operation. The most common solution for ejecting a cartridge and disc from a spindle is the technique used in most Japanese drives. In this type of disc unloading apparatus, a cartridge "box" has four pins at its sides, and the pins ride in tracks in an adjacent sheet metal guide. disc ejection, the cartridge box lifts the disc straight up and off the spindle. The apparatus then moves the disc horizontally, parallel to the baseplate and turntable, towards the disc receiving port in the front of the player. When the disc is thus lifted from the spindle during the unloading operation, it is necessary to generate sufficient upward force on the cartridge to overcome the magnetic clamping force holding the disc hub on the spindle magnet. The peak upward force required to overcome the magnetic clamping force may be produced by the manual operation of an ejection lever or by the activation of an electric ejection system.

5

10

15

20

25

In conventional electric ejection systems, wherein the disc cartridge unloading apparatus vertically lifts the disc cartridge to break the magnetic force between the spindle magnet and the disc hub, the electric ejection motor must generate a large load to effect removal of the disc cartridge. Consequently, when an operator opts to use the electric ejection system, a large motor having a large torque is required to generate sufficient vertical lifting force. Space must be reserved in the system housing to accommodate this large motor, thereby increasing the overall size of the housing for the cartridge-loading apparatus. In addition,

the large motor consumes a considerable amount of power.

It is thus desirable to reduce the complexity of the disc player, while reducing the overall size of the player to facilitate the drive's convenient use in computer applications. In order to be able to receive a 5 % inch disc cartridge and yet be small enough to be conveniently used in conjunction with a personal computer, optical disc drives must use compact and carefully located mechanical and electrical subsystems. With this in mind, it is desirable to reduce the size of the required ejection motor. One way to effect this result is to reduce the amount of force required to break the magnetic clamping force holding the disc hub on the spindle magnet. By reducing this required force, it is possible to use a smaller ejection motor in the player. It is thus desirable to design a disc loading apparatus wherein the disc is not vertically lifted off of the spindle magnet, but is, rather, "peeled" from the magnet.

A conventional method that attempts to achieve this peeling action has the turntable and spindle swing down away from the disc. This method is discussed in U.S. Patent No. 4,791,511 granted to Marvin Davis and assigned to Laser Magnetic Storage International. It remains desirable, however, to design a drive wherein the disc is peeled from the spindle magnet.

Focus and Tracking Actuation.

5

10

15

20

25

In order to attain a precise reading of the information stored on the disc, it is necessary to be able to move the objective lens in both a focusing (i.e., perpendicular to the



plane of the disc) or Z direction in order to focus the laser beam to a small point of light on a precise location of the disc to write or retrieve information, and in a tracking (i.e., radial from the center of the disc) or Y direction to position the beam over the exact center of the desired information track on the disc. Focus and tracking corrections may be effected by moving the objective lens in either the direction of the optical axis of the lens for focusing, or in a direction perpendicular to the optical axis for tracking.

5

10

15

20

25

In these systems, the position of the objective lens in the focus and tracking directions is commonly adjusted by control systems. Actuators support the objective lens and convert position correction signals from the feedback control systems into movement of the objective lens. Most commonly, these actuators comprise moving coils, stationary magnets, and a stationary yoke, wherein a magnetic field is produced in an air gap between the yoke and magnets. U.S. Pat. No. 4,568,142 issued to Iguma and entitled "Objective Lens Driving Apparatus" illustrates an actuator of this type wherein the actuator includes rectangular magnets positioned within U-shaped yokes. The yokes are spaced from one another with their north poles opposing, in close enough proximity to one another to form a magnetic circuit. A square-shaped focusing coil is bonded to the outsides of a square-shaped lens frame. Four tracking coils are bonded on the corners of the focusing coil. The ends of the focusing coil are then positioned within the air gaps formed by

each of the U-shaped yokes so that the focusing coil straddles the yokes. Because the focusing coil must extend around these "center" or "inner" yoke plates, the coil cannot be wound as tightly as desired and the rigidity of the coil construction is compromised. Further, in this type of closed magnetic circuit design, the majority of coil wire is positioned outside the air gaps, significantly reducing the efficiency of the actuator.

In most optical systems, the stiffness of the coil in the air gap has to be very high and the coil decoupling resonance frequency should be above 10 kHz, and is most desirably above 25 kHz. In many types of prior actuator designs, large amounts of coil wire in the magnetic air gap are often required to achieve maximum motor performance. To place such a large amount of coil within the air gap and still conform to the limited space constraints of the actuator design, the coil must be wholly or partially "freestanding", or must be wound on the thinnest bobbin possible. These types of coil configurations have low stiffness and typically decouple at lower frequencies. The dynamic resonance behavior of many actuator designs can also cause the coil to unwind during operation.

Other actuator designs have used the same magnetic air gap to develop focus and tracking motor forces such that the tracking coil(s) is glued onto the focus(s) coil or vice versa, in an attempt to save parts, space, and weight. In these types of designs, the decoupling frequency of the tracking coil(s) glued onto a freestanding focus coil is typically around 15 kHz,

significantly below the preferred decoupling frequency. Focus Sensing.

Optical recording and playback systems, such as those utilizing optical memory disks, compact disks, or video disks, require precise focusing of an illuminating optical beam through an objective lens onto the surface of an optical disc. The incident illuminating beam is generally reflected back through the objective lens, and is then used to read information stored on the disc. Subsequent to passing back through the objective lens, a portion of the reflected beam is typically directed to an apparatus designed to gauge the focus of the illuminating beam on the disc. Information extracted from the reflected beam by this apparatus may then be used to adjust the focus of the illuminating beam by altering the position of a movable objective lens relative to the disc.

A number of techniques for detecting the focus of an illuminating optical beam are known. For example, U.S. Pat. Nos. 4,423,495, 4,425,636 and 4,453,239 employ what has been termed the "critical angle prism" method of determining beam focus. In this method an illuminating beam reflected from a storage disc is made incident upon a detection prism surface which is set very close to a critical angle with respect to the reflected illuminating beam. When the focus of the illuminating beam on the surface of the disc deviates from a desired state, the variation in the amount of optical energy reflected by the detection prism surface may be used to derive a focus error signal used to adjust

the focus of the illuminating beam.

The critical angle prism method generally requires that the orientation of the detection prism surface relative to the reflected illuminating beam be precisely adjusted. This requirement arises as a result of reflectivity characteristic of the detection prism in the neighborhood of the critical angle and makes focus error detection systems based on this method extremely sensitive. However, the critical angle technique has several disadvantages. First, the focus error signal it produces depends on the light reflection at the interface between the detection prism surface and air; thus, changes in altitude, which change the index of refraction of the air, can cause false focus readings (offsets) to occur. Also, the critical angle technique is inherently unsuitable for use in differential focus sensing systems.

Differential systems are increasingly important because they allow cancellation of certain types of noise that can occur in optical disc drives. The critical angle method is unsuited to differential operation for two reasons. First, the transmitted beam produced by the sensing prism is compressed along one axis, making it unsymmetrical with the reflected beam. Symmetry of the two beams is preferred in a differential system to optimize the noise-cancellation properties in varied environments. Second, at the point on the reflectivity curve of a critical angle prism where the intensities of the two beams are balanced, the slope is far too low to produce a useful differential focus error signal.



A focus detecting apparatus which requires somewhat less precise adjustment of the optical surface on which the reflected illuminating beam is incident, when compared to the critical angle technique is disclosed in U.S. Pat. No. 4,862,442. In particular, the optical surface described therein comprises a dielectric multilayer coating having a reflectivity which varies continuously with respect to the angle of incidence of the reflected illuminating beam. It follows that rotational maladjustment of the surface comprising the multilayer coating will have smaller effect on the value of the focus error signal, but that also the technique will have reduced angular sensitivity. Also, inaccuracies in the focus error signal produced by multilayer dielectric systems may develop in response to relatively slight changes in the wavelength of the reflected illuminating beam. Such sensitivity to wavelength changes is undesirable since the focus error signal is designed to relate solely to the focus of the illuminating beam.

5

10

15

20

25

In addition, certain systems using a dielectric multilayer reflecting surface provide focus error signals having only a limited degree of sensitivity. For example, Fig. 37 of U.S. Pat. No. 4,862,442 shows a particular reflectivity characteristic for a layered dielectric reflecting surface, with the slope of the reflectivity characteristic being proportional to the sensitivity of the focus error signal. The disclosed reflected intensity ranges in value from approximately 0.75 to 0.05 over angles of incidence extending from 42 to 48 degrees. This reflectivity



change of approximately 10% per degree produces a focus error signal of relatively low sensitivity.

Accordingly, a need in the art exists for an optical arrangement characterized by a reflectivity profile which allows generation of a highly sensitive focus error signal relatively immune to changes in altitude and to chromatic aberration, and which is capable of use in differential systems.

Seek Actuation.

5

10

15

20

25

Optical data storage systems that utilize a focused laser beam to record and instantaneously playback information are very attractive in the computer mass storage industry. Such optical data storage systems offer very high data rates with very high storage density and rapid random access to the data stored on the information medium, most commonly an optical disc. In these types of optical disc memory systems, reading and writing data is often accomplished using a single laser source functioning at two respective intensities. During either operation, light from the laser source passes through an objective lens which converges the light beam to a specific focal point on the optical disc. During data retrieval, the laser light is focused on the recording medium and is altered by the information of the data storage medium. This light is then reflected off the disc, back through the objective lens, to a photodetector. It is this reflected signal that transmits the recorded information. It is thus especially important that, when information is being written to or read from the memory, the objective lens, and the exiting



focused beam, be precisely focused at the center of the correct track so that the information may be accurately written and retrieved.

In order to attain a precise reading of the information stored on the disc, it is necessary to be able to move the objective lens in both a focussing (i.e., perpendicular to the plane of the disc) or Z direction in order to focus the laser beam to a small point of light on a precise location of the disc to write or retrieve information, and in a tracking (i.e., radial) or Y direction to position the beam over the exact center of the desired information track on the disc. Focus and tracking corrections may be effected by moving the objective lens in either the direction of the optical axis of the lens for focussing, or in a direction perpendicular to the optical axis for tracking.

In these systems, the position of the objective lens in the focus and tracking directions is commonly adjusted by control systems. Actuators support the objective lens and convert position correction signals from the feedback control systems into movement of the objective lens. As will be appreciated, failure to focus the light on a small enough area of the medium will result in too large a portion of the disc being used to store a given amount of information, or in too broad of an area of the disc being read. Likewise, the failure to precisely control the tracking of the laser light will result in the information being stored in the wrong location, or in information

from the wrong location being read.

5

10

15

20

25

In addition to translation along the Z axis to effect focusing, and translation along the Y axis to effect tracking, there are at least four additional motion modes for the actuator, each of which reduces the accuracy of the reading and writing operations and is thus undesirable during normal operation of the system. These undesirable modes of motion are rotation about the X axis (an axis orthogonal to both the X direction and the Z direction), or pitch; rotation about the Z axis, referred to as yaw; rotation about the Y axis, called roll; and linear motion along the X axis, or tangential translation. Motion in these directions is often caused by motor and reaction forces acting on the carriage and/or actuator. These modes typically produce undesired movement during tracking or focusing operations which subsequently affects the alignment of the objective lens relative to the optical disc.

Anamorphic, Achromatic Prism System.

Optical disc systems often employ an anamorphic prism for adjustment of laser beam ellipticity, for the removal of laser beam astigmatism, and/or for beam steering. References such as U.S. Pat. No. 4,333,173 issued to Yonezawa, et al., U.S. Pat. No. 4,542,492 issued to Leterme, et al. and U.S. Pat. No. 4,607,356 issued to Bricot, et al. describe using simple anamorphic prisms for beam shaping in optical disc applications.

Frequently, the anamorphic prism systems have an embedded thin film to reflect some or all of a returning beam (reflected

from optical media) to a detection system. U.S. Pat. No. 4,573,149 to Deguchi, et al describes the use of thin films to reflect a return beam to detection systems. Furthermore, the entrance face of the anamorphic prism is often used to reflect the returning beam to a detection system as described in U.S. Pat. Nos. 4,542,492 and 4,607,356. Often, it is advantageous to have multiple detection channels. For instance, in optical disks, one detector may provide data signals and another detector may provide control signals such as tracking and/or focus servo signals.

A typical problem with conventional prisms is that the anamorphic prism suffers from chromatic dispersion which can result in lateral chromatic aberration. In other words, when the wavelength of the light source changes, the resulting angles of refraction through the anamorphic prism also change. These changes result in a lateral beam shift when the beam is focussed onto optical media such as an optical disc. In optical disc systems, a small shift in the beam may cause erroneous data signals. For instance, if the shift is sudden and in the data direction, the beam may skip data recorded on the optical disc.

If the light source (e.g., a laser) were truly monochromatic, the chromatic aberration in the prism would not cause a problem. However, several factors often cause the laser spectrum to change. For instance, most laser diodes respond with a change in wavelength when the power increases. In magneto-optic disc systems, an increase of power occurs when pulsing the laser

from low to high power to write to the optical disc, as is well understood in the art. This increase in laser power often causes a wavelength shift of around 1.5 to 3 nanometers (nm) in conventional systems. Most laser diodes also respond to a change in temperature with a change in the wavelength. Additionally, random "mode-hopping" can cause unpredictable wavelength changes commonly ranging from 1-2 nanometers. RF modulation is often applied to laser diodes operating at read power in order to minimize the effect that "mode-hopping" has on the system. However, the RF modulation increases the spectral bandwidth and

can change the center frequency. Moreover, RF modulation is not generally used when the laser is operating at write power. In a non-achromatic system, a sudden change in the wavelength of the incident light typically results in a lateral beam shift in the focussed spot of up to several hundred nanometers. A lateral beam shift of this magnitude could cause significant errors in the data signal.

Using multi-element prism systems to correct chromatic dispersion is known in the art of optical design. Textbooks such as Warren J. Smith, Modern Optical Engineering, McGraw-Hill, 1966, pp. 75-77 discuss this idea. Furthermore, some optical disc systems use multi-element anamorphic prism systems which are achromatic. However, typical existing multi-element prism systems require the multiple prism elements to be separately mounted. Mounting the multiple elements increases the expense and difficulty of manufacturing because each element must be

carefully aligned with respect to the other elements in the system. Small deviations in alignment can cause significant variations in function. This also complicates quality control. Other existing multi-element prism systems have attached elements to form a unitary prism, but these prism systems require that the prism material of each prism be different in order for the system to be achromatic. Finally, existing systems which are achromatic do not provide return beam reflections to multiple detection systems.

10 Data Retrieval - Transition Detection.

5

15

20

25

Various types of recordable and/or erasable media have been used for many years for data storage purposes. Such media may include, for example, magnetic tapes or disks in systems having a variety of configurations.

Magneto-optical ("MO") systems exist for recording data on and retrieving data from a magnetic disc. The process of recording in a magneto-optical system typically involves use of a magnetic field to orient the polarity of a generalized area on the disc while a laser pulse heats a localized area, thereby fixing the polarity of the localized area. The localized area with fixed polarity is commonly called a pit. Some encoding systems use the existence or absence of a pit on the disc to define the recorded data as a "1" or "0", respectively.

When recording data, a binary input data sequence may be converted by digital modulation to a different binary sequence having more desirable properties. A modulator may, for example,



convert m data bits to a code word with n modulation code bits (or "binits"). In most cases, there are more code bits than data bits -- i.e., m < n.

The density ratio of a given recording system is often expressed according to the equation $(m/n) \times (d + 1)$, where m and n have the definitions provided above, and d is defined as the minimum number of zeroes occurring between ones. Thus, the RLL 2/7/1/2 code has, according to the above equation, a density ratio of 1.5, while the GCR 0/3/8/9 code has a density ratio of 0.89.

5

10

15

20

25

For reading data in an MO system, a focused laser beam or other optical device is typically directed at the recording surface of a rotating optical disc such that the laser beam can selectively access one of a plurality of tracks on the recorded surface. The rotation of the laser beam reflected from the recorded surface may be detected by means of Kerr rotation. A change in Kerr rotation of a first type, for example, represents a first binary value. A change in Kerr rotation of a second type represents a second binary value. An output signal is generating from the first and second binary values occurring at specified clock intervals.

Although there has been a continual demand for disc systems capable of storing increasingly higher data densities, the ability to achieve high data storage densities has met with several limitations. As a general matter, the reasonable upper limit for data density is determined in part by reliability



requirements, the optical wavelength of laser diode, the quality of the optical module, hardware cost, and operating speed.

Maximum data densities are also affected by the ability to reject various forms of noise, interference, and distortion. For example, the denser that data is packed, the more intersymbol interference will prevent accurate recovery of data. Moreover, because the technology for many intermediate and high performance optical disc drives has been limited by downward compatibility constraints to older models, signal processing techniques have not advanced as rapidly as they might otherwise have.

When attempting to recover stored data, existing read channels of magneto-optical and other types of disc drives commonly suffer from a number of problems due to the unintended buildup of DC components in the read signal. One cause of DC buildup results from the recording of unsymmetrical data patterns over a number of bytes or data segments. A symmetrical data pattern may be considered as one having an average DC component of zero over a region of interest. Because sequences of recorded bits may be essentially random in many modulation codes, however, localized regions of recorded data having particular patterns of 1's and 0's will produce an unsymmetrical read signal having unwanted DC components. Because the data patterns vary over time, the level of DC buildup will also vary, causing wander of the DC baseline, reduction of threshold detection margins, and greater susceptibility to noise and other interference.

Undesired DC buildup is also caused by variance in pit size

due to thermal effects on the writing laser or the storage medium. As the writing laser heats up, for example, the spot size may increase leading to wider pits. When the recorded pits are read, variations in pit size will cause an unsymmetrical input signal having DC components. Variation in pit size not only causes undesired DC buildup but also causes the relative locations of the data to appear shifted in time, reducing the

5

10

15

20

25

Various attempts have been made to overcome the described problems. For example, various tape drive systems commonly use a DC-free code such as a 0/3/8/10 code, otherwise referred to simply as an 8/10 code. Because an 8/10 code requires 10 stored bits to yield 8 data bits, however, it is only 80% efficient which is a drawback when attempting to record high data densities.

timing margin and leading to possible reading errors.

Another method for handling DC buildup involves the use of double differentiation. This method typically involves detection of the peaks of a first derivative of the input signal by detecting zero-crossings of the second derivative of the input signal. Thus, the DC components are effectively filtered out. One drawback of this method is that differentiation or double differentiation can cause undesirable noise effects. A second drawback is that the method may decrease the timing margin to unacceptably low levels (e.g., by as much as 50 percent).

In another method for addressing DC buildup, the data to be stored is randomized prior to recording such that none of the



data patterns repeat over a data sector. However, this method may not acceptable by ISO standards and may lack downward compatibility with previous disc drive systems. As a further drawback to this method, de-randomizing the data may be complex.

5

10

15

20

25

Yet another method for controlling DC buildup involves the use of so-called resync bytes between data segments. This method generally involves the examination and manipulation of data before it is recorded in order to minimize DC buildup upon readback. Before recording, two consecutive data segments are examined to determine if the patterns of 1's and 0's are such as to cause positive DC, negative DC, or no DC components when read If, for example, two consecutive data segments have the same DC polarity, one of the data segments is inverted prior to being recorded on the medium. In order to stay within the constraints of the particular encoding system, however, a resync byte between the segments may need to be written so that the pattern of contiguous bits and of flux reversals is proper. A drawback of such a method is that it will not necessarily reduce all DC buildup, and time constants must be determined such that the predictable DC buildup will not affect performance. Further, the method requires additional overhead including the examination of data segments to determine their relative polarity.

It would therefore be advantageous to have a method and device for reading stored data from a medium without suffering the undesirable effects of DC buildup, without creating unacceptable levels of noise or significantly reducing timing

margins, without the requirement of large amounts of overhead or de-randomizing algorithms, and while providing high data storage efficiency.

Data Storage and Other Aspects of Data Retrieval

Recordable/erasable optical disks are currently available for use as data storage media. Magneto-optical recording is the technique commonly used to store the data on and/or retrieve the data from the disc. During recording, a magnetic field orients the polarity of a generalized area on the disc, while a laser pulse heats a localized area thereby fixing the polarity of the smaller area. The localized area with fixed polarity is commonly called a pit. Some encoding systems use the existence or absence of a pit on the disc to define the recorded data as a "1" or "0", respectively. The most commonly used encoding system for this pit-type recording is the run length limited (RLL) 2,7 code because it gives the highest data-to-pit ratio. This type of recording, however, does not lead to higher density because amplitude and timing margins deteriorate very rapidly as frequency is increased.

SUMMARY OF THE INVENTION

5

10

15

20

25

There is disclosed a method for moving a carriage assembly from an initial position to a target position relative to a storage medium rotating at a circumferential velocity. The method comprises the steps of determining a first radial distance between the initial position and a center of the storage medium, determining a second radial distance between the target position



and the center of the storage medium, determining a circumferential distance between the initial position and the target position, determining an initial circumferential velocity of the storage medium, calculating a velocity trajectory relative to the first radial distance, the second radial distance, the circumferential distance, and the initial circumferential velocity, and moving the carriage assembly from the initial position to the target position substantially at the velocity trajectory. The velocity trajectory is calculated such that the carriage assembly will arrive radially and circumferentially at the target position at substantially the same time. Additionally, a target circumferential velocity may be determined, the rotation of the storage medium may be changed from the initial circumferential velocity to the target circumferential velocity, and the velocity trajectory is further related to the target circumferential velocity.

Additional objects, advantages and features of the present invention will further become apparent to persons skilled in the art from a study of following description and of the accompanying drawings.

BRIEF DESCRIPTION OF THE DRAWING

5

10

15

20

25

Fig. 1 is an isometric view of an optical disk drive embodying the present invention.

Fig. 2 is a top view of the disk drive of Fig. 1, with the housing of the drive removed.

Fig. 3 is a cross-sectional view of the disk drive of Fig.

1, taken in the direction of arrows 3-3 in Fig. 1.

5

10

15

25

Fig. 4a is a top view of an Optics module of the disk drive of Fig. 1.

Fig. 4b is a diagram of the optical path of the disk drive of Fig. 1.

Fig. 5 is a system block diagram of the electronics of the disk drive of Fig. 1.

Fig. 6 is another isometric view of a disc drive with a disc cartridge about to be inserted therein.

Fig. 7 is an exploded isometric view of the disc drive of Fig. 6, depicting the major subassemblies of the disc drive.

Figs. 8A-8B are isometric views of the baseplate depicted in Fig. 7.

Fig. 9 is a top elevational view of the drive of Fig. 6 with some features removes to better show the tiller, the tiller-driving gears, the motor that drives these gears, and the operative relationship between these features.

Figs. 10A-10F comprise elevational and isometric views of a tiller.

Figs. 11A-11C comprise elevational and isometric views of a left slider.

Figs. 12A-12E comprise elevational and isometric views of a right slider.

Fig. 13 is an elevational view of the parking arm in two positions, one drawn in phantom, showing its action of parking the carriage at the back of the drive while the drive is at rest.



Figs. 14A-14C comprise elevational and isometric views of a parking arm.

Figs. 15A-15B are isometric views of a cartridge receiver.

Fig. 16A-16B are elevational views, during insertion of a disc cartridge, of the drive of Fig. 6 with some features removed to better show the trip lug on the right door link, the latch, and the operative relationship between these features.

Figs. 17A-17B are isometric views of a latch that holds the cartridge receiver in the up position.

Fig. 18 is an isometric view of a bias coil assembly clamp.

Fig. 19 is an isometric view of a bias coil assembly.

Fig. 20 is an exploded isometric view of the major components comprising the bias coil assembly.

5

10

15

20

25

Fig. 21 is an isometric view of a pivot bar or rail that rotatably supports the bias coil assembly.

Fig. 22 is an isometric view of the bias coil assembly flexure to which the bias coil assembly is mounted and which is in turn mounted to the pivot bar depicted in Fig. 21.

Fig. 23 is an elevational view of the right side of the cartridge receiver and the cartridge just before initiation of an cartridge-eject cycle, depicting the disc mounted in operating position on the spindle.

Fig. 24 is an elevational view of the right side of the cartridge receiver and the cartridge during the cartridge-eject cycle, depicting the cartridge being tipped and the disc being peeled off the spindle. and



Fig. 25 is an elevational view of the right side of the cartridge receiver and the cartridge during the cartridge-eject cycle, depicting the cartridge loading system in the up position and the disc starting to be ejected from the disc drive.

Fig. 26 is a schematic perspective view of an actuator in accordance with the present invention.

Fig. 27 is a perspective view of the lens holder for the actuator of FIG. 26.

Fig. 28 is a perspective view of the actuator of Figure 26 within a magnetic field housing.

10

25

Fig. 29 is a top plan view of the recording system of FIG. 28.

Fig. 30 is a right side elevational view of the recording system of FIG. 28.

Fig. 31 is a front elevational view of the recording system of FIG. 28.

Fig. 32 is a schematic perspective view illustrating the magnetic fields produced by the magnet pairs of the actuator of FIG. 26.

20 Fig. 33 is a perspective view of the focus coils and permanent magnets of the actuator of FIG. 26.

Fig. 34 is a schematic cross-sectional view of the focus coils and permanent magnets of the actuator of Fig. 26 taken along lines 9--9 of Fig. 33 illustrating the focus forces acting on the actuator.

Fig. 35 is a schematic cross-sectional view of the tracking



coil and permanent magnets of the actuator of Fig. 26 illustrating the tracking forces acting on the actuator.

5

10

15

20

25

Fig. 36 is a block diagrammatic presentation of a preferred embodiment of the beam focus sensing apparatus of the present invention.

Fig. 37 is a magnified top cross-sectional view of a differential version of the inventive beam separation module (FTR prism).

Fig. 38 is an illustrative front view of the first and second quad detectors included within the inventive focus sensing apparatus.

Fig. 39 is a graph showing the reflectivity of the FTR prism as a function of the angle of incidence of the servo beam.

Fig. 40 is a graph of the value of a differential focus error signal generated by a preferred embodiment of the apparatus of the present invention as a function of the position of the objective lens relative to an optical disc.

Fig. 41 schematically illustrates an exemplary optical read/write system in which the carriage and actuator assembly of the present invention may be used.

Fig. 42 is a perspective view of the carriage and actuator assembly.

Fig. 43 is an exploded view of the carriage and actuator assembly.

Fig. 44 is an exploded view of the actuator.

Fig. 45 is a schematic top view illustrating the coarse



tracking forces acting on the assembly.

5

10

15

20

25

Fig. 46 is a side schematic view further illustrating the coarse tracking forces.

Fig. 47 is an exploded view which illustrates the focus forces acting on the actuator.

Fig. 48 is an exploded view which illustrates the fine tracking forces acting on the actuator.

FIG. 49a is a schematic top view illustrating the symmetry of coarse tracking forces in the horizontal plane.

FIG. 49b is a schematic side view illustrating the symmetry of coarse tracking forces in the vertical plane.

FIG. 50a is a schematic top view illustrating the symmetry of fine tracking forces in the horizontal plane.

FIG. 50b is a schematic end view illustrating the alignment of the net fine tracking force with the center of mass of the fine tracking motor.

FIG. 51a is a schematic top view illustrating the symmetry of fine tracking reaction forces in the horizontal plane.

FIG. 51b is a schematic end view illustrating the alignment of the net fine tracking reaction force with the center of mass of the fine tracking motor.

FIG. 52a is a schematic side view illustrating the symmetry of focus forces in the horizontal plane.

FIG. 52b is a schematic end view of illustrating the alignment of the net focus force with the optical axis of the objective lens.



FIG. 53a is a schematic side view which illustrates the symmetry of focus reaction forces in the horizontal plane.

5

10

15

20

25

FIG. 53b is a schematic end view which illustrates the alignment of the net focus reaction force with the optical axis of the objective lens.

Fig. 54 is a schematic top view illustrating the flexure forces and fine motor reaction forces generated in response to the flexure forces.

FIG. 55a is a schematic side view which illustrates the symmetry of carriage suspension forces in the horizontal plane.

FIG. 55b is a schematic end view illustrating the alignment of the net carriage suspension force with the optical axis of the objective lens.

FIG. 56a is a schematic top view which illustrates the symmetry of friction forces in the horizontal plane.

FIG. 56b is a schematic side view illustrating the alignment of the friction forces with the center of mass of the carriage.

Fig. 57 is a schematic end view which illustrates the net inertial forces acting at the center of mass of the fine motor and center of mass of the carriage in response to a vertical acceleration.

FIG. 58a is a schematic side view illustrating the alignment of the net inertial force of the fine motor with the optical axis of the objective lens.

FIG. 58b is a schematic side view illustrating the alignment of the net inertial force of the carriage with the optical axis



of the objective lens.

5

15

20

FIG. 59a is a schematic top view which illustrates the inertial forces acting on components of the carriage and actuator assembly for horizontal accelerations.

FIG. 59b is a schematic top view illustrating the net inertial forces for horizontal accelerations.

FIG. 60a is a schematic end view which illustrates the fine motor and carriage inertial forces for accelerations above the flexure arm resonance frequency.

FIG. 60b is a schematic end view which illustrates the fine motor and carriage inertial forces for accelerations below the flexure arm resonance frequency.

FIGS. 61a-61b a diagram illustrating the relationship between the fine tracking position versus fine motor current.

FIGS. 62a-62c illustrate the effects of asymmetrical focus forces acting on the assembly.

Fig. 63 illustrates an alternative embodiment of a carriage and actuator assembly.

Fig. 64 illustrates the operation of the actuator to move the lens holder in a focusing direction.

Fig. 65 illustrates the operation of the actuator to move the lens holder in a tracking direction.

Fig. 66 depicts a simple anamorphic prism and illustrates the effect of chromatic aberration in the prism.

Fig. 67 depicts an existing multi-element anamorphic prism system.



Fig. 68 depicts an exemplary air-spaced prism system according to the present invention.

Figs. 69 and 69a depict one embodiment of an air-spaced, multi-element prism system of the present invention.

FIGS. 70, 70a and 70b depict side, bottom and top plan views, respectively, of the plate prism of the prism system embodiment depicted in Fig. 69.

5

10

15

20

FIGS. 71, 71a and 71b depict side, top and bottom plan views, respectively, of the trapezoidal prism of the embodiment of the prism system shown in Fig. 69.

FIGS. 72 and 72a depict a side view and a plan view of one optical surface, respectively, of an embodiment of the chromatic correcting prism of the prism system embodiment shown in Fig. 69.

Fig. 73 depicts an alternative embodiment of an air-spaced, multi-element prism system of the present invention.

Figs. 74, 74a, and 74b depict side, top and bottom plan views, respectively, of the quadrilateral prism of the alternative embodiment illustrated in Fig. 73.

Fig. 75 is a block diagram showing an optical data storage and retrieval system.

Fig. 76 is a series of sample waveforms.

FIGS. 77A and 77B are waveform diagrams of a symmetrical and unsymmetrical input signal, respectively.

Fig. 78 is a block diagram of a read channel.

25 Fig. 79 is a more detailed block diagram of various stages of a read channel.



FIG. 79B is a detailed circuit diagram of a partial integrator stage.

FIGS. 80A-80E are frequency response diagrams of various stages of a read channel.

FIG. 80F is a plot of group delay for a combination of stages in a read channel.

5

15

25

FIG. 80G is a waveform diagram showing signal waveforms at various stages in the read channel.

Fig. 81 is a block diagram of a peak detection and tracking circuit.

Fig. 82 is a schematic diagram of the peak detection and tracking circuit of FIG. 81.

Fig. 83 is a waveform diagram showing tracking by a threshold signal of the DC envelope of an input signal. and

FIGS. 84A-84D are diagrams showing exemplary waveforms at various points in a read channel.

Fig. 85 is a block diagram showing the optical data storage and retrieval system.

Fig. 86 is a series of waveforms showing uniform laser

pulsing under a pulsed GCR format and nonuniform laser pulsing

under an RLL 2,7 format.

Fig. 87 is a series of waveforms showing laser pulsing for various data patterns adjusted by the write compensation circuit.

Fig. 88 is a schematic diagram showing the write compensation circuit.

Fig. 89 is a series of waveforms showing laser pulsing for



amplitude asymmetry correction.

5

20

Fig. 90 is a schematic diagram showing the amplitude asymmetry correction circuit.

Fig. 91 is a block diagram showing the basic relationship of elements of the pulse slimming means.

Fig. 92 is a series of waveforms showing threshold adjustments by the dynamic threshold circuit.

Fig. 93 is a schematic diagram for the dynamic threshold circuit.

10 Fig. 94 is a schematic block diagram of an optical data storage and retrieval system incorporating downward compatibility.

Fig. 95 is a diagram of the track layout of the highdensity optical disks.

Fig. 96 is a diagram of the sector format of the highdensity optical disks.

Fig. 97 is a block diagram in more detail showing the read/write circuitry of FIG. 94.

Fig. 98 is a table depicting, for each of the 21 zones in the preferred format of the high-density optical disc, the tracks within the zone, the number of sectors per track within the zone, the total number of sectors in the zone, and the write frequency of the data recorded in the zone.

Fig. 99 provides the equations used to compute the CRC bits of the ID field.

FIG. 100a is the first half of a table (Hex 00 to 7F)

showing how the 8-bit bytes in the three address fields and in the data field, except for the resync bytes, are converted to channel bits on the disc. and

FIG. 100b is the second half of a table (Hex 80 to FF) showing how the 8-bit bytes in the three address fields and in the data field, except for the resync bytes, are converted to channel bits on the disc.

Figs. 101 - 119 are schematic diagrams of the electronic circuitry in a preferred embodiment of the invention.

Fig. 120 is an isometric view of a mechanical isolator and a pole piece in accordance with a first preferred embodiment.

Fig. 121 is an isometric view of the mechanical isolator in a second preferred embodiment.

DESCRIPTION OF THE PREFERRED EMBODIMENTS

15 System Overview

5

25

Main Optical, Electrical and Mechanical Components

Referring now to figure 1, there is shown an optical disk drive 10. Disk drive 10 plays and/or records on a disk (not shown) that is housed in removable disk cartridge 12.

20 Alternatively, the disk could be contained within the housing 14 of disk drive 10.

Referring now to figures 2 and 3, in figure 2 there is shown a top view of drive 10, with housing 14 removed to reveal certain important mechanical, electrical and optical components of drive 10. Figure 3 is a cross-sectional view of drive 10, taken in the direction of arrows 3-3 in figure 1. In figure 2 there is shown

base plate 16, spindle 17, linear actuator assembly 20, objective lens assembly 22, Optics module 24, drive circuit board 26, and flexible circuit connector 28. Figure 3 shows main circuit board 30, spindle motor 18, optics module circuit board 27, and drive circuit board 26.

In brief, base plate 16 acts as a base for the other components of drive 14, positioning and aligning the components with respect to each other. Preferably base 16 is made of cast steel for low cost.

5

25

Linear actuator assembly 20 includes a pair of linear voice coil actuators 23. Each voice coil actuator 23 consists of a rail 34 that is rigidly attached to base plate 16. Rails 34 are substantially parallel. Surrounding a portion of each pole piece 32 is an actuator coil 34. Each actuator coil 23 is attached to an opposite portion of carriage assembly 22, so that when coils 23 are properly energized, carriage assembly 22 moves along rails 34. Actuator coils 23 are driven by signals from drive circuit board 26, which result in linear motion of carriage assembly 22 relative to optics module 24, and relative to a disk (not shown) inserted in drive 10. In this manner, carriage assembly 22 enables coarse tracking of the disk.

Optics module 24 and carriage assembly 22 together contain the principle optics of drive 10. Optics module 24 is rigidly attached to base plate 16, and contains a laser, various sensors, and optics (not shown). In operation, the laser directs a beam (not shown) from optics module 24 towards carriage assembly 22,



and Optics module 24 in turn receives a return beam (not shown) from carriage assembly 22. Carriage assembly 22 is attached to linear actuator assembly 20, as described above. Carriage assembly 22 contains a pentaprism (not shown), an objective lens (not shown), servomotors (not shown) for focusing the objective lens, and servomotors (not shown) for fine adjustments of the objective lens position relative to the position of the linear actuator assembly 20 and to the inserted disk, to enable fine tracking of the disk. Electrical information and control signals are transferred between carriage assembly 22 on the one hand, and main circuit board 30 and drive circuit board 26 on the other hand by means of flexible circuit connector 28.

5

10

15

20

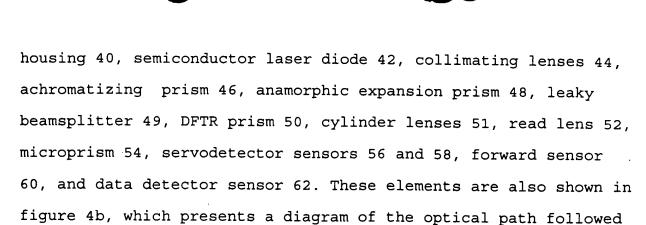
25

Optics module circuit board 27 contains a laser driver and preamplifiers (not shown). Drive circuit board 26 controls motor 18, linear actuators 23 of linear actuator assembly 20, and the servomotors of carriage assembly 22. Drive circuit board 28 is controlled by main circuit board 30. Main circuit board 30 includes most of the electronic components that various design considerations (e.g., noise reduction, EMI and power loss) do not require to be located on optics module circuit board 27, or drive circuit board 26.

Motor 18 is rigidly attached to base plate 16. Motor 18 directly drives spindle 17, which in turn spins the disk.

Optics: Optics module and Objective Lens Assembly

Referring now to figure 4, there is shown a top crosssectional view of Optics module 24. Optics module 24 includes



5

10

15

20

25

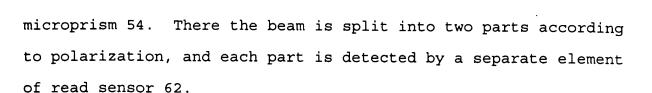
by laser beam 64. Figure 4b shows the Optics module 24 optical elements in conjunction with the pentaprism 66 and objective lens 68 of carriage assembly 22. For ease of illustration, in figure

objective lens 68 is shown to lie in the same plane as the portions of laser beam 64 that pass through Optics module 24. Actually, pentaprism 66 is positioned to direct laser beam portion 70 perpendicular relative to the portions of laser beam 64 that pass through Optics module 24.

4b portion 70 of laser beam 64 between pentaprism 66 and

Referring now to figure 4b, in operation laser beam 64 is a collimated beam produced by lenses 44 from the diverging beam emitted by laser 42. Beam 64 transmits through prisms 46 and 48, transmits through beamsplitter 49 and exits optics module 24 toward carriage assembly 22. There it passes through penta prism 66 and is focused onto the disk surface by objective lens 68.

Upon reflection from the disk, the reflected portion of laser beam 64 returns through objective lens 68 and penta prism 66 to re-enter optics module 24. A first portion of beam 64 reflects on the beamsplitter interface between prisms 48 and 49, transmits through and is focused by read lens 52, and enters



A second portion of beam 64 transmits through beamsplitter 49 and is internally reflected in anamorphic prism 48. This second portion of beam 64 them exits anamorphic prism 48 and enters DFTR prism 50. There this second portion of beam 64 is divided into two parts, which are focused by cylinder lenses 51 onto the surfaces of respective servo sensors 56 and 58. In response, sensors 56 and 58 generate signals that are directed to optics module circuit board 27, where the signals are used to generate tracking and focus error signals.

Electronic Systems: Main Circuit Board, Drive Circuit Board, and Optics module Circuits

Referring now to figures 1, 2 and 5, in figure 5 there is shown a system block diagram of the electronic subsystems of drive 10. In figure 5, block 80 encompasses read sensor preamplifier 82, laser driver 84 and servo sensor preamplifiers 86. Referring now to figures 4a and 5, read sensor preamplifier 82 is connected to data detector 62, and amplifies the signal generated by data detector 62. Similarly, servo sensor preamplifiers 86 are connected to servo detectors 56 and 58, and amplifies the signal generated by servo detectors 56 and 58.

Laser 42 is connected to laser driver 84, which provides signals that drive laser 42. The subsystems 82, 84 and 86 of block 80 are grouped together on a printed circuit board 27 that is



positioned in close proximity to Optics module 24. This minimizes the distance that signals must travel from sensors 62 to preamplifier 82, and from sensors 56 and 58 to preamplifiers 86, to reduce the adverse effect of noise on these signals. Since the signal that laser driver 84 generates to drive laser 42 is a relatively high frequency, good design practice requires laser driver 84 to be positioned close to laser 42.

Referring now to figures 1, 2 and 5, in figure 5 block 88 encompasses spindle motor interface 90, mechanical subassembly (MSA) interface 92, and position sensor interface 94. The components 90, 92, 94 and 96 of block 88 all reside on drive circuit boards 26. Spindle motor interface 90 controls spindle motor 18. MSA interface 92 interfaces with various displays and switches 96, including the front panel displays, the eject circuit, and switches related to disk cartridge 12. Position sensor interface 94 connects to actuators 98, which are powered by power amplifiers 102.

The remaining subsystems of system block diagram of figure 5 reside on main circuit board 30. These subsystems include analog read channel 100, encoder/decoder 104, SCSI chip set 106, buffer dram 108, and GLIC interface 110 and associated EEPROM 112. Main circuit board 30 also includes Analog interface circuit 114, Digital Signal Processor (DSP) 116, embedded controller 118 and its associated RAM/EPROM 120. Note that for optical drives 10 that are MO recordable drives, power amps 102 also drive bias coil 122.



Cartridge Loading Apparatus.

5

Referring first to Fig. 6, there is shown a magnetic disc storage system, generally designated 1-10. Fig. 6 depicts a replaceable disc cartridge 1-13 positioned for insertion into the disc drive 1-10 incorporating the cartridge loading and unloading apparatus of the instant invention. The disc drive 1-10 includes a bottom housing 1-16 and a face plate 1-19. The face plate 1-19 comprises a disc receiving port 1-22, a drive activity indicator light 1-25, and an ejection button 1-28.

10 Continuing to refer to Fig. 6, the disc cartridge 1-13, which is of a conventional type, comprises the following primary components. Its outer housing includes a upper planar surface 1-31 and a lower planar surface 1-32 (shown in, for example, Fig. The disc cartridge also has a forward-facing label end 15 1-34. In the preferred embodiment, the forward-facing label end 1-34 of the disc cartridge 1-13 remains visible to a user while the disc cartridge 1-13 is inserted in the disc drive 1-10. walls, for example side wall 1-37, extend between the upper planar surface 1-31 and the lower planar surface 1-32, and the 20 cartridge further comprises a rear wall 1-38 (shown in, for example, Fig. 24) extending between the upper planar surface 1-31 and the lower planar surface 1-32 parallel to the forward-facing label end 1-34. Near the label end 1-34 of the side walls 1-37 are channels 1-40 to accommodate cartridge locating pins 1-43 25 (Figs. 8A-8B) located on the base plate 1-46.

The disc cartridge 1-13 also includes a cartridge door or



shutter 1-49. The shutter 1-49 is spring-loaded in a closed position (Figs. 6, 7, and 16). When the shutter 1-49 is open, it rests in a recessed portion 1-52 of the upper planar surface 1-31. Since the disc drive 1-10 of the preferred embodiment reads two-sided disc cartridges 1-13, a similar shutter and recessed portion exists on the lower planar surface 1-32, but these features are not shown in the figures. The shutter typically has a shutter latch 1-55 (not shown) on the rear wall 1-38 of the disc cartridge 1-13.

Protected within the disc cartridge 1-13 is a disc 1-14 (Figs. 23-25), having a metallic disc hub 1-15. As is known in the relevant arts, the disc 1-14 may be formed as a rigid substrate having a magnetic material coating thereon. Embedded in the magnetic material coating are tracks in the form of concentric or spiraling rings. The magnetic coating may be on either one or both surfaces of the rigid substrate, and the coating enables data to be magnetically recorded on the disc 1-14 by magnetic transducers, typically referred to as heads. At the center of the rigid substrate is the metallic disc hub 1-15.

Referring now to Fig. 7, the primary component groups within the disc drive 1-10 of the instant invention include the following. There is a bottom housing 1-16 in which a base plate 1-46 rests. In Fig. 7, the spindle motor 1-61 is shown mounted on the base plate 1-46. The spindle motor 1-61 includes a spindle magnet 1-63 which attracts the metallic disc hub 1-15 of the disc 1-14 when the disc cartridge 1-13 is installed in the



disc drive 1-10. The ejection mechanism of the instant invention is shown generally at 1-67. The ejection mechanism 1-67 includes a left slider 1-70, a right slider 1-73, and a tiller 1-76. The ejection mechanism 1-67 is described more fully below. A parking arm 1-79 is also depicted in Fig. 7 in its position above the left slider 1-70. The cartridge receiver is shown generally at 1-82. Also shown in Fig. 7 are the left door link 1-85, the right door link 1-88, and the receiver door 1-91, each of which is pivotally attached to the cartridge receiver 1-82. The drive face plate 1-19 is depicted in front of the cartridge receiver 1-82. Finally, the rotatable, magnetic bias coil assembly 1-94 is depicted attached to the bias coil arm 1-97, with the bias coil clamps 1-100 depicted above the bias coil arm. Further details about each of these primary component assemblies will next be provided.

Continuing to refer to Fig. 7, one can see that the bottom housing 1-16 includes side walls 1-103 and a back wall 1-106. On the inside base of the bottom housing 1-16 are four mounting stations 1-109 to which the base plate 1-46 is secured. The bottom housing 1-16 would also encase the control electronics, which are not depicted in the figures.

Referring now to Figs. 8A and 8B, further details of the construction of the base plate 1-46 will now be provided. The base plate 1-46 is mounted on the four mounting stations 1-109 (Fig. 7) of the bottom housing 1-16. The base plate 1-46 has many components either molded into, embedded into, attached to,

or associated with it. It is the "glue" that brings the many components of this invention together and permits them to interact. Around the periphery of the base plate 1-46 there is a forward wall 1-112, a left outer side wall 1-115, a left inner side wall 1-118, a right outer side wall 1-121, a right inner side wall 1-124, and a rear vertical wall 1-127. The left and right outer side walls 1-115, 1-121, respectively, each comprises a vertical slot 1-130, 1-133, respectively. The left vertical slot 1-130 accommodates the left lift pin 1-136 (Fig. 15A) on the cartridge receiver 1-82 when the cartridge receiver 1-82 is in place around the base plate 1-46. The right vertical slot 1-133 similarly accommodates the right lift pin 1-139 (Fig. 15B) of the cartridge receiver 1-82.

5

10

15

20

25

The two cartridge locating pins 1-43 are positioned near the forward ends of the left and right outer side walls 1-115, 1-121, respectively. These locating pins 1-43 are adapted to engage the cartridge channels 1-40 (Fig. 6). When the pins 1-43 are located in the channels 1-40, the pins 1-43 hold the disc cartridge 1-13 and prevent it from moving both laterally (i.e., side-to-side) and longitudinally (i.e., forward and backward).

The spindle motor mount 1-142 is molded into the bottom of the base plate 1-46. The spindle motor 1-61 (Fig. 7) may be held on the spindle motor mount 1-142 by, for example, spring clips (not shown) attached to the intermediate rib 1-145.

The base plate 1-46 has various axes and mounting pins associated therewith. For example, a tiller pivot axis 1-148 is



mounted on the base plate 1-46 adjacent to the spindle motor mount 1-142. A tiller-spring pin 1-151 is fixed to the bottom of the base plate 1-46 near the forward wall 1-112 (Fig. 8A). other pins attached to the bottom of the base plate 1-46 near the forward wall 1-112 act as pivot shafts for the gears in the ejection gear train. The base plate 1-46 also includes a left slider channel 1-154 and a right slider channel 1-157. slider channels 1-154, 1-157 extend along the sides of the base plate 1-46. The left slider channel 1-154 is formed between the left outer side wall 1-115 and the left inner side wall 1-118. When in position, the left slider is sandwiched between the left inner side wall 1-118 and the left outer side wall 1-115, and rides in the left slider channel 1-154 (see, e.g., Figs. 9, 13, and 16). Similarly, the right slider channel 1-157 is formed between the right outer side wall 1-121 and the right inner side wall 1-124. When in position, the right slider 1-73 is sandwiched between the right inner side wall 1-124 and the right outer side wall 1-121, and rides in the right slider channel 1-157. The left and right sliders 1-70, 1-73, respectively, may be held in their respective channels 1-154, 1-157 by, for example, "ears" on the spring clips (not shown) that hold the spindle motor 1-61 in position on the spindle motor mount 1-142.

5

10

15

20

25

At the end of the right slider channel 1-157, adjacent to the rear vertical wall 1-127, a socket 1-160 is formed in the base plate 1-46 where the rear of the right inner side wall 1-124 merges with the rear of the right outer side wall 1-121. This

socket 1-160 accommodates the pivot pin 1-163 (Figs. 17B and 17A) of the receiver latch 1-166. The receiver latch 1-166 has a vertical surface 1-169 (Fig. 17B) upon which a latch-release trip lug 1-172 (Figs. 7 and 16), which is fixed to the right door link 1-88, impacts to release the receiver latch 1-166.

5

10

15

20

25

The base plate 1-46 has a port 1-175 in the rear vertical wall 1-127. The laser diode (not shown), which would be located behind the rear vertical wall between the left corner pillar 1-178 and the right corner pillar 1-181, shines through the port 1-175 and into the carriage 1-184 (Figs. 9, 13, and 16), which contains the optics that focus the laser beam on an information track on the disc 1-14. The carriage 1-184 is discussed further below.

The base plate 1-46 also has a hole 1-187 molded therein to accommodate the pivot shaft 1-190 (Fig. 13B) of the parking arm 1-79. This hole 1-187 is molded as an integral part of the left inner side wall 1-118. Fig. 9, for example, shows the parking arm 1-79 in place with its pivot shaft 1-190 in the hole 1-187.

Referring now to Figs. 13A through 13C, further features of the parking arm will be described. In addition to the pivot shaft 1-190, the parking arm 1-79 comprises a pressing end 1-193. The parking arm 1-79 has a jaw 1-196 formed on the end remote from the pressing end 1-193. The jaw 1-196 has a long side 1-199 and a short side 1-202. When the parking arm 1-79 is in position, the jaw 1-196 straddles the lug 1-205 (Fig. 11C) on the left slider 1-70. The parking arm 1-79 in position, with its jaw



1-196 straddling the lug 1-205 of the right slider 1-70, may be seen to best advantage in Figs. 9, 13, and 16. The position of the parking arm 1-79 is thereby dictated by the location of the left slider 1-70 in the left slider channel 1-154.

5

10

15

20

25

As seen to best advantage in Fig. 13, the parking arm 1-79 parks the carriage 1-184. The carriage 1-184 focuses the laser beam coming through the port 1-175 in the rear vertical wall 1-127 of the base plate 1-46. In particular, the carriage positions the laser beam over the center of a data track containing data to be read. The carriage 1-184 rides on support rails 1-208. A conventional magnetic arrangement drives the carriage 1-184 along the rails 1-208. When the cartridge receiver 1-82 is in the up condition, the parking arm 1-79, which is powered by the left slider 1-70, holds the carriage 1-184 toward the rear of the drive. This condition is illustrated in Figs. 9 and 16, and is illustrated in Fig. 14b by the parking arm 1-79 shown in solid lines. When the left slider 1-70 is driven forward by the tiller 1-76 during ejection of the disc cartridge 1-13, the parking arm 1-79 is rotated by the lug 1-205 pressing against the short side 1-202 of the jaw 1-196 until the pressing end 1-193 of the parking arm 1-79 holds the carriage 1-184 toward the back of the disc drive 1-10. When the cartridge receiver 1-82 is in its down position, the left slider 1-70 has been driven toward the rear of the disc drive 1-10 by the tiller 1-76. Under this scenario, the lug 1-205, which was driven rearward with the left slider 1-70, has rotated the parking arm 1-79

toward the front of the disc drive 1-10. With the left slider 1-70 and parking arm 1-79 in these positions, the carriage 1-184 is not influenced by the pressing end 1-193 of the parking arm 1-79 and may move freely below the disc 1-13 in the disc drive 1-10.

5

10

15

20

25

The ejection mechanism 1-67, which may be seen to best advantage in Figs. 7 and 9, comprises the following key features. An ejection motor 1-208 powers the ejection mechanism. particular, the ejection motor 1-208 powers a gear train that powers the output cam which, in turn, forces the tiller to rotate in a first direction (counterclockwise in Fig. 9), thereby ejecting a disc cartridge 1-13 from the disc drive 1-10. When user initiates the ejection process, the motor 1-208 drives the worm gear 1-211. The worm gear 1-211 is fixed to the central shaft of the ejection motor 1-208. This worm gear 1-211 drives a first large gear 1-214 about a first axis 1-217. This rotation of the first large gear 1-214 rotates a first small gear 1-220, which is fixed to the bottom of the first large gear 1-214 for rotation therewith about the first gear axis 1-217. The first small gear 1-220 drives a second large gear 1-223 about a second gear axis 1-226. A second small gear 1-229 is fixed to the top of the second large gear for rotation therewith about the second gear axis 1-226. The second small gear 1-229, in turn, drives a third large gear 1-232 about a third gear axis 1-235. large gear 1-232 drives the cam 1-238 that forces the tiller 1-76 to rotate about the tiller axis 1-148.

5

10

15

20

25

The tiller 1-76 will now be described with reference to Figs. 10A-10F and Fig. 9. The tiller 1-76 is pivotally attached to the base plate 1-46 by the tiller axis 1-148. A tiller-spring hook 1-238 is molded on the slender portion of the tiller 1-76. A tiller spring 1-241 (Fig. 9) is attached between the tillerspring hook 1-238 and the tiller-spring pin 1-151. The tillerspring 1-241 biases the tiller 1-76 in a second direction (clockwise in Fig. 9) about the tiller axis 1-148. cartridge-loading direction, which drives the right slider 1-73 forward and the left slider 1-70 rearward, to seat the disc cartridge 1-13 on the spindle motor 1-61. The tiller further includes a tiller skirt or webbed portion 1-244 that rides on top of the tiller gear train and thereby helps to contain the ejection gears in position on their respective gear axes. end of the tiller near the tiller skirt 1-244 comprises a Ushaped jaw 1-247, and the tiller end remote from the skirt 1-244 comprises a similar U-shaped jaw 1-250. The U-shaped jaw 1-247 fits rotatably around the cylindrical connection post of the left slider 1-70 (Fig. 11C). Similarly, the U-shaped jaw 1-250 of the tiller 1-76 fits rotatably around the cylindrical connection post 1-256 (Fig. 12E) of the right slider 1-73. The tiller 1-76 is thereby pivotally connected to the forward ends of the left and right sliders 1-70, 1-73, respectively. In addition, since the left and right sliders 1-70, 1-73 are held in their respective slider channels 1-154, 1-157 by the spring clips (not shown) which also hold the spindle motor 1-61 in position, the tiller



1-76 is held on the tiller axis 1-148 by the interaction between the U-shaped jaws 1-247, 1-250 and the cylindrical connecting posts 1-253, 1-256.

5

10

15

When the tiller 1-76 rotates in a first direction (counterclockwise in Fig. 9), the left slider 1-70 is driven forward in the left slider channel 1-154, while the right slider 1-73 is simultaneously driven rearward in the right slider channel 1-157. Thus, rotation of the tiller 1-76 in the first direction (counterclockwise in Fig. 9) raises the cartridge receiver 1-82 so that a disc cartridge 1-13 may be ejected from or loaded into the disc drive 1-10. On the other hand, when the tiller 1-76 rotates in a second direction (clockwise in Fig. 9), the left slider 1-70 is driven rearward in the left slider channel 1-154, while the right slider 1-73 is simultaneously driven forward in the right slider channel 1-157. Rotation of the tiller 1-76 in this direction lowers the cartridge receiver 1-82, placing the disc on the spindle motor. The raising and lowering of the cartridge receiver 1-82 by the rotation of the tiller 1-76 is discussed further below.

As discussed above, the left slider 1-70 rides in the left slider channel 1-154, and the right slider 1-73 rides in the right slider channel 1-157 under the influence of the tiller 1-76. Further details concerning the sliders 1-70, 1-73 is provided next.

25 Referring now to Figs. 11A-11C, the features of the left slider 1-70 are as follows. The left slider comprises a



cylindrical connecting post 1-253 on its forward end. A parking arm lug 1-205 exists on a first recessed portion 1-259. parking arm 1-79 slides along the first recessed portion 1-259 of the left slider 1-70 under the influence of the lug 1-205. An Sshaped slot 1-262 is formed into the left slider 1-70. When the left slider 1-70 is in position in the left slider channel 1-154, the S-shaped slot 1-162 opens toward the left outer side wall, adjacent to and behind the left vertical slot 1-130. When the cartridge receiver 1-82 is in position around the base plate 1-46, the left lift pin 1-136 (Fig. 15A) of the cartridge receiver 1-82 rides in the left vertical slot 1-130 of the base plate 1-46. The left lift pin is longer than the left outer side wall 1-115 is thick. Therefore, the left lift pin 1-136 projects through the left vertical slot 1-130 and rides in the S-shaped slot 1-262 in the left slider 1-70. When the cartridge receiver 1-82 is thus positioned about the base plate 1-46, with the left lift pin 1-136 riding in the vertical slot 1-130 and the S-shaped slot 1-262, the cartridge receiver 1-82 is restricted from traveling forward or backward and may only travel up and down vertically. The vertical slot 1-130 restricts the forward-tobackward movement of the cartridge receiver 1-82, while the Sshaped slot 1-262 in the left slider 1-70 defines the vertical height of the cartridge receiver. In other words, depending upon which portion of the S-shaped slot 1-262 is behind the vertical slot 1-130 at any particular moment, the cartridge receiver 1-82 may be in its highest position, its lowest position, or at some

5

10

15

20

25



position between its highest and lowest positions.

5

A second recessed portion 1-265 is present on the top of the left slider 1-70. A horizontal pin (not shown) may be attached to the base plate 1-46 so as to slip along the second recessed portion 1-265. This horizontal pin (not shown) would limit the most forward and most rearward positions of the left slider because the pin would impact the edges of the second recessed portion 1-265 upon reaching one of the extreme positions of the left slider.

The rear-most end of the left slider 1-70 includes a notch 1-268, which may be seen to good advantage in both Fig. 11B and Fig. 7. The notch 1-268 is located on a displaced portion 1-272 of the left slider 1-70. The notch 1-268 receives the lever arm 1-275 of the bias coil arm 1-97. This lever arm 1-275 rotates the bias coil arm 1-97 depending upon the position of the left slider 1-70, and in particular, the position of the notch 1-268. The displaced portion 1-272 of the left slider 1-70 rides in a recess 1-278 (Fig. 8B) in the left outer side wall 1-115 of the base plate 1-46.

Referring now to Figs. 12A-12E, the features of the right slider 1-73 will be presented. As stated above, the tiller 1-76 is connected to the right slider 1-73 via the cylindrical connection post 1-256. The right slider 1-73 has an S-shaped slot 1-281 formed therein. This S-shaped slot 1-281 is a flipped version of the S-shaped slot 1-262 in the left slider 1-70. This may be seen to best advantage in Fig. 7. In this figure, it is

apparent that, when the sliders 1-70, 1-73 are connected to the tiller 1-76, the S-shaped slots 1-262, 1-281 are flipped mirror images of each other. This arrangement is necessary since the sliders 1-70, 1-73 move in opposite directions under the influence of the tiller 1-76. The S-shaped slot 1-281 in the right slider 1-73 also opens toward the right outer side wall when the right slider 1-73 is in its operating position in the right slider channel 1-157. Similar to what was described above with reference to the left slider 1-70, when the cartridge receiver 1-82 is in position around the base plate 1-46, the right lift pin 1-139 (Fig. 15B) rides in the right vertical slot 1-133 (Fig. 8B). Since the right lift pin 1-139 is longer than the right outer side wall 1-121 is thick, the right lift pin 1-139 projects through the right outer side wall 1-121 at the right vertical slot 1-133 and rides in the S-shaped slot 1-281 in the right slider 1-73. The right vertical slot 1-133 restricts the right lifting pin 1-139 from traveling parallel to the longitudinal axis of the base plate 1-46 (i.e., parallel to a line passing perpendicularly through the forward wall 1-112 and the rear vertical wall 1-127). Since the right lift pin 1-139 rides in the S-shaped slot 1-281, the vertical height of the cartridge receiver 1-82 is defined by the location of the right lift pin 1-139 in the S-shaped slot 1-281. The S-shaped slot 1-281 in the right slider 1-73 travels behind the right vertical slot 1-133 at the same rate that the S-shaped slot 1-262 in the left slider 1-70 passes behind the left vertical slot 1-130, but

5

10

15

20

25

in an opposite direction. The flipped mirror image design of the S-shaped slots 1-262, 1-281, however, insures that the left and right lift pins 1-136, 1-139, respectively, are held at substantially the same vertical height above the bottom of the base plate 1-46 at any particular time.

5

10

15

20

25

Still referring primarily to Figs. 12A-12E, the right slider comprises the following additional features. A recessed portion 1-284 is present on the top surface of the right slider 1-73. A pin (not shown) may be mounted horizontally across the right slider channel 1-157 so as to slide along the recessed surface 1-284. The horizontal pin sliding along the recessed surface 1-284 would limit the maximum forward and rearward travel of the right slider 1-73 since the horizontal pin would hit the edges of the recess 1-284 at the extremes of travel of the right slider 1-73. The right slider 1-73 also includes a notched region 1-287 to accommodate the paw 1-290 (Figs. 17A and 17B) of the receiver latch 1-166. A raised portion 1-293 is present on the rear end of the right slider 1-73. When the tiller 1-76 rotates in the first direction (counterclockwise in, for example, Fig. 14b), driving the right slider 1-73 rearward in the right slider channel 1-157, a latching action takes place between the paw 1-290 of the receiver latch 1-166 and the raised portion 1-293 of the right slider 1-73. In particular, the first slipping surface 1-296 (Fig. 17A), which is located on the paw 1-290, slides past the second slipping surface 1-299 (Figs. 12C and 12E), which is on the raised portion 1-293 of the right slider 1-73. When the

surfaces 1-296, 1-299 slip past each other, the paw 1-290, which is spring-loaded in the direction indicated by the arrow 1-302 in Fig. 17A, enters the notched region 1-287 of the right slider 1-73, which holds the right slider 1-73 in the rearward position and, consequently, holds the cartridge receiver 1-82 in its uppermost position. When the cartridge receiver is in this position, any disc cartridge 1-13 in the drive 1-10 would be ejected, or, alternatively, a disc cartridge 1-13 could be loaded into the disc drive 1-10.

5

20

25

The S-shaped slots 1-262, 1-281 in the left and right sliders 1-70, 1-73, respectively, play a significant role in generating the peeling action accomplished by the instant invention when loading a disc cartridge onto and unloading a disc cartridge from the spindle motor. This role of the S-shaped slots 1-262, 1-281 in facilitating the peeling action generated by the instant invention is discussed further below.

Referring now to Figs. 15A and 15B, the cartridge receiver and the components attached to it will be described. The cartridge receiver 1-82 is a one-piece, injection molded piece of plastic to which the left door link 1-85 (Fig. 7) and right door link 1-88 are added. When the disc drive 1-10 is fully assembled, the cartridge receiver 1-82 rides on the outside of the left and right outer side walls 1-115, 1-121 of the base plate 1-46. The cartridge receiver 1-82 travels vertically up and down as the lift pins 1-136, 1-139 move up and down as they follow their respective S-shaped slots 1-262, 1-281. The

cartridge receiver 1-82 also pitches slightly up and down about an imaginary lateral axis passing through the left and right lift pins 1-136, 1-139. It is this slight pitching motion in conjunction with the up and down motion that generates the beneficial peeling action achieved by the instant invention. The cartridge receiver 1-82 may be snapped or lifted off of the remainder of the mechanism if the cover of the disc drive 1-10 is removed.

5

10

15

20

25

The cartridge receiver 1-82 has a left cartridge receiving channel 1-305 and a right cartridge receiving channel 1-308 formed therein. A stop bumper 1-311 is positioned in the rear of the right cartridge-receiving channel 1-308 to prevent improper insertion of a disc cartridge 1-13. As may be seen in Figs. 6 and 7, the disc cartridge 1-13 has a pair of slots 1-314 molded into the side walls 1-37. If the disc cartridge 1-13 is inserted correctly, with its rear wall 1-38 entering the disc receiving port 1-22 first, one of the slots 1-314 in the disc cartridge 1-13 will accommodate the stop bumper 1-311 and permit the cartridge 1-13 to be fully inserted into the drive 1-10. If, on the other hand, the user inserts the disc cartridge 1-13 with the forward-facing label end 1-34 entering the disc receiving port 1-22 first, the stop bumper 1-311 will impact the label end 1-34 of the disc cartridge 1-13, thereby preventing full insertion of the disc cartridge 1-13 into the disc drive 1-10. The rear wall 1-317 of the cartridge receiver 1-82 has a notched region 1-320 formed therein. This notched region permits the latch-release

trip lug 1-172 (Fig. 16) fixed to the right door link 1-88 to impact the vertical surface 1-169 (Fig. 17B) of the receiver latch 1-166. Since the left and right door links 1-85, 1-88, respectively, are rotated toward the rear of the disc drive 1-10 as the disc cartridge 1-13 is inserted in the cartridge receiver 1-82, as the disc cartridge 1-13 approaches full insertion, the trip lug 1-172 trips the receiver latch 1-166 by pressing against the vertical surface 1-169 to rotate the receiver latch 1-166. This rotation of the receiver latch 1-166 frees the paw 1-290 from its latched position around the raised portion 1-293 of the right slider 1-73. When the receiver latch 1-166 is tripped in this manner, the cartridge receiver 1-82 can be lowered, placing the disc cartridge 1-13 in operating position on the spindle motor 1-61.

5

10

25

Referring to Figs. 7, 15A, 15B, and 16, the attachment of the left door link 1-85 and the right door link 1-88 to the receiver cartridge 1-82 will now be described. The left and right door links 1-85, 1-88 are attached to the rear corners of the cartridge receiver 1-82, near the rear wall 1-317.

Specifically, the left door link 1-85 is rotatably mounted to the cartridge receiver 1-82 at a first pivot point 1-323, and the

cartridge receiver 1-82 at a first pivot point 1-323, and the right door link 1-88 is rotatably mounted to the cartridge receiver 1-82 at a second pivot point 1-326. The door links 1-85, 1-88 are biased by a spring (not shown) toward the face plate 1-19 of the disc drive 1-10. In operation, one or the other of the door links 1-85, 1-88 unlatches the cartridge

shutter lock and opens the cartridge shutter 1-49 as the disc cartridge 1-13 is inserted into the drive 1-10. Whether the left door link 1-85 or the right door link 1-88 opens the cartridge shutter 1-49 is determined by which side of the disc cartridge 1-13 is facing up when the cartridge 1-13 is inserted into the drive 1-10. If the disc cartridge 1-13 is inserted with a first side up, the right door link 1-88 operates the shutter latch and opens the shutter 1-49. If the disc cartridge 1-13 is inserted with its other side up, the left door link 1-85 operates the shutter latch and opens the shutter 1-49. When no disc cartridge 1-13 is in the drive 1-10, the door links 1-85, 1-88 rest against door link stops 1-329, which are integrally formed as part of the cartridge receiver 1-82. These door link stops 1-329 insure that the free ends 1-332 of the door links 1-85, 1-88 are properly positioned to release the shutter latch and open the shutter 1-49 as the disc cartridge 1-13 is inserted into the drive 1-10.

5

10

15

20

25

Referring now to Figs. 19-22, the rotatable, magnetic bias coil assembly 1-94 will be more fully described. The bias coil assembly 1-94 is used during writing and erasing operations of the disc drive 1-10. The bias coil assembly 1-94 comprises a steel bar 1-335 wrapped in a coil of wire 1-338. When the bias coil assembly 1-94 is positioned over a disc 1-14, as shown to best advantage in Fig. 23, it extends radially across the disc 1-14 and is thus capable of generating a strong magnetic field over a radial strip of the disc 1-14, extending from near the spindle 1-62 (Figs. 23-25) to the edge of the disc 1-14. When

the disc 1-14 is rotated under the bias coil assembly 1-94 by the spindle motor 1-61, it is possible to generate a magnetic field over the entire surface of the disc 1-14, thus enabling the user to write information to all portions of the disc 1-14 from its innermost to its outermost tracks. The coil 1-338 and bar 1-335 are covered by a bias coil housing top 1-341, which is mounted to a bias coil housing bottom 1-344.

5

10

15

20

25

The bias coil assembly 1-94 is mounted to the bias coil flexure 1-347 (Fig. 22), which is, in turn, mounted on the bias coil arm 1-97 (Fig. 21). The bias coil arm 1-97 straddles the width of the base plate 1-46 and is rotatably held by a pair of bias coil clamps 1-100 (Fig. 18) to the corner pillars 1-178, 1-181 (Figs. 8A and 8B) of the base plate 1-46. The bias coil clamps 1-100 thus act as bearing blocks under which the bias coil arm 1-97 can rotate. The bias coil clamps 1-100 include a stop ledge 1-350, which terminates the upward travel of the cartridge receiver 1-82 during an ejection operation, as discussed more fully below with reference to Figs. 23-25. As previously discussed, the bias coil arm 1-97 includes a lever arm 1-275 in operative association with a notch 1-268 on the rearward end of the left slider 1-70 to lift and lower the bias coil assembly 1-94. Since the lever arm 1-275 engages the notch 1-268 in the left slider 1-70, the left slider 1-70 controls when the bias coil assembly 1-97 is rotated onto or off of the disc cartridge 1-13.

The bias coil assembly 1-94 may tilt or rotate about a point

1-353 near its center, and it is spring-loaded downward. In this manner, the bias coil assembly 1-94 can remain parallel to the disc cartridge 1-13 when in the down condition (i.e., the position depicted in Fig. 23, wherein the disc cartridge 1-13 is fully loaded), and when in the up condition (i.e., the position depicted in Fig. 25, wherein the disc cartridge 1-13 is unloaded). The ability of the bias coil assembly 1-94 to remain parallel to the disc cartridge 1-13 when in the up condition provides the clearance needed for the drive 1-10 to be able to complete a disk-ejection operation, as discussed below. When in the down condition and loaded in the disc cartridge 1-13, the bias coil assembly 1-94 rests on the disc cartridge 1-13 in three places.

5

10

Referring now to Figs. 23-25, the ejection of a disc cartridge 1-13 from the disc drive 1-10 will be described. 15 23 depicts a disc cartridge 1-13 with the disc hub 1-15 fully loaded onto the spindle 1-62 of the spindle motor 1-61. configuration, the bias coil assembly 1-94 is loaded into the disc cartridge 1-13 through the open shutter 1-49. When the disc cartridge 1-13 is fully loaded in this manner, the left slider 20 1-70 has been slid to its most rearward position by the tiller 1-76. The lever arm 1-275 of the bias coil arm 1-97 has been rotated toward the rear of the disc drive 1-10. It is this rotation of the lever arm 1-275 which has installed the bias coil assembly 1-94 into the disc cartridge 1-13. Since the lift pins 25 1-136, 1-139 of the cartridge receiver 1-82 are restrained to

only vertical movement by the vertical slots 1-130, 1-133 (Figs. 8A and 8B), when the left slider 1-70 has been driven toward the rear of the disc drive 1-10 by the tiller 1-76, as depicted in Fig. 23, the cartridge receiver 1-82, via its lift pins 1-133, 1-136, has been driven to the lowest point in the S-shaped slots 1-262, 1-281.

5

10

15

20

25

Referring now to Fig. 24, an intermediate stage of the ejection cycle will now be described. After a user initiates the ejection of the disc cartridge 1-13 from the disc drive 1-10, the ejection motor 1-208 (Fig. 9) rotates the tiller 1-76 in a first direction (counterclockwise in Fig. 9). This rotation of the tiller pulls the left slider 1-70 toward the front of the drive 1-10, as depicted in Fig. 24. As the left slider 1-70 slides forward, the notch 1-268 rotates the lever arm 1-275 forward, thereby lifting the bias coil assembly 1-94 out of the disc cartridge 1-13. As may also be seen from Fig. 24, the lift pins 1-136, 1-139, which are fixed to the cartridge receiver 1-82, are being forced up the S-shaped slots 1-262, 1-281 by the motion of the tiller 1-76. Since the lift pins 1-136, 1-139 are positioned on the cartridge receiver at a point where a lateral axis passing through both lift pins 1-136, 1-139 would not also pass through the spindle 1-62, a "peeling" action for removal of the disc hub 1-15 from the spindle magnet 1-64 is achieved as the cartridge receiver 1-82 is raised. In other words, as depicted in Fig. 24, the disc 1-14 is not lifted vertically from the spindle 1-62 during the ejection cycle. Rather, due to the location of the

lift pins 1-136, 1-139 on the cartridge receiver 1-82, the rear portion of the disc cartridge 1-13 is lifted before the forward end of the disc cartridge 1-13 as the lift pins 1-136, 1-139 follow their respective S-shaped slots 1-262, 1-281. This peeling action lowers the peak force required to remove the disc hub 1-15 from the magnetic clamp 1-64 of the spindle motor 1-61.

5 -

10

15

20

25

Referring still to Fig. 24, it is apparent that after the cartridge receiver 1-82 has been lifted a predetermined amount by the motion of the sliders 1-70, 1-73, the lip 1-356 (Fig. 15A) on the rear wall 1-317 of the cartridge receiver 1-82 impacts the lower surface of the stop ledge 1-350 (Fig. 18) on the bias coil clamps 1-100. This contact between the bottom surface of the stop ledge 1-350 and the top surface of the lip 1-356, in conjunction with the continued rotation of the tiller 1-76 and the resulting longitudinal motion of the sliders 1-70, 1-73, causes the cartridge receiver 1-82 to pitch slightly upward in Fig. 24, substantially about the point of contact between the stop ledge 1-350 and the lip 1-356, as the lift pins 1-136, 1-139 continue to pick up the receiver. This slight pitching motion of the cartridge receiver 1-82 effects the "peeling" action referred to above.

Fig. 25 depicts the configuration of the disc drive 1-10 after the slight upward pitching of the cartridge receiver 1-82 is complete and the cartridge receiver 1-82 has impacted the stops adjacent to the disc receiving port 1-22. At this point, the left slider 1-70 has reached its furthest forward position

and has pulled the lever arm 1-275 to its furthest forward position, thereby rotating the bias coil assembly 1-94 out of the disc cartridge 1-13. The bias coil assembly is thus parked parallel to and above the disc cartridge 1-13, substantially against the inside of the top surface of the disc drive 1-10 or substantially against a printed circuit board located against the inside of the top surface of the disc drive 1-10. The bias coil assembly 1-94 travels vertically about 9mm from its loaded position in the disc cartridge 1-13 to its just-described raised position.

As the cartridge receiver 1-82 is raised to its highest position (about 5mm above its lowest position), the right slider 1-73 (Figs. 12A-12E) is latched in its rear-most position by the receiver latch 1-166 (Figs. 17A and 17B), as fully described above. When the cartridge receiver 1-82 is in the up position depicted in Fig. 25, the cartridge receiver 1-82 is positioned parallel to the base plate 1-46, ready for the cartridge 1-13 to be ejected. The spring force of the door links 1-85, 1-88, which are biased toward the forward end of the disc drive 1-10 as described above, and the spring force of the cartridge shutter 1-49, which is biased toward a closed position, cause the disc cartridge 1-13 to be ejected from the disc drive 1-10, as depicted in Fig. 25.

The disc loading process is essentially the reverse of the above described ejection process. Therefore, a detailed description of the disc insertion process will not be provided.

In the instant invention, where the disc hub 1-15 is peeled from the spindle magnet 1-64, the required ejection force is effectively reduced by the manner in which the disc 1-14 is moved from the loaded position to the unloaded position. Through the use of the "peeling" motion of the instant invention, a smaller force is required to remove the disc hub 1-15 than is required in conventional, vertical-lifting systems. In addition, the design conserves overall drive height. The above-described design accomplishes the peeling of the disc hub 1-15 from the spindle magnet 1-64 with a mechanism that uses available space at the sides of the drive 1-10, rather than requiring parts that straddle the width of the base plate 1-46 to tie the motion of both sides of a cartridge receiver 1-82 together and using additional height to do so. Another advantageous feature of the design is the noncritical nature of most of the dimensions required.

5

10

15

20

25

Further, the bias coil actuating mechanism that loads the bias coil assembly into the cartridge 1-13 is simple and has almost no wear points. The entire design is easy to assemble and for the most part can be executed using simple and easy to fabricate parts.

While what has been described above is a preferred embodiment of this invention, it will be obvious to those skilled in the art that numerous changes may be made without departing from the spirit or scope of the invention. For example, the instant invention may be used for media systems which do not

require the bias coil assembly 1-94 (i.e., phase change or write once systems), by eliminating the parts used to operate the bias coil arm 1-97. In addition, although in the preferred embodiment the storage media is a 5 ¼ inch magneto-optic disc cartridge, the invention is applicable to all types of media and all sizes of drives.

Two-Axis Moving Coil Actuator.

5

10

15

20

25

Fig. 26 schematically illustrates a two-axis electromagnetic actuator 2-10 constructed in accordance with the present invention. The actuator 2-10 includes an objective lens 2-12 positioned within a lens holder 2-14 (shown in phantom). A radial or tracking coil 2-16 is wound around and affixed to the lens holder 2-14 so as to be generally positioned perpendicular to the Z axis. First and second focus coils 2-18, 2-20 are positioned at the sides of the lens holder 2-14 and are affixed to the tracking coil 2-16 so as to be generally positioned perpendicular to the Y axis. A first pair of permanent magnets 2-22 is positioned adjacent the first focus coil 2-18 and a second pair of permanent magnets 2-24 is positioned adjacent the second focus coil 2-20.

As shown in Fig. 27, the lens holder 2-14 includes a generally rectangular collar 2-30 having a circular aperture 2-32 centered therein. The objective lens 2-12 is glued into position on top of the circular aperture 2-32 in the collar 2-30. The collar 2-30 is supported by a generally I-shaped platform 2-34 having a pair of grooves 2-44 formed at the edges thereof to align and secure the tracking coil 2-16 therein when it is wound

around the platform. A base 2-36 supporting the platform 2-34 includes first and second "t" shaped sections 2-46, 2-48 having a slot 2-50 formed therebetween. As will be explained in more detail below, this base 2-36 acts as a mass balance for the lens holder 2-14. The collar, platform, and base are aligned on two sides to form first and second opposing faces 2-52, 2-54 of the lens holder.

5

10

15

20

25

The focus coils 2-18, 2-20 are affixed to the tracking coil 2-16 such that the central axes of the focus coils are coincident, and intersect and are preferably perpendicular to the central axis of the tracking coil. The focus coils 2-18, 2-20 are preferably formed from thermally bonded wire having a bond material layer thereon and are preferably wound on a suitable tool or support. The coils 2-18, 2-20 are preferably wound around the support as tight as possible without deforming the wire. As those skilled in the art will appreciate, this tightness will vary with the type of wire. During the winding process, the focus coils 2-18, 2-20 are preferably heated to melt the bond material layer on the wire, advantageously increasing the solidity and rigidity of the wound coils. The temperature is advantageously selected so as to be high enough to melt the bond material, but not so high as to melt the insulation. After cooling, the coils 2-18, 2-20 are removed from the support and these freestanding coils are then affixed to the tracking coil 2-16 in a well-known manner using a suitable adhesive.

Each freestanding focus coil 2-18, 2-20 is oval in shape and

has two elongate sides 2-56 joined by a pair of shorter ends 2-58. The sides 2-56 and ends 2-58 of the coils 2-18, 2-20 surround an open or hollow annular center 2-60. The tracking coil 2-16 is wound around the I-shaped platform 2-34 of the lens holder 2-14 such that the coil is received by and secured within the grooves 2-44 and positioned against the opposed faces 2-52, 2-54 of the lens holder. Referring to Fig. 26 and Fig. 27, the two focus coils 2-18, 2-20 are affixed to the tracking coil 2-16 such that the tracking coil is positioned within the center 2-60 of each focus coil. The focus coils 2-18, 2-20 are further positioned such that each coil abuts the opposed faces 2-52, 2-54 of the lens holder 2-14. In this manner, the tracking coil 2-16 and focus coils 2-18, 2-20 are rigidly secured to the lens holder 2-14, thereby creating a more rigid driven unit that behaves as a single lumped mass.

Referring to FIGS. 28, 29, 30, and 31, in operation, a light source element (not shown), typically a laser diode, emits a laser light beam 2-70 (Fig. 31). The beam 2-70 is incident upon a prism 2-72 which orthogonally reflects the light beam upward toward the objective lens 2-12. The lens 2-12 converges the beam 2-70 to a precise focal point or optical spot 2-74 on the surface of a recording medium, such as an optical disc 2-76. Upon striking the disc 2-76, the light beam 2-70 is altered by the information stored on the disc 2-76 and is reflected as a divergent light beam carrying information identical to that encoded on the disc 2-76. This reflected beam re-enters the

objective lens 2-12 where it is collimated and is again reflected by the prism 2-72 to a photodetector (not shown) which detects the data stored on the disc 2-76. In addition, if the light beam falling on the photodetector is out of focus or misaligned, the amount of misalignment or defocusing is measured electronically and used as feedback for a servo system (not shown) well-known in the art which properly realigns the objective lens 2-12 relative to the disc 2-76.

5

10

15

20

25

It is these feedback signals which determine the amount and direction of movement of the actuator 2-10 and objective lens 2-12 carried thereon needed to bring the light beam into the desired focus condition with respect to the disc 2-76. When radial or tracking movement is required to position the objective lens 2-12 beneath the center of a selected track on the optical disc 2-76, current is applied to the tracking coil 2-16. The current interacts with the magnetic field produced by the permanent magnet pairs 2-22, 2-24 to produce forces which move the actuator 2-10 in the tracking direction. The forces are generated according to the Lorentz law F = B X I multiplication dot 1, wherein F represents the force acting on the tracking coil 2-16, B represents the magnetic flux density of the magnetic field between the permanent magnet pairs 2-22, 2-24, I represents the current through the tracking coil 2-16, and 1 represents the length of the coil 2-16. When the current I applied to the tracking coil 2-16 travels through the coil in a counterclockwise direction (as shown in Fig. 29), a force is produced which moves



the actuator 2-10 to the right (as shown in Fig. 31) by the arrow 2-15. When the current applied to the coil 2-16 travels through the coil in the opposite, or clockwise direction (as shown in Fig. 29), a force is produced which moves the actuator 2-10 to the left (as shown in Fig. 31) by the arrow 2-17. In this manner, the actuator 2-10 is moved radially to position the objective lens 2-12, beneath the center of a desired information track on the surface of the optical disc 2-76.

5

25

Movement of the actuator 2-10 to effect focusing is produced 10 when current is generated in the two focus coils 2-18, 2-20 affixed to the tracking coil 2-16 at the sides of the lens holder 2-14. When the current through these coils 2-18, 2-20 is applied so that the current travels in a counterclockwise in the plane of Fig. 30, a force is produced which acts to move the lens holder 15 2-14 and objective lens 2-12 upward (as shown by the arrow 2-19 in Fig. 31) towards the surface of the optical disc 2-76. Conversely, when current is applied such that current travels through the coils 2-18, 2-20 in a direction clockwise in the plane of Fig. 30, a force is produced which moves the lens holder 20 2-14 downward (as shown in Fig. 31) by the arrow 2-21, or farther away from the surface of the disc 2-76.

Because the tracking coil 2-16 is coupled to the lens holder 2-14, and, in turn, the focus coils 2-18, 2-20 are coupled directly to the tracking coil 2-16, the coils and lens holder behave as a "lumped mass" and the frequencies at which the coils decouple with respect to the lens holder are significantly

increased. Decoupling frequencies of up to 30 kHz have been measured with the actuator design of the present invention.

5

10

15

20

25

Referring to Fig. 28, the magnet pairs 2-22, 2-24, remain stationary during movement of the lens holder 2-14 and are affixed within a generally rectangular housing or base 2-80. Two pairs of suspension wires 2-82, 2-84 are provided to suspend the objective lens holder 2-14 between the magnet pairs 2-22, 2-24. The wire pairs 2-82, 2-84 are attached to a stationary printed circuit board 2-85 which is positioned vertically with respect to the lens holder 2-14 and acts as a support for the wire pairs 2-82, 2-84. The wire pairs 2-82, 2-84 are further attached to electrical contacts on a moving circuit board 2-87 which is attached to the lens holder 2-14, again in a vertical orientation. In particular, a free end of each focus coil 2-18, 2-20 is soldered to electrical contacts 2-86 such that current is supplied to the focus coils 2-16, 2-18, through the second or bottom wire pair 2-84 which is also soldered to the contacts 2-86. The other free end of each focus coil 2-18, 2-20 is soldered to the circuit board 2-87 and joined along an electrical contact 2-88. The free ends of the tracking coil 2-16 and the first or top suspension wire pair 2-82 are soldered to electrical contacts 2-89 on the moving circuit board 2-87 such that current is supplied to the coil through the top pair of wires. The base 2-36 of the lens holder 2-14 acts as a mass balance by offsetting the weight of the objective lens 2-12 and the circuit board 2-87 to which the lens holder 2-14 is attached.

Alternatively, four flexures could be used to suspend the lens holder 2-14. The flexures would desirably act as parallel leaf springs which permit the objective lens holder 2-14 to move up-and-down for focusing while prohibiting changes in the orientation of the optical axis of the lens 2-12. In this manner, the objective lens 2-12 will not be canted with respect to the surface of the optical disc 2-76 as the lens holder 2-14 is moved in the focusing direction. Each flexure further includes narrow portions which operate as a hinge so as to allow some movement of the lens holder 2-14 in a side-to-side direction for tracking adjustments.

In addition to accomplishing fine focusing and tracking movements of the lens holder 2-14, it is often desirable to detect the position of the lens holder 2-14 with respect to the base 2-80. To ascertain the position of the objective lens 2-12 in both a tracking and/or a focusing direction, the actuator 2-10 is equipped with a position sensor 2-90. Preferably, a light emitting diode (LED) 2-92 is positioned on one side of the actuator 2-10, opposite the sensor 2-90, such that when the objective lens holder 2-14 is centered within the base 2-80, light emitted by the LED 2-92 will shine through the slot 2-50 in the lens holder 2-14 to illuminate a portion of the sensor 2-90. A position sensitive detector is advantageously implemented as the sensor 2-90 and the sensor is positioned such that when the lens holder 2-14 is centered within the base 2-80, light emitted by the LED 2-92 will pass through the slit 2-50 and will be

distributed on the detector. Thus, as the lens holder 2-14 moves in a side-to-side direction, i.e., the tracking direction, various portions of the sensor 2-90 will be illuminated, indicative of the position of the lens holder 2-14 in the tracking direction. Consequently, when the lens holder 2-14 is not centered with respect to the base 2-80, a portion of the light emitted from the LED 2-92 will be blocked by the lens holder 2-14, causing an unequal distribution of light on the sensor 2-90. This unequal distribution may then be analyzed to determine the position of the lens holder 2-14 with respect to the base 2-80 by well-known circuitry and methods.

When a control signal is generated by the servo system, a given current is applied to the tracking coil 2-16 and/or the focus coils 2-18, 2-20 depending on the direction in which the displacement of the lens holder 2-14 and objective lens 2-12 attached thereto is required. Such servo systems and feedback circuits which control the amount of current are well known in the art. As discussed above, this current interacts with the electromagnetic field produced by the permanent magnet pairs 2-22, 2-24 to create a force which displaces the lens holder 2-14 and objective lens 2-12 attached thereto in the appropriate focusing or tracking direction.

The operation and structure of the focus and tracking mechanism will now be described in greater detail. As illustrated in FIGS. 32 and 33, the permanent magnet pairs 2-22, 2-24, are oriented with opposite poles opposing each other. More



specifically, the first pair of magnets 2-22 includes a first or top magnet 2-100 and a second or bottom magnet 2-102 in a stacked relationship joined along a planar interface, such that the north pole of the top magnet 2-100 and the south pole of the bottom magnet 2-102 (as illustrated in Fig. 33) are positioned adjacent the lens holder 2-14. The second pair of magnets 2-24 includes a third or top magnet 2-104 and a fourth or bottom magnet 2-106 in a stacked relationship joined along a planar interface having the opposite orientation, such that the south pole of the top magnet 2-104 and the north pole of the bottom magnet 2-106 (as illustrated in Fig. 33) are positioned adjacent the lens holder 2-14. As shown in Fig. 32, the field lines produced by this orientation originate at the north pole of each magnet pair 2-22, 2-24, and terminate at the south pole of each magnet pair. Iron plates 2-110 (shown in phantom for clarity) may be attached to each magnet pair 2-22, 2-24 on the sides of the permanent magnets opposite the lens holder 2-14. The iron plates 2-110 effectively "shunt" the magnetic flux emanating from the sides of the magnets 2-100, 2-102, 2-104, 2-106, opposite the lens holder 2-14, increasing the magnetic flux adjacent the lens holder and producing a corresponding increase in actuator power.

5

10

15

20

25

The focus forces acting on the actuator 2-10 are illustrated in more detail in Fig. 34. When a current I is applied to the focus coils 2-18, 2-20 in the direction indicated, i.e., out of the plane of the figure adjacent the top magnets 2-100, 2-104 and into the plane of the figure adjacent the bottom magnets 2-102,

2-106, forces F_{FOCUS1} and F_{FOCUS2} are generated which are translated to the lens holder 2-14 to accelerate or decelerate the moving mass (lens holder) and to the suspension wire pairs 2-82, 2-84, bending the suspension wires to move the lens holder 2-14 and associated objective lens 2-12 closer to the optical disc 2-76. Because the lines of magnetic flux curve as described above, the direction of the magnetic field varies vertically in the focus coils 2-18, 2-20. For example, for the focus coil 2-18 positioned adjacent the first magnet pair 2-22, in the plane of Fig. 34 which vertically bisects the coil adjacent the top magnet 2-100, the magnetic field has a first direction at the top of the coil 2-18 given by B, and a second direction in the bisecting plane adjacent the bottom magnet 2-102 at the bottom of the coil 2-18 given by B2. In accordance with the Lorentz law F=BXI multiplication dot 1, the current interacts with the magnetic field B1 to produce a first force component F1 acting on the portion of the focus coil 2-18 adjacent the top magnet 2-100, and interacts with the magnetic field B2 to produce a second force component F2 acting on the portion of the focus coil adjacent the bottom magnet 2-102. As the magnitude of the horizontal portions of the force components F1 and F2 are equal in magnitude but opposite in direction, these horizontal force components cancel one another in accordance with the rules of vector addition to produce a resultant force F_{FOCUS1} which is vertically upward in the plane of Fig. 34. Similarly, the horizontal force components throughout the rest of the coil 2-18 are canceled, giving a

5

10

15

20

25

vertical resultant force which is strictly vertically upward (i.e., is vertically upward and has effectively no horizontal component) and therefore moves the lens holder 2-14 closer to the surface of the optical disc 2-76.

5

10

15

20

25

As the lines of flux generated by the second magnet pair 2-24 curve oppositely of those generated by the first magnet pair 2-22, the direction of the magnetic field at any point in the focus coil 2-20 is different than the direction of the field at the corresponding point in the focus coil 2-18. Again, because the flux lines curve, the direction of the field acting on the coil 2-20 varies vertically along the coil. In the plane of Fig. 34 which vertically bisects the coil adjacent the top magnet 2-104 of the second magnet pair 2-24, the magnetic field direction is given by B₃ at the top of the coil 2-20 and a force is generated in accordance with Lorentz law in the direction F3, while in the bisecting plane adjacent the bottom magnet 2-106, the magnetic field direction is given by B4 at the bottom of the coil 2-20 and a force F4 is generated. The forces add to produce a resultant force F_{FOCUS2} , which, as shown, is strictly vertically upward.

Thus, it can be seen that the forces F_{FOCUS1} and F_{FOCUS2} , act on the focus coils 2-18 and 2-20, respectively, to move the lens holder 2-14 upward. Conversely, if the current was applied to the focus coils 2-18, 2-20, in the opposite direction, forces would be generated to move the lens holder 2-14 downward, or farther away from the surface of the optical disc 2-76. By moving the

objective lens 2-12 closer to or farther away form the surface of the optical disc 2-76, the focus coils 2-18, 2-20 act to precisely focus the laser beam exiting the objective lens 2-12 on the disc 2-76.

5

10

15

20

25

As illustrated in Fig. 35, movement of the actuator 2-10 to effect fine tracking is produced when current is generated in the tracking coil 2-16 affixed to the lens holder 2-14. In the plane of Fig. 35 which horizontally bisects the tracking coil 2-16, a magnetic field having direction B1 acts on the cross-section of the coil 2-16 located closest to the first magnet pair 2-22 and a magnetic field having the direction B2 acts on the cross-section of the coil located closest to the second magnet pair 2-24. If, for example, a current I is applied in a counterclockwise direction around the tracking coil 2-16, a force F1 acts on the portion of the tracking coil adjacent the first magnet pair 2-22 and a force F2 acts on the portion of the tracking coil adjacent the second magnet pair 2-24. These forces add under the laws of vector addition to produce a resultant force $\boldsymbol{F}_{\text{TRACK}}$ which acts to move the lens holder 2-14 to the right in the plane of Fig. 35. When the forces act on the tracking coil 2-16 in this manner, they are translated through the lens holder 2-14 to accelerate or decelerate the moving mass (lens holder) and to the suspension wire pairs 2-82, 2-84 which bend in the corresponding direction to move the objective lens 2-12 and precisely center the laser beam exiting therefrom within the center of a selected data track on the surface of the optical disc 2-76. Conversely, if a current

I is applied in a clockwise direction around the coil 2-16, a resultant force is produced which moves the lens holder 2-14 to the left in the plane of the Fig. 35.

Thus, it can be seen that the coupling arrangement of the present invention further reduces the distance between the resultant forces acting on the coils 2-16, 2-18, 2-20 and the optical axis of the objective lens 2-12, decreasing adverse modes of motion such as pitch, roll, and yaw during focusing and tracking operations.

5

10

15

20

25

With the actuator design of the present invention, only two pairs of permanent magnets, i.e., four total magnets, and three coils are required to effect movement in both the tracking and focusing directions, thereby reducing both the size and weight of actuator and yielding higher decoupling frequencies. As the component count for the actuator is low, the actuator is easy to manufacture and assemble as compared to prior actuator designs having many more coils, magnets, and pole pieces. In addition, because the tracking and focus coils 2-16, 2-18, 2-20 are coupled directly to the lens holder 2-14 and are not wound around yokes or poles, coil rigidity and resonance frequency response is significantly improved. Further, direct coupling of the coils 2-16, 2-18, 2-20, reduces the distance between the point where the effective tracking and focus forces are generated and the optical axis of the objective lens, decreasing adverse motions such as pitch, roll, and yaw.

The present invention improves motor performance; Figures of

merit as high as 130 m/s² /sq. rt. (W) for the focus direction and 70 m/s² /sq. rt. (W) for the radial direction have been measured for actuators constructed in accordance with the present invention, significantly higher than previously realized. As those skilled in the art will recognize, the design of the present invention also ensures that approximately 40% of the coil wire is utilized, increasing the efficiency of the actuator over prior designs.

The preferred embodiment has been described with reference to the coordinate system illustrated in Fig. 26 wherein the optical disc 2-76 is positioned above the objective lens 2-12 such that focusing is effected by moving the actuator 2-10 up and down along the Z-axis and tracking movement is effected by moving the actuator in a side-to-side motion along the Y-axis. Those skilled in the art will recognize, however, that the actuator 2-10 of the present invention could also be incorporated in optical systems having different orientations than those illustrated.

Focus Sensing Apparatus.

5

10

15

20

25

Fig. 36 is a block diagrammatic representation of a preferred embodiment of the beam focus sensing apparatus 3-10 of the present invention. The apparatus 3-10 includes an optical arrangement 3-12 for providing a servo beam S indicative of the focus of an illuminating beam I upon an optical disc 3-14. The servo beam S comprises a portion of the illuminating beam I reflected by the disc 3-14. Techniques for generating such a

servo beam are well known to those skilled in the art. For example, an optical system such as the optical arrangement 3-12 for generating the servo beam S is described in U.S. Pat. No. 4,862,442, which is herein incorporated by reference. A brief summary of the operation of the optical arrangement 3-12 is set forth below.

5

10

15

20

25

As shown in Fig. 36, the optical arrangement 3-12 includes a laser source 3-16 which generates a linearly polarized beam B. The beam B is collimated by a collimating lens 3-18, and the collimated beam is directed by an optical beamsplitting arrangement 3-20 to an objective lens 3-24. The collimated beam is then converged by the objective lens 3-24 onto the surface of the optical disc 3-14. The optical disc may, for example, comprise a compact disc, video disc, or optical memory disc. The disc 3-14 reflects the illuminating beam focused thereon back through the objective lens 3-24 to beamsplitting arrangement 3-20. Those skilled in the art will appreciate that the beamsplitting arrangement 3-20 may include a first beamsplitter (not shown) to redirect a first portion of the reflected illuminating beam in order to form the servo beam S. The beamsplitting arrangement 3-20 will also generally include a second beamsplitter (not shown) to redirect a second portion of the reflected illuminating beam to create a data beam. Such a data beam carries information stored on the optical disc 3-14. The servo beam S is intercepted by the FTR prism 3-30, the design and construction of which is discussed more fully hereinafter.

As is also described more fully below, the servo beam S is divided into a transmitted beam T and a reflected beam R by the FTR prism 3-30. In the embodiment of Fig. 36 the transmitted and reflected beams T,R are of substantially equal cross section and intensity. The transmitted beam T is incident on a first quad detector 3-32, while the reflected beam R is incident on a second quad detector 3-34. Electrical signals produced by the quad detectors 3-32, 3-34 in response to the intensity distributions of the transmitted and reflected beams T, R are utilized by a control unit 3-37 to generate a differential focus error signal (DFES) indicative of the focus of the illuminating beam I on the disc 3-14. One preferred embodiment of a control unit 3-37 and associated method for generating the DFES is discussed hereinafter. The focus error signal may, for example, be used to control a mechanical arrangement (not shown) disposed to adjust the focus of the illuminating beam I by altering the displacement of the objective lens 3-24 relative to the disc 3-14.

5

10

15

20

25

Fig. 37 shows a magnified top cross-sectional view of the FTR prism 3-30. The prism 3-30 includes first and second optical members 3-35, 3-36 which sandwich a separation layer 3-38. The optical members 3-35, 3-36 may be realized from glass having an index of refraction larger than that of the separation layer 3-38. For example, in one preferred embodiment the optical members 3-35, 3-36 may be manufactured from glass having an index of refraction of 1.55, while the separation layer 3-38 is composed of a solid such as either magnesium fluoride (MgF₂) or

fused silica (SiO₂) having indices of refraction of 1.38 and 1.48, respectively. The separation layer 3-38 need not consist of a solid, and may be realized from a liquid or air provided that the optical members 3-35, 3-36 are of a larger index of refraction.

5

10

15

20

25

A brief description of the physics of the interaction of the light in beam S with layer 3-38 is as follows. If layer 3-38 and optical member 3-35 are not present, the well-known phenomenon of total internal reflection takes place at the hypotenuse face of optical member 3-36, sending all of beam S in the direction of beam R. However, some light energy exists behind the hypotenuse face of optical member 3-36 in the form of "evanescent waves", which do not propagate. When optical member 3-35 is brought close enough to optical member 3-36, this energy is coupled without loss into member 3-35 and propagates in the direction of beam T. This phenomenon is known as frustrated total reflection (FTR). In this condition, if the FTR prism is disposed with respect to beam S such that the incidence angle A of beam S at separation layer 3-38 is close to the region of frustrated total reflection, the transmission and reflection curves will have very steep slopes (angular sensitivities). This allows the fabrication of a very sensitive focus sensing system. Further, the transmission and reflection curves for such a system based on the FTR principle will be relatively insensitive to the wavelength of the light in beam S, as compared to the curves of a multilayer structure.

The prism 3-30 may be fabricated by first depositing the

separation layer on either of the optical members via conventional thin film techniques. The complementary optical member may then be affixed to the exposed surface of the separation layer with an optical glue. Although the indices of refraction of the first and second optical members 3-35, 3-36 will generally be chosen to be identical, differing indices of refraction may also be selected. In the preferred embodiment, the first and second optical members have identical indices of refraction in such a geometry that the transmitted and reflected beams T and R are of substantially equal cross-section.

As shown in the illustrative front view of Fig. 38, the first quad detector 3-32 includes first, second, third and fourth photodetective elements 3-40, 3-42, 3-44, 3-46, respectively, which produce electrical signals hereinafter referred to as T1, T2, T3, and T4 in response to the intensity of the transmitted beam T impinging thereon. Similarly, the second quad detector 3-34 includes fifth, sixth, seventh and eighth photodetective elements 3-50, 3-52, 3-54, 3-56, respectively, which provide electrical signals hereinafter referred to as R1, R2, R3 and R4 in response to incidence of the reflected beam R. The photodetective elements may be realized by PIN diodes, wherein the level of the electrical output from each diode is proportional to the optical energy received thereby.

When the objective lens 3-24 (Fig. 36) is situated relative to the disc 3-14 such that the illuminating beam I is properly focused, the rays included within the servo beam are well

collimated (i.e. substantially parallel) and are therefore incident on the separation layer 3-38 at a substantially identical angle A shown in Fig. 37. Contrary to this, when the objective lens 3-24 does not focus the illuminating beam in the plane occupied by the surface of the disc 3-14 the rays comprising the servo beam S will be either mutually convergent or divergent. It follows that all rays within the servo beam S will impinge on the separation layer 3-38 at the substantially same angle when the illuminating beam I is suitably focused, while rays of a different range of angles of incidence will address the separation layer 3-38 when the beam I is out of focus. The prism 3-30 is designed such that the reflectivity and transmissivity of the separation layer 3-38 is extremely sensitive to the angle at which optical energy is incident on the separation layer 3-38. Thus, the spatial distribution in the intensity of the transmitted and reflected beams T, R will vary as the focus position of the illuminating beam I varies relative to the surface of the disc 3-14. That is, an illuminating beam I which is properly focused gives rise to a well collimated servo beam S such that all the rays thereof experience the same degree of reflection by the separation layer 3-38. Accordingly, the transmitted and reflected beams T, R will be of substantially uniform intensity when the illuminating beam I is appropriately focused. Conversely, a convergent or divergent servo beam S will engender transmitted and reflected beams T, R of nonuniform spatial intensity distributions since the rays within the servo

5

10

15

20

25

beam S will be subject to a variety of degrees of reflection by the separation layer 3-38. By detecting these spatial variations in the intensity of the transmitted and reflected beams the photodetectors 3-32, 3-34 produce electrical signals which may be utilized to produce a DFES indicative of the focus position of the illuminating beam I.

5

10

15

20

25

The manner in which a DFES may be synthesized in response to the degree of collimation of the servo beam S may be further understood with reference to Fig. 39. Fig. 39 is a graph showing the reflectivity (intensity of beam R/intensity of beam S) of the FTR prism 3-30 as a function of the angle of incidence of rays within the servo beam S relative to the separation layer 3-38. Specifically, the graph of Fig. 39 depicts the reflectivities Rs and Rp of the prism 3-30 in response to illumination by both s-polarized and p-polarized optical energy of wavelength 0.78 microns. The reflectivity profiles of Fig. 3-39 pertain to a FTR prism 3-30 having a separation layer with a thickness of 4.5 microns and an index of refraction of 1.38, with the separation layer being sandwiched by glass members having an index of refraction of 1.55. As shown in Fig. 39, the prism 3-30 is preferably positioned relative to the servo beam S at an angle of incidence A_1 such that the prism 3-30 is operative about a working point P. That is, at the working point P the prism 3-30 is positioned such that an illuminating beam I properly focused on the disc 3-14 engenders a well collimated servo beam S having rays which impinge on the separation layer 3-38 at the angle A_1 .

Since the reflectivity of the prism 3-30 is approximately 0.5 at the operating point P, the transmitted and reflected beams produced by the module 3-30 are of substantially identical average intensity.

5

10

15

20

25

When the separation between the objective lens 3-24 and the disc 3-14 varies such that the servo beam S decollimates in either a convergent or divergent manner, a first portion thereof will impinge on the separation layer 3-38 at an angle of incidence larger than the angle A_1 . For example, at an angle of incidence of A_2 (Fig. 39) a corresponding portion of the servo beam will experience a reflectivity of approximately 0.7. Since the first servo beam portion is subject to a reflectivity of only 0.5 when the servo beam S is well collimated, the regions of the detectors 3-32, 3-34 which receive the parts of the reflected and transmitted beams R, T derived from the first servo beam portion will collect more and less optical energy, respectively, than when the illumination beam I is properly focused. Similarly, the areas of the detectors 3-32, 3-34 in optical alignment with parts of the transmitted and reflected beams T, R arising from a second portion of the servo beam S incident on the separation layer 3-38 at an angle of incidence A_3 (smaller than the angle A_1) will be illuminated by more and less optical energy, respectively, than in a condition of proper focus. The DFES is produced in response to electrical signals engendered by the photodetectors 3-32, 3-34 indicative of this spatial nonuniformity in the intensity distribution of the transmitted and reflected beams T, R.

Moreover, since in the preferred embodiments described herein the module 3-30 is optically nonabsorbing, variation in the intensity of the transmitted beam T arising from a change in the angle of incidence of a portion of the servo beam S is mirrored by an equal, oppositely directed variation in the magnitude of the part of the reflected beam R engendered by the identical servo beam portion. Non-differential error signals may be generated independently from either the transmitted or reflected beam, using the equations:

10 FES (transmitted) =
$$(T1 + T2) - (T3 + T4)$$
 [1]

5

20

25

FES (reflected) =
$$(R1+R2)-(R3+R4)$$
 [2]

In the differential system, the differential focus error signal (DFES) is generated by the control unit 3-37 in accordance with the following expression:

DFES =
$$(R1+R2+T3+T4) - (T1+T2+R3+R4)$$
 [3]

The control unit 3-37 includes circuitry suitable for carrying out the arithmetic operations of equation [3] and for generating a DFES based on these operations. Preamplifiers (not shown) are included to amplify the electrical signals from the photodetectors 3-32, 3-34 prior to processing by the control unit 3-37.

Utilizing the dual quad photodetector arrangement described herein leads to the synthesis of differential focus error signals having a reduced sensitivity to certain beam imperfections not induced by inaccuracies in the focus position of the illuminating beam relative to the disc 3-14. Since a localized decrease in the

intensity of the servo beam S unrelated to the focus position of the illuminating beam affects the detectors 3-32 and 3-34 in a substantially similar manner, such a decrease does not affect the value of the DFES due to the corresponding cancellation which occurs in equation [3].

As mentioned in the Background of the Invention, prior focusing systems were generally ill-equipped to implement the differential focus sensing scheme described by equation [3]. In particular, a feature of the present invention lies in the ability of the FTR prism 3-30 to provide transmitted and reflected beams of substantially similar cross section and intensity such that both may effectively contribute to the synthesis of a DFES.

In addition to providing a DFES for maintaining the focus of the illuminating beam I in the direction normal to the surface of the disc 3-14, the electrical outputs from the photodetectors 3-32, 3-34 may also be used by the control unit 3-37 to generate a tracking error signal (TES). The TES is indicative of the radial position of the illuminating beam I relative to the conventional spiral or concentric guiding tracks (not shown) imprinted on the surface of the disc 3-14. The TES enables the beam I to follow the guiding tracks despite eccentricities therein by controlling a mechanical arrangement (not shown) operative to adjust the radial position of the objective lens 3-24 relative to the disc 3-14. The TES is calculated by the control unit 3-37 on the basis of electrical outputs from the

photodetectors 3-32, 3-34 in accordance with the following equation:

TES = (T1+T3+R3+R1) - (T2+T4+R2+R4) [4]

5

10

15

20

25

Again, the manner in which a tracking error signal may be derived from the relationship existing between spatial intensity changes of the servo beam and the tracking position of the illuminating beam is disclosed in, for example, U.S. Pat. No. 4,707,648.

In perhaps the majority of systems operative to control the focus of an illuminating beam relative to an optical disc it will be desired to generate both tracking and focus error signals in response to the electrical outputs of the photodetective elements. Since generation of both the focus and tracking error signals is known to generally require at least one quad photodetector, the embodiments of the present invention disclosed herein have been described with reference to quad photodetectors. However, it is also known that a focus error signal may be derived on the basis of electrical signals produced by photodetectors having only two independent photosensitive regions (bicell detectors). Accordingly, in applications requiring only the generation of a focus error signal a single photodetective element could be substituted for the first and second elements 3-40, 3-42 of the photodetector 3-32, and a single photodetective element could replace the third and fourth elements 3-44, 3-46. Similarly, a single photodetective element could be used in lieu of the fifth and sixth elements 3-50, 3-52 of the photodetector 3-34, and a single element could be substituted for the seventh

and eighth elements 3-54, 3-56.

5

10

15

20

25

The slope of the reflectivity profile of Fig. 39 about the working point P is proportional to the sensitivity of the DFES generated by the apparatus 3-10. Specifically, the sensitivity of the apparatus 3-10 to changes in the focus of the illuminating beam I is augmented by increases in the slope of the reflectivity profile. Accordingly, it is an object of the present invention to provide a prism 3-30 characterized by a reflectivity profile which is as steep as practically possible.

The shape of the reflectivity profile of Fig. 39 about the working point P may be altered by adjusting the thickness of the separation layer 3-38. For example, increasing the thickness of the separation layer 3-38 translates the angle of minimum reflectivity A_m towards the critical angle A_c (see Fig. 39) without affecting the value of the latter. It follows that increasing the separation layer thickness serves to increase the slope of the reflectivity profile in the vicinity of the working point P. Similarly, reducing the thickness of the separation layer 3-38 enlarges the angular displacement between the critical angle A_c and the angle of minimum reflectivity A_m . The shape of the reflectivity profile of the prism 3-30 may be varied in order to adjust the sensitivity of the DFES. A reasonable slope can be obtained, for example, by use of a separation layer having a thickness that is greater than one half of the wavelength of the illuminating beam I.

The value of the critical angle A_c may be adjusted by

varying the index of refraction of the separation layer 3-38 relative to that of the glass members 3-35, 3-36. Thus, adjustment of the separation layer thickness in conjunction with manipulation of the indices of refraction of the separation layer and surrounding glass members allows the prism 3-30 to be fabricated in accordance with a desired reflectivity profile.

5

10

15

20

25

Fig. 40 is a graph of the value of a normalized DFES (NDFES) generated by the apparatus 3-10 as a function of the deviation from the desired displacement of the objective lens 3-24 relative to the disc 3-14.

Again, the data in Fig. 40 was obtained by utilizing a prism 3-30 having a separation layer of index of refraction 1.38 and thickness 4.5 microns sandwiched between glass members of index of refraction 1.55, with the prism 3-30 being illuminated by a servo beam of wavelength 0.78 microns. As is shown in Fig. 40, the value of the DFES is preferably zero when the desired displacement exists between the objective lens 3-24 and the disc 3-14. The sign (+ or -) of the DFES is thus indicative of whether the displacement between the objective lens and disc surface exceeds or is less than that required for proper focusing. As mentioned above, the DFES may be used to control a mechanical arrangement (not shown) disposed to adjust the separation between the objective lens 3-24 and the disc 3-14. It may be appreciated that the slope of the NDFES is approximately 0.16 micron⁻¹ at the working point defined by 0 (zero) disc displacement.

Although the servo beam S has been represented herein to be

substantially collimated when incident on the separation layer 3-38, the present invention is not limited to configurations giving rise to collimated servo beams. When a convergent or divergent servo beam is utilized, inaccuracies in the focus position of the illuminating beam will alter the degree of convergence or divergence thereof. Those skilled in the art will appreciate that the focus sensing apparatus of the present invention may be utilized to generate a DFES in response to such changes in convergence or divergence.

The inventive focus sensing apparatus has thus been shown to overcome the disadvantages inherent in other focus detection systems by providing reflected and transmitted beams of substantially similar shape and intensity from which a high precision, altitude insensitive focus error signal may be differentially derived. The focus sensing technique disclosed herein nonetheless retains features present in certain related focus detection systems such as low sensitivity to mechanical vibration, decreased sensitivity to disc tilt, and increased thermal stability.

20 Seek Actuator

5

10

15

25

Fig. 41 schematically illustrates the operation of an exemplary optical read/write system 4-50 in reading data from a precise location 4-52 on an information storage medium, such as an optical disc 4-54. While the system 4-50 illustrated is a write-once or WORM system, those skilled in the art will recognize that the carriage and actuator assembly of the present



invention could also be used in magneto-optical erasable system. Information is transmitted to and read from the disc 4-54 utilizing a light beam 4-56 produced by a light source 4-58 which passes through a plurality of components including a cube-shaped beamsplitter 4-60 which separates the light beam 4-56 according to its polarization, a quarter wave plate 4-62 which changes the polarization of the light beam 4-56, a collimator lens 4-64, and an objective lens 4-66, which, in combination, direct the light beam 4-56 toward the desired location 4-52 on the disc 4-54.

5

10 In operation, the light source element 4-58, typically a laser diode, emits the light beam 4-56 toward the convex collimator lens 4-64. The collimator lens 4-64 converts this source beam 4-56 into a parallel, linearly S polarized light beam 4-70 and conducts the beam 4-70 toward the beamsplitter 4-60. 15 This cube-shaped beamsplitter 4-60 is formed by attaching two right angle prisms 4-72, 4-74 along their respective hypotenuses and includes a polarization sensitive coating forming a beamsplitting interface 4-76 between the two hypotenuses. The beamsplitter 4-60 separates and/or combines light beams of differing polarization states, namely linear S polarization and 20 linear P polarization. Separation is accomplished in conjunction with the polarization sensitive coating which transmits linearly P polarized light beams and reflects linearly polarized S light beams. Light exiting the beamsplitter 4-60 passes through the quarter wave plate 4-62 which converts the linearly polarized 25 light beam 4-70 to a circularly polarized light beam 4-78. Upon

exiting the quarter wave plate 4-62, the circularly polarized beam 4-78 enters an actuator 4-80.

5

10

15

20

25

The actuator 4-80 includes a mirror 4-82 which orthogonally reflects the light beam 4-78 upward toward the objective lens 4-66. This objective lens 4-66 converges the circularly polarized beam 4-78 to the precise focal point 4-52 on surface of the optical disc 4-54. Upon striking the disc 4-54, the circularly polarized light beam 4-78 is altered by the information stored on the disc 4-54 and is reflected as a divergent circularly polarized light beam 4-84 carrying information identical to that encoded on the disc 4-54. This reflected circularly polarized light beam 4-84 re-enters the objective lens 4-66 where it is collimated. The light beam 4-84 is again reflected from the mirror 4-82 and re-enters the quarter wave plate 4-62. Upon exiting the quarter wave plate 4-62, the circularly polarized beam 4-84 is converted to a linearly P polarized light beam 4-86. As linearly P polarized light beams are transmitted through the beamsplitter 4-60 without reflection at the splitting interface, this light beam 4-86 continues to a photodetector 4-88, which detects the data stored on the disc 4-54. In addition, if the light beam 4-86 falling on the photodetector 4-88 is out of focus or misaligned, the amount of misalignment or defocusing is measured electronically and used as feedback for a servo system (not shown) which properly realigns the objective lens 4-66.

Fig. 42 illustrates an electromagnetic carriage and actuator assembly 4-100 constructed in accordance with the present

invention. The assembly can be used with an optics module 4-102 to read and write data onto the surface of an optical disc as described above in connection with Fig. 41, wherein the light source 4-58, detector 4-88, collimating lens 4-64, quarter wave plate 4-62, and beamsplitter 4-60 are all incorporated within the module 4-102. A spindle motor 4-104 is located adjacent the assembly 4-100 and rotates an optical disc (not shown) about an axis of rotation A above the assembly 4-100. The assembly 4-100 includes a carriage 4-106 having first and second bearing surfaces 4-108, 4-110 slidably mounted on first and second guide rails 4-112, 4-114, respectively, and an actuator 4-116 which is mounted on the carriage 4-106. As will be appreciated, these rails 4-112, 4-114 provide a frame along which the carriage moves. A beam of light 4-120 emitted from the light source 4-58 in the optics module 4-102 enters the actuator 4-116 through a circular aperture 4-118 and is reflected by a mirror contained inside the actuator through an objective lens 4-122 defining an optical axis O to the surface of the disc. As will be appreciated, the axis of rotation A of the disc is parallel to the optical axis O of the objective lens 4-122.

5

10

15

20

25

The carriage 4-106 and actuator 4-116 carried thereon are moved horizontally along the rails 4-112, 4-114 in a tracking direction by a coarse tracking motor to access various information tracks on the surface of the disc. The tracking motor includes two permanent magnets 4-130, 4-132 wherein each magnet is attached to a C-shaped outer pole piece 4-134, 4-136,

respectively. Two inner pole pieces 4-138, 4-140 are positioned across the ends of the outer pole pieces 4-134, 4-136 so as to form a rectangular box around the permanent magnets 4-130, 4-132. Two coarse coils 4-142, 4-144 of equal length are affixed to the vertical plates 4-174, 4-176 (Fig. 43) and surround the inner pole pieces 4-138, 4-140 with sufficient clearance to move over the pole pieces 4-138, 4-140 when the carriage 4-106 is moved in the tracking direction. In this embodiment, these coarse coils 4-142, 4-144 are the only portion of the course tracking motor that are movable. As will be described in more detail below, the actuator 4-116 can also move the objective lens 4-122 closer to or farther away from the disc, thereby focusing the exiting light beam 4-120 upon the desired location on the surface of the disc.

5

10

15 Fig. 43 is an exploded view illustrating the carriage 4-106 and actuator 4-116 in greater detail. The carriage 4-106 includes a generally rectangular base 4-150 to which the actuator 4-116 is attached. The base 4-150 has a substantially flat top surface 4-152 having a generally rectangular chamber 4-154 formed
20 therein. The first bearing surface is cylindrical in shape, while the second bearing surface 4-110 consists of two elliptical bearing sections 4-160, 4-162 of approximately equal length which meet inside the base 4-150. The spacing of the rails 4-112, 4-114 relative to the optical axis 0 is selected such that each bearing surface 4-108, 4-110 is subjected to the same amount of preload. The bearing surfaces 4-108, 4-110 are further designed such that

both surfaces have substantially the same amount of surface area contacting the rails 4-112, 4-114. The length of the bearing sections comprising the second bearing surface is approximately equal to the length of the first bearing surface, although minor variations in length may be necessary to account for wear.

Two vertical walls 4-156, 4-158 extend upwardly from the top surface 4-152 of the base 4-150 adjacent the ends of the chamber 4-154. The base 4-150 further includes two platform regions 4-164, 4-166 formed at the ends of the base 4-150 above the bearing surfaces 4-108, 4-110. A step 4-168 joins the top surface 4-152 of the base 4-150 with the second platform region 4-166. A first U-shaped notch 4-170 is formed in the first platform region 4-164, and a second U-shaped notch 4-172 is formed in the second platform region 4-166 and step 4-168.

The coarse coils 4-142, 4-144 are attached to two vertical plates 4-174, 4-176 respectively. The plates 4-174, 4-176 are positioned in notches 4-180, 4-182 formed in the ends of the base 4-150. The base 4-150 further includes a mass balancing plate 4-184 which is attached to a bottom surface 4-186 of the base 4-150 via a screw 4-188, and a mass balancing projection 4-190 which extends outwardly from the base 4-150 adjacent the first coarse coil 4-142. A circular aperture 4-192 is formed in a front side 4-194 of the base 4-150 and receives the light beam 4-120 emitted from the optics module 4-102 (Fig. 42). A bracket 4-196 having a circular aperture 4-198 therein is positioned between the second vertical wall 4-158 and the first platform region

4-164 along the front side 4-194 of the base 4-150. The bracket 4-196 additionally includes a notch 4-200 which receives a photodetector 4-202 such that the photodetector 4-202 is positioned between the bracket 4-196 and the first platform region 4-164.

5

10

15

The actuator 4-116, often referred to as a "2-D" actuator for 2 degrees of motion, i.e. focussing and tracking, is mounted on the base 4-150 between the vertical walls 4-156, 4-158 and the platform regions 4-164, 4-166. A prism (not shown) is positioned within the chamber 4-154 in the base 4-150 to deflect the light beam 4-120 emitted from the optics module 4-102 such that the beam 4-120 exits the actuator 4-116 through the objective lens 4-122. The objective lens 4-122 is positioned within a lens holder 4-210 attached to a focus and fine tracking motor which moves the lens 4-122 so as to precisely align and focus the exiting beam 4-120 upon a desired location on the surface of the optical disc. The objective lens 4-122 defines an optical axis 0 which extends vertically through the center of the lens.

The components of the actuator 4-116 are best seen in Fig.

44. The lens holder 4-210 is generally rectangular in shape and includes a generally rectangular opening 4-212 formed therethrough. A top surface 4-214 of the lens holder 4-210 includes a circular collar 4-216 positioned between two shoulders 4-218, 4-220. A circular aperture 4-222 having a diameter substantially equal to that of the collar 4-216 is formed in a bottom surface 4-224 of the lens holder. A rectangular focus coil

4-230 is positioned within the rectangular opening 4-212 in the lens holder 4-210. Two oval-shaped, fine tracking coils 4-232, 4-234, are positioned at the corners of a first end 4-240 of the focus coil 4-230, and two more identical tracking coils 4-236, 4-238 are positioned at the corners of a second end 4-242 of the focus coil 4-230. A first pair of U-shaped pole pieces 4-244 is positioned to surround the first end 4-240 of the focus coil 4-230 and tracking coils 4-232, 4-234 attached thereto, while a second pair of U-shaped pole pieces 4-246 surrounds the second end 4-242 of the focus coil 4-230 and tracking coils 4-236, 4-238 attached thereto. In addition, two permanent magnets 4-250, 4-252 are positioned between the pole piece pairs 4-244, 4-246, adjacent the tracking coils 4-232, 4-234; 4-236, 4-238 respectively.

5

10

Two top flexure arms 4-260, 4-262 are attached to the top surface 4-214 of the lens holder 4-210 while two additional bottom flexure arms 4-264, 4-266 are attached to a bottom surface of the lens holder 4-210. Each flexure arm preferably consists of a thin sheet of etched or stamped metal (typically steel or beryllium copper) with a thickness in the order of 25 micrometers to 75 micrometers. For simplicity, only the flexure arm 4-260 will be described, however, it should be noted that the remaining flexure arms 4-262, 4-264, 4-266 are of identical structure. The flexure arm 4-260 includes a first vertical section 4-270 attached to first, second and third horizontal sections 4-272, 4-274, 4-276. The third horizontal section 4-276 is further

attached to a perpendicular crossbar 4-280. The first horizontal section includes a shoulder 4-272 which attaches to the corresponding shoulder 4-218 on the lens holder 4-210. Further, the shoulder of the second top flexure arm 4-262 attaches to the corresponding shoulder 4-220, while the shoulders of the bottom flexure arms 4-264, 4-266 attach to similar structures on the bottom surface of the lens holder 4-210.

5

10

15

20

25

The flexures 4-260, 4-262, 4-264, 4-266 are further attached to a support member 4-290. The support member 4-290 includes a central notch 4-292 which receives the second pair of pole pieces 4-246. A ledge 4-294 is formed on each side of the notch 4-292 on the top and bottom surfaces of the support member 4-290. The crossbar sections 4-280 of the flexure arms 4-260, 4-262 are attached to these ledges 4-294, while flexure arms 4-264, 4-266 are connected to corresponding ledges on the bottom of the support member 4-290 so as to cooperatively suspend the lens holder 4-210 from the support member 4-290. The support member 4-290 further includes an aperture 4-296 for receiving a light emitting diode 4-300. The diode 4-300 is in alignment with the aperture 4-198 in the bracket 4-196 (Fig. 43) and photodetector 4-202 positioned within the notch 4-200 in the bracket, such that when the light emitting diode 4-300 is energized, substantially collimated light is emitted through the aperture 4-198 in the bracket 4-196 and is incident upon the photodetector 4-202. Depending on the position of the lens holder 4-210 with respect to the support member 4-290, light emitted by the diode 4-300

will fall onto various portions of the detector 4-202. By analyzing the amount of light incident upon the detector 4-202, a position correction signal can be generated to determine the amount of displacement required for precise focusing and tracking at the desired location on the surface of the disc.

In the illustrated embodiment, the fine motor mass consists of the lens holder 4-210, the objective lens 4-122, the focus coil 4-230, and the fine tracking coils 4-232, 4-234, 4-236 and 4-238. The carriage mass consists of the base 4-150, course tracking coils 4-142 and 4-144, the bracket 4-196, and photodetector 4-202, the support member 4-290, the vertical plates 4-174 and 4-176, the mass balancing plate 4-184 and screw 4-188, the permanent magnets 4-250 and 4-252, the pole pieces 4-244 and 4-246, and the bearing surfaces 4-108 and 4-110.

With reference to the above description in connection with FIGS. 43 and 44, the coarse tracking coils 4-142, 4-144 have equal dimensions and are symmetric about optical axis 0 of the objective lens. Further, the tracking coil pairs 4-232, 4-234 and 4-236, 4-238 have equal dimensions and are symmetric about optical axis 0 of the lens 4-122. The dimensions of the mass balance plate 4-184 and mass balance projection 4-190 are advantageously selected to compensate for the mass of the support member 4-290, flexures 4-260, 4-262, 4-264, 4-266, bearing surfaces 4-108, 4-110, bracket 4-196 and photodetector 4-202, such that the center of mass of the carriage and the center of mass of the fine and focus drives (consisting of the pole pieces

4-244, 4-246, the permanent magnets 4-250, 4-252, the focus coil 4-230, and tracking coils 4-232, 4-234, 4-236, 4-238) are generally intersected by the optical axis O of the lens 4-122. As will be described in more detail below, alignment of these centers of gravity with the optical axis O of the lens 4-122, and the symmetry of the motor forces and reaction forces acting on the carriage 4-106 and actuator 4-116 ensure that undesirable modes of motion which adversely affect position of the objective lens 4-122 are minimized.

5

10

15

20

25

Referring to Fig. 45, the permanent magnets 4-130, 4-132 adjacent the coarse tracking coils 4-142, 4-144 generate a magnetic field B whose lines of flux extend inwardly toward the coarse coils 4-142, 4-144. When coarse tracking movement is required to position the objective lens 4-122 beneath a selected track on the optical disc, current is applied to the coarse tracking coils 4-142, 4-144. The current interacts with the magnetic field B to produce forces which move the carriage 4-106 in the tracking direction. The forces are generated according to the Lorentz law F=BXI1, wherein F represents the force acting on the focus coil, B represents the magnetic flux density of the magnetic field between the two permanent magnets, I represents the current through the focus coil, and 1 represents the length of the coil. For example, when the current I applied to the first coarse tracking coil 4-142 travels through the portion of the coil positioned within the magnetic field B in the direction into the plane of the figure, a force F_{Coarsel} in the direction of the

arrow 4-320 is produced. Similarly, when current I travels through the portions of the second tracking coil 4-144 positioned within the magnetic field B in the direction out of the plane of the figure, a force F_{Coarse2} in the direction of the arrow 4-322 is produced. The forces F_{Coarse1} and F_{Coarse2} act to move the carriage 4-106 horizontally to the left.

Conversely, Fig. 46 shows that if the direction of the current I within the portions of the tracking coils 4-142, 4-144 within the magnetic field B is reversed, forces F_{coarsel} ', and F_{coarse2} ', are produced which act to move the carriage into the plane of the figure (to the right in Fig. 45). The amount of movement in the tracking direction depends on the amount of current applied to the coarse coils 4-142, 4-144. In this manner, the carriage 4-106 is moved to position the objective lens 4-122 such that the laser beam 4-120 exiting the lens 4-122 is focused within a desired information track on the surface of the optical disc.

When a control signal is generated by the optics module 4-102, a given current is applied to either the fine tracking coils 4-232, 4-234, 4-236, 4-238, or the focus coil 4-230 depending on the direction in which the displacement of the lens holder 4-210 and objective lens 4-122 attached thereto is required. Such servo system and feedback circuits which control the amount of current are well known in the art. This current interacts with the electromagnetic field produced by the permanent magnets 4-250, 4-252 to create a force which displaces

the lens holder 4-210 and the objective lens 4-122 attached thereto in the appropriate tracking or focussing direction. For example, if re-positioning is desired in the focus direction, according to a focus error signal, this signal is transmitted to a servo amplifier (not shown), which generates a current through the focus coil 4-230. As described above, a force is generated according to the Lorentz law F=BXI1.

5

10

15

20

25

Referring to Fig. 47, the permanent magnets 4-250, 4-252 of the 2-D actuator 4-116 are oriented such that the south poles of each magnet 4-250, 4-252 face the lens holder 4-210. In this configuration, a magnetic field B is formed whose lines of flux originate at the magnets 4-250, 4-252 and are directed inwardly toward the lens holder 4-210 as shown. When a current I is applied to the focus coil 4-230 and travels through the portions of the coil 4-230 positioned within the magnetic field B in the direction shown, an upward force F_{Focus} is generated at each section of the focus coil 4-230 which is translated to the flexure arms 4-260, 4-262, 4-264, 4-266, bending the flexure arms to move the lens holder 4-210 and associated objective lens 4-122 closer to the optical disc. Conversely, when the current I is run through the coil sections in the opposite directions as those illustrated, a downward force is generated which acts on the flexures to move the lens holder 4-210 and objective lens 4-122 farther away from the surface of the optical disc. The magnitude of the displacement is dependent upon the amount of current applied to the focus coil 4-230. By moving the objective lens

4-122 closer to or farther away from the surface of the optical disc, the focus coil 4-230 acts to precisely focus the laser beam 4-120 exiting the objective lens 4-122 within the desired information track on the disc.

5

10

15

20

25

As shown in Fig. 48, movement of the actuator 4-116 to effect fine tracking is produced when current is generated in the four fine tracking coils 4-232, 4-234, 4-236. 4-238 affixed to the focus coil 4-230. When current is applied to the tracking coils in the directions shown through the portions of the tracking coils positioned within the magnetic field B, forces F_{Track} are produced which move the lens holder 4-210 to the right. When the forces F_{Track} act on the tracking coils 4-232, 4-234, 4-236, 4-238, they are translated through the focus coil 4-230 and lens holder 4-210 to the flexures 4-260, 4-262, 4-264, 4-268 which bend in the corresponding direction and the objective lens 4-122 is moved in the direction of the forces, to the right in Fig. 48. When current travels through the tracking coils 4-232, 4-234, 4-236, 4-238 in the opposite direction, a force is generated which acts to move the lens holder 4-210 to the left. The amount of current applied to the fine tracking coils 4-232, 4-234, 4-236, 4-238 is relatively small in comparison with the amount applied to the coarse tracking coils 4-242, 4-244, and the dimensions of the fine tracking coils much smaller than the coarse coils to increase resonance frequencies and thus enable higher servo bandwidths which can then control to tighter track errors.

FIGS. 49-56 are schematic diagrams of the actuator and carriage assembly 4-100 which illustrate the symmetry and balancing of forces achieved with the design of the present invention.

5

10

15

20

25

FIG. 49a is a schematic diagram illustrating the symmetry of coarse or carriage motor forces acting on the actuator 4-116 in the horizonal plane. When current is applied to the coarse tracking coils 4-142, 4-144 as described above, forces F_{Coarsel} and F_{Coarse2} are produced which are centered within the portion of the coarse coils 4-142, 4-144 located adjacent the permanent magnets 4-130, 4-132, respectively. The dimensions of the first coarse coil 4-142 are selected to equal the dimensions of the second coarse coil 4-144, and the current applied to each coil is the same, such that the forces F_{Coarse1} and F_{Coarse2} acting on the coils are equal. Further, the coarse coils 4-142, 4-144 are positioned at equal distances L_{c1} and L_{c2} from the objective lens 4-122 such that the resulting moments about the optical axis O of the objective lens 4-122 are equal, and the carriage yaw is minimized. In FIG. 49b, the centers of the coarse motor forces F_{Coarsel} and F_{Coarse2} are illustrated in the vertical plane. Because the forces F_{Coarsel} and F_{Coarse2} are vertically aligned with the center of mass of the carriage CM_c (i.e., are generally intersected by a line orthogonal to the radial direction and the optical axis O containing the center of mass of the carriage CM_c), the moments about the horizontal axis are equal, and carriage pitch which can cause the prism to deflect the beam

angle, thereby introducing track offset, is reduced.

5

10

15

20

25

The fine tracking motor forces in the horizontal and vertical planes are illustrated in FIGS. 50a and 50b. The forces F_{Track1} and F_{Track2} produced by the energization of the fine tracking coils 4-232, 4-234, 4-236, 4-238 within the magnetic field induced by the permanent magnets 4-250, 4-252 are centered between the pairs of fine tracking coils 4-232, 4-234 and 4-236, 4-238, and extend horizontally in the tracking direction. The dimensions of the coils are equal and the amount of current applied to the coils is equal as well, such that the magnitude of the resulting forces F_{Track1} and F_{Track2} is equal. Additionally, the fine tracking coils 4-232, 4-234, 4-236, 4-238 are positioned at equal distances $L_{\scriptscriptstyle T}$ from the optical axis O of the objective lens 4-122, and thus, the moments produced about the optical axis O are equal, such that yaw of the lens holder 4-210 and lens 4-122 carried thereon about the vertical axis is decreased. As illustrated in FIG. 50b, the resultant fine tracking force F_{Track} acts on the center of mass of the fine motor mass CM, such that lens holder pitch is minimized.

FIG. 51a illustrates the reaction forces F_{React1} and F_{React2} resulting from the fine tracking motor which act upon the carriage 4-106 in opposition to the fine tracking motor forces F_{Track1} and F_{Track2} illustrated in FIG. 50a. These reaction forces F_{React1} and F_{React2} act on the pole pieces 4-244, 4-246 positioned over the tracking coils 4-232, 4-234, 4-236, 4-238 on each side of the lens holder 4-210. As described above, the magnitude of

the tracking forces F_{Track1} and F_{Track2} is equal. Further, the dimensions of the pole pieces 4-244, 4-246 are equal, such that the reaction forces F_{React1} and F_{React2} produced are equal. Because the pole pieces 4-244, 4-246 are positioned at equal distances L_R from the optical axis O of the lens 4-122, the moments about the optical axis O are equal in magnitude, reducing rotation about the vertical axis, or yaw. FIG. 51b illustrates the resultant reaction force F_{React} in the vertical plane. As shown, the reaction force F_{React} acts at the center of mass of the fine motor mass CM_F , at a distance L_{RM} above the center of mass of the carriage mass CM_C , and thus a moment will act on the carriage 4-106, however, because the distance L_{RM} and the reaction forces F_{React1} and F_{React2} are fairly small, this moment is relatively small and does not significantly affect carriage performance.

The resultant focus forces F_{Focus1} and F_{Focus2} acting on the 2-D actuator 4-116 are illustrated in FIG. 52a. The focus forces F_{Focus1} and F_{Focus2} are centered in the portions of the focus coil 4-230 located between the tracking coils 4-232, 4-234, 4-236, 4-238 and pole pieces 4-244, 4-246, adjacent the permanent magnets 4-250, 4-252. The focus coil 4-230 is wound within the opening 4-212 in the lens holder 4-210 (Fig. 44) such that the same amount of current flows through each side of the coil 4-230 adjacent the magnets, thus producing equal forces F_{Focus1} and F_{Focus2} at the sides of the lens holder 4-210 which act to move the lens holder and objective lens 4-122 carried thereon in a vertical direction. The coil is positioned symmetrically within the

opening 4-212 in the lens holder 4-210 such that the centers of the forces F_{Focus1} and F_{Focus2} produced are positioned equidistantly at distances L_F from the optical axis O of the objective lens 4-122. In this configuration, the moments produced about the optical axis O of the lens 4-122 are equal, reducing roll of the lens holder 4-210. Additionally, as illustrated in FIG. 52b, when viewed from the end of the carriage, the focus forces F_{Focus1} and F_{Focus2} (F_{Focus} in the drawing) are aligned with the center of mass CM_C of the carriage mass, thereby reducing pitch of the carriage 4-106.

The reaction forces F_{Focus1} and F_{Focus2} produced in response to the focus forces F_{Focus1} and F_{Focus2} shown in FIG. 52a are illustrated in the horizontal plane in FIG. 53a. The reaction forces F_{FR1} and F_{FR2} are equal in magnitude and opposite in direction to the focus forces F_{Focus1} and F_{Focus2} and are centered adjacent the fine motor permanent magnets 4-250, 4-252 intermediate the pole pieces 4-244, 4-246. As described above, the focus forces F_{Focus1} and F_{Focus2} are equal, and thus, the reaction forces F_{FR1} and F_{FR2} are equal as well. Further, the reactions forces F_{FR1} and F_{FR2} act at equal distances L_{FR} from the optical axis 0 of the objective lens 4-122 to further reduce pitch. Additionally, as illustrated in FIG. 53b, when viewed from the end of the carriage 4-106, the reaction forces F_{FR1} and F_{FR2} (F_{FR} in the drawing) are aligned with the center of mass CM_C of the carriage mass, thereby reducing pitch of the carriage.

The forces F_{Flex1} and F_{Flex2} generated by the flexure arms

4-260, 4-262, 4-264, 4-266 on the lens holder 4-210 are illustrated in Fig. 54. The forces F_{Flex1} and F_{Flex2} illustrated are those acting on the upper flexure arms 4-260, 4-262, however, those skilled in the art will recognize that identical forces act on the lower flexure arms 4-264, 4-266, as well. The forces F_{Flex1} and F_{Flex2} acting on the upper flexure arms 4-260, 4-262, respectively, are centered at the crossbar sections 4-280 of the flexure arms 4-260, 4-262 where the flexure arms are attached to the support member 4-290. As previously described, when these forces F_{Flex1} and F_{Flex2} act on the flexure arms 4-260, 4-262, the flexure arms bend in the appropriate direction to achieve fine tracking. To maintain the flexure arms 4-260, 4-262 in their bent condition, the fine motor generates reaction forces F_{RA} and F_{RB} which are centered at the pole pieces 4-244, 4-246 on either side of the lens holder 4-210. As shown, the flexure forces F_{Flex1} and F_{Flex2} act a distance L_{Flex} from the optical axis 0 of the focus lens 4-122, while the reaction forces F_{RA} and F_{RB} act distances L_{RA} and L_{RB} from the optical axis O, respectively. It will be apparent to those skilled in the art that the moments produced about the optical axis O of the lens 4-122 by the pairs of forces are not equal, since $(F_{Flex1} + F_{Flex2})$ does not equal $(F_{RA} \perp_{RA} + F_{RB} \perp_{RB})$. However, since these forces are effectively decoupled from the carriage except at very low frequencies (typically below around 40 hz), these forces do not affect actuator performance at most normal operating conditions.

5

10

15

20

25

As described above, the carriage 4-106 includes two bearing

surfaces 4-108, 4-110 which are slidably mounted on the guide rails 4-112, 4-114 in order to position the carriage 4-106 beneath various data tracks on the optical disc. In essence, the bearings 4-108, 4-110 act as "springs" which hold the carriage 4-106 above the rails 4-112, 4-114. The bearing "spring" stiffness forces $F_{Bearing1}$ and $F_{Bearing2}$ are illustrated in FIG. 55a. The forces $F_{ exttt{Bearing1}}$ and $F_{ exttt{Bearing2}}$ are centered at the point of contact between the bearing surfaces 4-108, 4-110 and the rails 4-112, 4-114 and extend downwardly through the center of the rails. As described above, the surface contact area between the bearing surface 4-108 and rail 4-112 is approximately equal to the surface contact area between the bearing surface 4-110 and rail 4-114, and thus these stiffness forces F_{Bearing1} and F_{bearing2} are substantially equal. Further, the bearing surfaces 4-108, 4-110 are positioned at equal distances L_{Bearing} from the optical axis O of the lens 4-122 so that the moments about the optical axis O produced by these forces $F_{bearing1}$ and $F_{bearing2}$ are equal, minimizing carriage yaw. Referring to FIG. 55b, in the vertical plane, the net carriage suspension force $F_{Bearing}$ acts at a point directly between the two bearings and aligned with the optical axis O.

5

10

15

20

25

The friction forces $F_{\text{Friction1A}}$, $F_{\text{Friction1B}}$, and $F_{\text{Friction2}}$ acting on the bearing surfaces 4-108, 4-110 and rails 4-112, 4-114 are illustrated in FIG. 56a. As the first bearing surface 4-108 comprises two sections 4-160, 4-162, two friction forces $F_{\text{Friction1A}}$ and $F_{\text{Friction1B}}$ are present, one associated with each bearing section 4-160, 4-162, respectively, which are centered at the middle of

the bearings along the area of contact with the rail 4-114. A second friction force $F_{\text{Friction2}}$ acts on the second bearing surface 4-108 and is centered in the middle of the bearing along its contact with the rail 4-112 as shown. Because the area of contact of the bearing sections 4-160, 4-162 forming the first bearing surface 4-110 substantially equals the area of contact of the second bearing surface 4-108, and the amount of pre-loading and coefficient of friction is the same for both bearing surfaces, the sum of the friction forces $F_{\text{Friction1A}}$ and $F_{\text{Friction1B}}$ equals the friction force $F_{Friction2}$. The bearing surfaces 4-112, 4-114 are located at equal distances $L_{\scriptscriptstyle F}$ from the optical axis O of the focus lens 4-122, and the resulting moments about the optical axis of the lens are then equal as well. In the vertical plane, the forces $F_{\text{Friction1A}}$, $F_{\text{Friction1B}}$, and $F_{\text{Friction2}}$, act at the areas of contact between the rails 4-112, 4-114 and the bearing surfaces 4-108, 4-110, as shown in FIG. 56b which are advantageously designed to be horizontally aligned with the center of mass of the carriage mass CM_c , such that moments about the center of mass which can produce carriage pitch are reduced.

5

10

15

20

25

FIGS. 57 through 60 illustrate the inertial forces acting on the carriage 4-106 and 2-D actuator 4-116 for both vertical and horizontal accelerations. The inertial forces acting on the fine motor and carriage in response to a vertical acceleration of the assembly are shown in Fig. 57. A first downward inertial force $F_{\rm IF}$ equal to the mass of the fine motor multiplied by the acceleration acts at the center of mass of the fine motor mass

 ${\rm CM_F}$. A second downward inertial force ${\rm F_{IC}}$ acts at the center of mass of the carriage mass ${\rm CM_C}$ and is equal to the mass of the carriage multiplied by the acceleration. FIGS. 58a and 58b further illustrate that the inertial forces ${\rm F_{IF}}$ and ${\rm F_{IC}}$ are horizontally aligned with the optical axis 0 of the objective lens 4-122.

5

10

15

20

25

FIG. 59a illustrates the inertial forces acting on the coarse coils 4-142, 4-144 and fine motor pole pieces 4-244, 4-246 for horizontal accelerations of the carriage and fine motor, respectively. An inertial force F_{IC1} acts at the center of upper portion of the first coarse coil 4-142 and an inertial force F_{IC} acts at the center of the upper portion of the second coarse coil 4-144. As described above, the coils 4-142, 4-144 are of identical dimensions, such that the mass of the first coil 4-142 equals the mass of the second coil 4-144. The magnitude of each force F_{IC1} , F_{IC2} is equal to mass of the respective coil multiplied by the acceleration, and thus, the inertial forces acting on the coils 4-142, 4-144 are equal. Because the coils 4-142, 4-144 are positioned at equal distances L_{c} from the optical axis O of the objective lens 4-122, the resulting moments about the optical axis of the lens produced by the inertial forces F_{ICl} and F_{IC2} are equal. Similarly, because the fine motor pole pieces 4-244, 4-246 are of equal dimensions and are located at equal distances L_p from the optical axis O, the inertial forces F_{IP1} and F_{IP2} acting on the pole pieces are equivalent, and the resulting moments about the optical axis O of the objective lens 4-122 are equal.

Applying this same analysis to all other components or "subparts" of the carriage and actuator assembly, and as will be explained in more detail below, the inertial forces produced by horizontal and vertical accelerations above the resonance frequency of the flexure arms are balanced and symmetric with respect to the optical axis 0. The net inertial forces of the fine motor and carriage $F_{\rm IF}$ and $F_{\rm IC}$ for acting on the assembly for horizontal accelerations thus act along a line through the center of the carriage which intersects the optical axis 0 as shown in FIG. 59b. The net inertial force due to the coarse motor $F_{\rm IC}$ is equal to the mass of the coarse motor multiplied by the acceleration, while the net inertial force due to the fine motor $F_{\rm IF}$ is equal to the mass of the fine motor multiplied by the acceleration.

At high frequencies, i.e., accelerations in the tracking direction above the lens holder--flexure arm resonance frequency, approximately 40 Hz, components of the assembly 4-100 decouple and do not affect the position of the objective lens 4-122. Consequently, the inertial forces differ for accelerations above and below the flexure arm resonance frequency. The inertial forces for horizontal accelerations at these high frequencies are illustrated in FIG. 60a. At these high frequencies, the actuator 4-116 is decoupled from the carriage 4-106, such that a first inertial force F_{11} equal to the mass of the fine motor multiplied by the acceleration acts at the center of mass of the fine motor mass CM_F , and a second inertial force F_{12} equal to the mass of the coarse motor multiplied by the acceleration is centered at the

center of mass of the carriage mass CMc.

FIG. 60b illustrates the inertial forces at horizontal accelerations below the flexure arm resonance frequency. At these lower frequencies, the fine motor mass and carriage mass move as a unit which has a net center of mass at CM_c '. As illustrated, this net center of mass CM_c ' is located at a distance x vertically above the center of mass of the carriage mass CM_c , and thus the coarse motor forces $F_{Coarse1}$ and $F_{Coarse2}$, and the friction forces $F_{Friction1}$ and $F_{Friction2}$, are no longer aligned with the carriage mass center of mass, now shifted to CM_c '. Although this vertical shift in the carriage center of mass occurs, the symmetrical design of the assembly 4-100 ensures that the center of mass of the carriage mass CM_c does not shift in the horizontal plane, and the forces acting on the carriage remain symmetrical about the center of mass and optical axis 0 in spite of the vertical shift in the center of mass from CM_c to CM_c '.

Further, the symmetry of the design ensures that horizontal shifting of the center of mass $CM_{\rm c}$ does not occur when subparts or components of the carriage decouple at high frequencies. For example, at frequencies in the KHz range, the fine motor poles pieces 4-244, 4-246 and magnets 4-250, 4-252 will decouple, however, due to the symmetry of the design, the center of mass will not shift in the horizontal plane. Because there is no shift of the center of mass $CM_{\rm c}$ in the horizontal plane, reaction forces of the focus motor will not pitch or roll the carriage at frequencies above those where subparts have come "loose". Thus,

by horizontally aligning the center of mass with the optical axis O of the objective lens 4-122, the lens sits "in the eye of the storm", where its position is minimally affected by resonance, motor, and reaction forces acting on the assembly 4-100.

5

10

15

20

25

FIGS. 61a illustrates the Bode transfer diagram of fine tracking position versus fine motor current of the actuator 4-116 of the present invention for an objective lens of 0.24 grams suspended in a fine motor having a mass of 1.9 grams. As illustrated, the actuator exhibits almost ideal dB curve having an approximate 40 dB/decade slope and an ideal phase shift curve. FIG. 61b illustrates the same transfer function when the lens is off centered in the horizontal or tracking direction by 0.15 mm. Both the dB and phase shift curves reveal a disturbance, or glitch, which occurs at approximately 3.2 kHz. The phase margin dips approximately 25 degrees, reducing loop damping and increasing settling time and overshoot. In terms of lens positioning, the horizontal shift in lens position disturbs the symmetry or balance of the fine tracking forces acting on the lens and results in a moment about the optical axis of the lens, resulting in yaw. Thus, it can be seen that the balancing of forces in the assembly 4-100 about the optical axis O of the objective lens 4-122 markedly improves tracking position.

Fig. 62 illustrates the effects of asymmetrical focus forces acting on the assembly 4-100. FIG. 62a illustrates the tracking signal while crossing tracks for a track pitch of 1.5 um, wherein each sine wave corresponds to an information track on the surface

of the optical disc. In FIG. 62b, the focus force is centered with the center of mass of the fine motor $CM_{\scriptscriptstyle F}$ and the optical axis O. The top trace shows the current applied to the focus coil during the step, while the bottom trace shows the tracking error signal while following a particular track, for a focus current of 0.1 Amp, and a focus acceleration of 0.75 m/s^2 . As illustrated, the tracking error signal remains virtually unaffected by the focus current level. FIG. 62c shows the effect on the current and tracking error signals as in FIG. 62b when the focus force is shifted out of alignment with the optical axis O and center of mass $CM_{\scriptscriptstyle F}$ by approximately 0.2 mm. The tracking signal is now visibly affected by the focus current. With the same focus current and acceleration, a tracking offset of 0.022 um results. Typically, the total allowable track offset in an optical drive is in the range of 0.05 um to 0.1 um, and thus, by aligning the forces as in FIG. 62b, the tracking offset is significantly reduced.

5

10

15

20

25

An alternative embodiment of a carriage and actuator assembly 400 in which the center of mass of the 2-D actuator coincides with the center of mass of the carriage mass is illustrated in Fig. 63. In addition to being substantially symmetrical about the optical axis of the objective lens, the center of mass of the fine motor mass coincides with the center of mass of the carriage mass and is aligned with the optical axis. The carriage and actuator assembly 4-100 of the first embodiment is adequate for most frequency ranges, however, the

assembly 400 of the alternative embodiment may be used in applications where it is desirable to avoid the shift in the center of mass of the carriage mass at frequencies below the flexure arm resonance frequency.

The assembly includes a carriage having first and second bearing surfaces substantially identical to those in assembly 4-100 which can be slidably mounted on guide rails (not shown), and a 2-D actuator which is mounted within the carriage. The carriage includes a pair of coarse tracking coils positioned within notches formed in the carriage, adjacent the bearing surfaces, which act to move the carriage horizontally in a tracking direction to access various information tracks on the surface of an optical disc.

The actuator includes a lens holder having an objective lens mounted thereon. A pair of ledges formed on the top surface of the carriage support a pair of top flexure arms which are further attached to the top surfaces of a pair of projections formed on the lens holder. A pair of bottom flexure arms which are identical in structure to the top flexure arms are supported by corresponding ledges in the bottom of the carriage (not shown), and attach to the bottom surfaces of the projections on the lens holder. A beam of light enters the actuator through a oval aperture and is reflected by a mirror contained inside the actuator through the objective lens along an optical axis O'. The actuator is further attached to a focus and fine tracking motor which moves the lens so as to precisely align and focus the

exiting beam upon a desired location on the surface of the optical disc. The focus and fine tracking motor includes two permanent magnets affixed to opposing ends of the lens holder. An oval-shaped fine tracking coil is affixed to each permanent magnet, adjacent the carriage bearings. Two focus coils are attached to the top and bottom surfaces of the carriage and supported by ledges formed within the interior of the carriage such that the lens holder is positioned between the focus coils.

Coarse tracking movement of the carriage and actuator is effected in a manner identical to that of the assembly 4-100 illustrated in FIGS. 46 and 47. When a current is applied to the coarse tracking coils in the presence of a magnetic field, a force is generated according to Lorentz law which acts to move the carriage and actuator in a tracking directions so as to position the objective lens beneath various information tracks on the optical disc.

Fig. 64 illustrates the operation of the actuator to move the lens holder and objective lens carried thereon in a focussing direction. When a current is generated in the focus coils, an electromagnetic field is induced in each of the coils. This electromagnetic field differs in direction for the respective focussing coils as shown. In the example shown, both permanent magnets will be attracted by the bottom focus coil and repelled by the top focus coil, thus moving the objective lens holder toward the bottom focus coil and away from the top focus coil to position the objective lens farther away from the surface of the

optical disc, wherein the magnitude of the displacement depends on the strength of the induced electromagnetic field.

In a similar manner, Fig. 65 illustrates the permanent magnets interacting with the fine tracking coils. Energization of the tracking coils moves the lens holder horizontally in the tracking direction to the right or to the left depending upon the direction of current through the coils. For example, in the presence of the magnetic field illustrated, the lens holder and objective lens are moved towards the left. In this manner, the fine tracking coils act to more precisely position the light beam exiting the objective lens within the center of a desired information track on the optical disc.

As described above, the coarse tracking motor operates in a manner identical to that of the coarse tracking motor in the assembly 4-100. The coarse tracking coils are of identical dimensions and are positioned at equal distances from the optical axis O' of the objective lens. Equal currents are applied to the coils such that forces F_{Coarsel} ' and F_{Coarse2} ' acting on the carriage act at equal distances L_{Cl} ' and L_{C2} ' from the optical axis O'. In the vertical plane, in the radial direction, these forces F_{Coarsel} ' and F_{Coarse2} ' are aligned with the coincident centers of gravity of the fine motor mass CM_F ' and carriage mass CM_C ', thereby minimizing carriage and actuator pitch. In a similar manner, the bearing surfaces are positioned at equal distances from the optical axis O' such that the carriage suspension forces are also symmetric about the optical axis O'. Each force F_{bearing1} and F_{bearing2}

acts an equal distance $L_{Bearing1}$ ' from the optical axis O' such that the moments produced about the optical axis are equal and carriage and actuator pitch is further reduced. The surface area of the bearings which contacts the rails is designed to be substantially equal such that the friction forces acting on the carriage are substantially equal. Since the bearing surfaces are positioned equidistantly from the optical axis O', the moments acting about the optical axis are equal and carriage and actuator is minimized. The assembly is further designed such that the friction forces are vertically aligned with the center of mass of the carriage and actuator.

The fine tracking coils are of equal dimensions and the current applied to the coils is equal such that the fine tracking forces acting on the actuator are equal. Further, the fine tracking coils are positioned at equal distances L_T ' from the optical axis 0' such that the moments produced about this axis are equal. In the vertical plane, these forces F_{Track1} ' and F_{Track2} ' are also aligned with the centers of gravity of the actuator and carriage, such that pitch of the actuator is reduced. Since the fine tracking forces acting on the assembly are equal, it follows that the reaction forces F_{React1} ' and F_{React2} ' produced in response to the tracking forces F_{Track1} ' and F_{Track2} ' are equal as well. These reaction forces act at equal distances L_R ' from the optical axis and are vertically aligned with the centers of gravity, such that moments about the optical axis are equal and yaw is reduced.

In a similar manner, the focus coils have substantially

equal dimensions and current applied to them such that the focus coils produce equal forces F_{Focus1} and F_{Focus2} ' acting on the actuator. However, in this embodiment, the focus coils are located at equal distances L_F ' from the coincident centers of gravity of the fine motor mass and carriage mass such that the moments about the optical axis O' are equal. Further, because the focus forces F_{Focus1} and F_{Focus2} ' are equal, the focus reaction forces F_{FR1} ' and F_{FR2} ' acting on the fine motor mass are equal and act at equal distances L_{FR} ' from the coincident centers of gravity of the carriage mass CM_C ' and fine motor mass CM_F '. Thus, moments produced by the reaction forces about the optical axis are equal and actuator pitch is further minimized.

The flexure forces F_{Flex1} ', F_{Flex2} ', acting on the actuator and fine motor reaction forces F_{RA} ', F_{RB} ', produced in response to the flexure forces are effectively the same as those illustrated in Fig. 54 for the assembly 4-100. Because the flexure and reactions forces are not symmetrical about the optical axis O', the moments produced by these pairs of forces about the axis O' are not equal, however, these forces are effectively decoupled from the carriage except at low frequencies (typically below around 40 Hz), such that these moments do not affect actuator performance under most operating conditions.

Thus, the motor and reaction forces acting on the assembly 400 are symmetric about the optical axis O' and are vertically in alignment with the centers of gravity of the fine motor mass CM_F ' and carriage mass CM_C '. Because the centers of gravity of the

fine motor mass and carriage mass coincide, decoupling of the actuator or any of the subparts of the assembly will not shift the center of mass, and the forces and moments acting on the assembly will remain balanced for virtually all horizontal and vertical accelerations.

Anamorphic, Achromatic Prism System.

5

10

15

20

25

Fig. 66 depicts a prior art optical system 5-100 having a light source 5-102, which provides an incident light beam 5-106 depicted in dashed lines, a simple anamorphic prism 5-108, a focussing lens 5-110, and optical media 5-112. The light beam 5-106 enters the prism 5-108 at an incidence angle 5-114 with respect to the normal to the entrance face 5-116 of the prism.

Laser light sources usually generate an elliptical beam with some astigmatism, as is well understood in the art. The anamorphic prism 5-108 provides expansion along the minor axis of the ellipse to correct for beam ellipticity. The angle of incidence 5-114 is selected to provide the desired expansion along the minor axis. The anamorphic prism 5-108 can also correct astigmatism in the incident light beam. The lens 5-110 focusses a resulting corrected beam 5-118 to form a spot 5-120 on the optical media 5-112.

The simple prism 5-108 is adequate as long as the wavelength of the incident light beam 5-106 remains constant. However, in practice, light sources typically change wavelength due to temperature changes, power shifts, random "mode hopping" and other conditions, as is well known in the art. In magneto-optic

disc systems, the laser power continually shifts between the power level required for write operations and the power level required for read operations.

The angle of refraction of light at the interface of materials is calculated with Snell's law, as is well known in the art:

 $n_1 \sin \theta_1 = n_2 \sin \theta_2$

where:

5

10

15

20

25

 n_1 = index of refraction of material 1;

 θ_1 = angle of incidence with respect to normal;

 n_2 = index of refraction of material 2; and

 θ_2 = angle of refraction with respect to normal.

This relationship governs the refraction of the light beam 5-106 when it enters the prism 5-108. As seen in Fig. 66, when an incident beam 5-106 of one wavelength enters the anamorphic prism 5-108, the beam is refracted at a given angle dictated by the index of refraction of the prism 5-108 and the angle of incidence 5-114 of the light beam 5-106. The resulting light beam 5-118, corrected for ellipticity, and possibly, astigmatism of the incident beam 5-106, enters the focussing lens 5-110 and results in the focussed light spot 5-120 on the optical media 5-112. The index of refraction, however, changes with wavelength. This is referred to as chromatic dispersion. Accordingly, when the wavelength of the incident light beam 5-106 changes, the angle of refraction resulting from the interface between air and the prism 5-108 is different than the angle of refraction for the previous

wavelength. Fig. 66 depicts with dotted lines, the effect of a shift in the wavelength of the incident beam 5-106. The incident light beam 5-106 refracts at a different angle and results in the light beam 5-122 which enters the focussing lens 5-110 at a different angle to result in a focussed light spot 5-124 on the optical media 5-112. As illustrated in Fig. 66, the light spot 5-124 is displaced from the light spot 5-120. This displacement, resulting from a change in wavelength in the incident light beam, is referred to herein as lateral beam shift.

5

10

15

20

25

The lateral beam shift may be avoided by not employing the anamorphic prism 5-108. For instance, a system may employ a circular lens to provide a circular spot on the optical media. However, to form the circular spot with a lens, the lens only focusses a circular aperture within the elliptical light beam. This results in an inefficient use of the laser power because portions of the light beam outside the circular aperture are discarded. Accordingly, a system which does not employ the anamorphic prism for beam shaping does not benefit from the prismatic correction of ellipticity and astigmatism in the incident light beam. The beam shaping capabilities of the anamorphic prism provide efficient use of the laser power by expanding the elliptical beam into a circular beam. The efficient use of power is advantageous, particularly in optical disc systems when increased power is necessary in order to write to the disc.

Fig. 67 depicts a conventional configuration for a

multi-element prism system 5-130, as is well known in the art. The system depicted consists of three prism elements, prism 5-132, prism 5-134 and prism 5-136, a focussing lens 5-138 and reflective-type optical media 5-140. The prism system 5-130 could be designed to be achromatic by proper selection of the individual prism geometries, indexes of refraction and dispersions for prism 5-132, prism 5-134 and prism 5-136.

5

10

15

20

25

The prism system 5-130 depicted in Fig. 67 also allows reflection of a return beam from the optical media 5-140 to a detection system 5-144 by including a beam-splitting thin film 5-146 between the prism 5-134 and the prism 5-136.

As seen in Fig. 67, an entering light beam 5-148 passes through the prism 5-132, the prism 5-134 and the prism 5-136 and is focussed by the lens 5-138 to form a spot 5-137 on the optical media 5-140. The light beam reflects from the optical media 5-140 back through the focussing lens 5-138 into the prism 5-136, and reflects from the thin film 5-146 as a light beam 5-150. The light beam 5-150 enters the detection system 5-144.

If designed to be achromatic, changes in the input light beam 5-148 wavelength should not result in a lateral shift in the focussed light spot 5-137 on the optical media 5-140.

As previously explained, optical systems often benefit from more than one detector. A prism system with an air space in the light path could provide significant advantages, particularly in providing a compact, achromatic prism system capable of reflecting portions of the incident and return beams to multiple

detectors. Furthermore, by using an air space, a symmetrical correcting prism can be added to an existing anamorphic prism system. Finally, a unitary prism system with an air space would be advantageous in order to provide a stable, compact and easy to manufacture and install, prism assembly.

5

10

15

20

25

In order to more fully explain the design of an achromatic prism system with an air space between prisms, reference is made to Fig. 68, which depicts a two-element prism system 5-152 having a chromatic correcting prism 5-154 added to a simple anamorphic prism 5-156. The correcting prism 5-154 has an index of refraction of n_1 and the simple anamorphic prism 5-156 has an index of refraction of n_2 , at a selected wavelength. The angles in the system are represented as shown in Fig. 68 as Φ , a_1 , a_2 , a_3 , a_4 , a_5 , a_6 , a_7 , β_1 , β_2 , and β_{air} . The deviation angle from the incident beam to the exit beam is referenced as α , where

$$\alpha = \beta_1 + \beta_{air} - (a_2 + \Phi + \beta_2)$$

and a_7 can be calculated through repeated applications of Snell's law and the geometry of triangles.

The design conditions are chosen to achieve a desired result (e.g., total deviation through the system). For instance, to design an achromatic system, the condition is that α be constant over some range of wavelengths.

For a total desired deviation angle, α = A, from the entrance beam to the exit beam, the condition is met as follows:

$$A = \beta_1 + \beta_{air} - (a_7 + \Phi + \beta_2)$$

Furthermore, the condition for making the correcting prism

5-154 a symmetrical prism with no net expansion of the incident light beam so that it can be added to the simple anamorphic prism 5-156, as shown in Fig. 68, is as follows:

$$\Phi = \sin^{-1} \left[n_1 * \sin(\beta_1/2) \right]$$

By selecting this condition, the correcting prism does not expand the incident light beam. Therefore, the correcting prism can be added to an existing anamorphic prism system selected to provide the appropriate expansion.

Finally, the prism assembly 5-152 can meet all of the desired design restraints by proper selection of Φ , β_1 , β_2 , β_{air} , and of the glass dispersions.

10

15

20

25

In some cases it may be desirable for the exit beam to have a significant deviation angle from the entrance beam. For instance, a deviation of 90 degree(s) may be advantageous. This can be accomplished by providing a total internal reflection in prism 5-156 before the beam exits the prism. This changes the above calculations, but the design goals can still be met by proper selection of the parameters.

Applying the above principles for adding a symmetrical correcting prism to an existing anamorphic prism, a prism system was designed which has multiple surfaces to partially reflect the return beam to different detectors. Embodiments of unitary, air-spaced, achromatic prism systems with significant deviation angles between the entrance beam and the exit beam, along with multiple reflections to various detection systems are described below.

Fig. 69 depicts an embodiment of an air-spaced, anamorphic, achromatic prism system 5-170 according to the present invention. Preferably, the prism system 5-170, as depicted in Fig. 69, has three prisms bonded as a single unit. As previously explained, this provides the advantage that the prism assembly 5-170 is mounted as a single unit. Because the prisms are bonded together, they need not be separately mounted in the optical system. This reduces mounting time, increases stability of the system, decreases mounting costs, and minimizes functional deviations between different optical systems. The three prism elements are a plate prism 5-172, a trapezoidal prism 5-174 and a correcting prism 5-176. Fig. 69 also depicts the light beam path as a light beam 5-178 from the light source 5-102, an air gap light beam 5-180, an exit/reflected light beam 5-182, a first detector channel light beam 5-184 to a first detector 5-185, a second detector channel light beam 5-186 to a second detector 5-187, and a third detector light beam 5-188 to a third detector 5-189. By including an air gap between the correcting prism 5-176 and the plate prism 5-172 through which the air gap light beam 5-180 passes, the correcting prism 5-176 can be designed as a symmetrical corrector with no net expansion to the incident beam 5-178. Therefore, the correcting prism 5-176 can be added to the plate prism 5-172 and the trapezoidal prism 5-174 combination in order to achromatize the prism system 5-170 shown in Fig. 69.

5

10

15

20

25

Fig. 69 also depicts a lens 5-190 positioned to focus the exit light beam 5-182 onto optical media 5-191. The specifics of

the design shown in Fig. 69 are described and designed to be substantially achromatic for a design wavelength of 785 +- 22 nm. At this wavelength, the system will have the properties described below.

5

10

15

20

25

The plate prism 5-172 is depicted in more detail in FIGS. 70, 70a and 70b. Fig. 70 is a side view of the plate prism 5-172; FIG. 70a'is a bottom plan view illustrating the surface S1 5-200; and FIG. 70b is a top plan view illustrating the surface S2 5-202. The plate prism has an optical surface S1 5-200, an optical surface S2 5-202, an optical surface S3 5-204, a surface S4 5-206 and a surface S5 5-208. In one embodiment, the surface S1 5-200 and the surface S2 5-202 are substantially parallel and spaced apart at a distance designated in Fig. 70 as 5-210. In the present embodiment, the distance 5-210 is advantageously 6.27 mm. The surface S5 5-208 and the surface S3 5-204 are also substantially parallel in the present embodiment. The surface S1 5-200 and the surface S3 5-204 intersect and terminate at an edge 5-211 (i.e., the S1/S2 edge) in Fig. 70, at an angle 5-212 (i.e., the S1/S2 angle), which is advantageously 50 degree(s) 21' +- 10' in the present embodiment. The surface S3 5-204 and the surface S2 5-202 intersect and terminate at an edge 5-214; the surface S2 5-202 and the surface S4 5-206 intersect and terminate at an edge 5-216; the surface S4 5-206 and the surface S5 5-208 intersect and terminate at an edge 5-218; and the surface S5 5-208 and the surface S1 5-200 intersect and terminate at an edge 5-220, as designated in Fig. 70. The surface S2 5-202 has a length

referenced as 5-222 in Fig. 70 and a width referenced as 5-224 FIG. 70a. In the present embodiment, the length 5-222 is 13.34 mm and the width 5-224 is 8.0 mm. The overall length of the prism, referenced as 5-225 in Fig. 70, from the edge 5-218 to the edge 5-211 measured parallel to the surface S1 5-200 is advantageously 23.61 mm in the present embodiment. The distance from the edge 5-218 and the edge 5-220, referenced as 5-227, measured along a reference plane 5-226 defined perpendicular to the surface S1 5-200 and the surface S2 5-202 is advantageously 2.14 mm. The plan view in FIG. 70a illustrates a clear aperture 5-230 and a clear aperture 5-232 defined on the surface S1 5-200. A clear aperture is simply an area of the surface of the prism over which the surface is specified to meet a selected quality. In the present embodiment, the clear apertures 5-230 and 5-232 are 8.5 mm by 6.5 mm ovals. Advantageously, the oval 5-230 is centered with its minor axis a distance referenced as 5-233 from the edge 5-211 and with its major axis centered in the middle of the surface S1 5-200 as shown in FIG. 70a. In the present embodiment, the clear aperture 5-232 is centered with its minor axis a distance referenced as 5-234 from the edge 5-220, and with its major axis centered along the middle of the surface S1 5-200. Advantageously, in the present embodiment, the distance 5-233 is 6.15 mm and the distance 5-234 is 5.30 mm.

5

10

15

20

25

The plan view depicted in FIG. 70b illustrates a clear aperture 5-235 defined on the surface S2 5-202. The present embodiment defines this clear aperture as an 8.5 mm by 6.5 mm

oval with its minor axis centered a distance referenced as 5-236 from the edge 5-214 and its major axis centered in the middle of the surface S2 5-202 as depicted in FIG. 70b. In the present embodiment the distance 5-236 is 5.2 mm. The clear apertures 5-230, 5-232, and 5-235 define portions of the surfaces over which the surface quality is preferably at least 40/20, as is well known in the art. In the embodiment depicted, BK7 grade A fine annealed glass, well known in the art, is an appropriate optical material for the prism 5-172.

5

10

15

20

25

Fig. 71 depicts additional detail of the trapezoidal prism 5-174 of the embodiment depicted in Fig. 69. The trapezoidal prism 5-174 has an optical surface S6 5-240, an optical surface S7 5-242, an optical surface S8 5-244, and an optical surface S9 5-246. The surface S6 5-240 and the surface S7 5-242 terminate and intersect at an edge 5-248. The surface S7 5-242 and the surface S8 5-244 intersect and terminate at an edge 5-250 at an angle referenced as 5-251. Advantageously, the angle 5-251 is substantially 135 degree(s). The surface S8 5-244 and the surface S9 5-246 intersect and terminate at an edge 5-252 at an angle 5-254 which is advantageously 50 degree(s) 21' in the present embodiment. The surface S9 5-246 and the surface S6 5-240 intersect and terminate at an edge 5-256. The surface S6 5-240 has a length referenced as 5-258 in Fig. 71. Advantageously, the length 5-258 is 9.5 mm in the present embodiment. The surface S6 5-240 and the surface S8 5-244 are substantially parallel and spaced at a distance referenced as 5-260 in Fig. 71. In the

present embodiment, the distance 5-260 is 8.0 mm measured in a direction perpendicular to the surface S6 5-240 and the surface S8 5-244. The edge 5-250 and the edge 5-248 are spaced at a distance referenced as 5-261 along a plane 5-262 defined parallel with the surface S8 5-244. Advantageously, the distance 5-261 is 8.0 mm in the present embodiment. FIG. 71a is a top plan view of the trapezoidal prism 5-174 illustrating the surface S6 5-240 and the surface S9 5-246. As depicted in FIG. 71a the trapezoid prism 5-174 has a thickness referenced as 5-263. Preferably, the thickness 5-263 is approximately 8 mm in the present embodiment. As shown in FIG. 71a, the surface S6 5-240 has a clear aperture 5-264 defined in the present embodiment as a 6.5 mm minimum diameter circular aperture centered across the width of the surface and centered at a distance 5-265 from the edge 5-248. Preferably, the distance 5-265 is 4.0 mm in the present embodiment. The surface S9 5-246 has a clear aperture 5-266 centered on the surface. In the present embodiment, the clear aperture 5-266 is defined as a 6.5 mm by 8.5 mm minimum oval.

5

10

15

20

25

FIG. 71b depicts a bottom plan view of the trapezoidal prism 5-174 illustrating the surface S7 5-242 and the surface S8 5-244 with clear apertures 5-268 and 5-270, respectively. As depicted in FIG. 71b, the trapezoid prism 5-174 has a length referenced as 5-272 from the edge 5-252 to the edge 5-248 measured along the reference plane 5-262. Preferably, the length 5-272 is 16.13 mm in the present embodiment. In one embodiment, the clear aperture 5-268 for the surface S7 5-242 is defined as a 6.5 mm by 9.2 mm

oval centered on the surface S7 5-242 with its minor axis parallel to and centered between the edge 5-248 and the edge 5-250. Advantageously, the clear aperture 5-270 is a 6.5 mm by 6.7 mm oval centered on the surface S8 5-244 with its major axis centered parallel between the edge 5-250 and the edge 5-252. In the present embodiment, the surface quality of the clear apertures 5-264, 5-266, 5-268 and 5-270 is advantageously 40/20, well known in the art.

Many of the surfaces in the prisms have coatings to facilitate the function of the prism. In the present embodiment, the surface S6 5-240 has an anti-reflection coating with transmission \geq 99.8% at 90° \pm 0.5 degree(s) angle of incidence. The surface S8 5-244 has a coating with transmission \geq 98.5% at 10.7° \pm 0.5 angle of incidence for internally incident light. The surface S9 5-246 has a low extinction thin film coating with reflection of the s polarization state (R_s) (i.e., normal to the plane of incidence) >90%, and with reflection of the p polarization state (R_p) = 12.5% \pm 2.5% at 39° 39' \pm 0.5° angle of incidence. The material for the trapezoidal prism 5-174 of the embodiment depicted in Fig. 69 is BK7 grade A fine annealed optical glass, as is well known in the art.

The chromatic correcting prism 5-176 of the embodiment of the prism system 5-170 depicted in Fig. 69 is shown in more detail in Fig. 72. As depicted, the chromatic correcting prism 5-176 has an optical surface S10 5-290, an optical surface S11 5-292, and a surface S12 5-294 configured to form a triangular

prism. The surface S11 5-292 and the surface S12 5-294 intersect and terminate at an edge 5-296. The surface S10 5-290 and the surface S12 5-294 intersect and terminate at an edge 5-298.

Preferably, the surfaces S10 5-290 and S11 5-292 are symmetrical. The surface S12 5-294 has a length referenced as 5-300, which is 7.78 mm in the present embodiment. Thus, the edge 5-296 and the edge 5-298 are separated by the distance 5-300. The surface S10 5-290 and the surface S11 5-292 approach each other at an angle referenced as 5-302. In the present embodiment, the angle 5-302 is advantageously 38° 20'. The surface S11 5-292 and the surface S10 5-290 are terminated a distance referenced as 5-303 from the surface S12 5-294, measured perpendicular to the surface S12 5-294. The distance 5-303 is 10.5 mm in the present embodiment.

FIG. 72a depicts a view of the surface S10 5-290. In this embodiment, the prism 5-176 has a thickness referenced as 5-304 in FIG. 72a. In the present embodiment, the thickness 5-304 is advantageously 8.0 mm. Desirably, the surface S10 5-290 has an oval clear aperture 5-306. In the present embodiment, the clear aperture is an oval centered with the major axis parallel to, and a distance referenced as 5-308 from, the intersection at 5-298. The minor axis is centered on the surface S10 5-290 as depicted. Preferably, the clear aperture 5-306 is defined as a 6.5 mm by 2.8 mm oval in the present embodiment, and the surface quality across the clear aperture 5-306 is advantageously 40/20, as known in the art. In the present embodiment, the surface S11 5-292 also has a similar clear aperture defined on its surface.

As with the trapezoidal prism 5-174, the chromatic correcting prism 5-176 has coatings on some of its surfaces to facilitate performance. In one embodiment, each surfaces S10 5-290 and S11 5-292 have an anti-reflective coating (e.g. reflectance <=3% at $35.5^{\circ}\pm1.0^{\circ}$ angle of incidence, as is well known in the art). In the present embodiment, SFII grade A fine annealed glass is the material for the correcting prism 5-176.

5

10

15

20

25

When the prisms as described above are assembled as the unitary prism system 5-170 of the embodiment shown in Fig. 69, the light beams reflect as depicted and explained below for a wavelength of 785 \pm 22 nm. For discussion purposes, a reference plane 5-237 is defined along one side of the prism system 5-170 as illustrated in FIG. 69a. The incident beam 5-178 from the light source 5-102 enters the surface S10 5-290 at an incidence angle 5-326 and parallel with the reference plane 5-237. The light beam exits the prism 5-176 into the air-gap as the light beam 5-180 and enters the prism 5-172 through surface S2 5-202. A portion of the light beam reflects at the thin film on the surface S9 5-246 and exits the surface S3 5-204 as the light beam 5-188. In one embodiment, the beam 5-188 may be directed to the detection system 5-189. Because this reflected beam is a portion of the input beam, the detection system 5-189 receiving the light beam 5-188 may monitor the intensity of the incident light. The remainder of the light beam which does not reflect at the thin film on the surface S9 5-246, passes into the trapezoidal prism 5-174, reflects internally at the surface S7 5-242 and exits as

the light beam 5-182 through the surface S6 5-240.

5

10

15

20

25

In the embodiment described, if the angle of incidence 5-326 of the light beam 5-178 is 35° 26° , the light beam exits the prism 5-174 with a total deviation from the entrance beam 5-178 to the exit beam 5-182 of 87° 37° \pm 5° , parallel to the reference plane 5-237 within 5° , and the light beam 5-182 exits normal to the surface 86 5-240 within 5° .

The lens 5-190 focusses the light beam 5-182 onto the optical media 5-191. The light beam reflects back through the lens and enters normal to the surface S6 5-240, reflects internally at the surface S7 5-242, and then reflects at the thin film between the trapezoidal prism 5-174 and the plate prism 5-172. The resulting beam exits the trapezoidal prism 5-174 through the surface S8 5-244 as the light beam 5-184 at a deviation angle 5-328. The light beam 5-184 enters a detection system 5-185.

Part of the light beam returned from the optical media 5-190 also passes through the thin film, reflects at the surface S2 5-202 and exits the plate prism 5-172 as the light beam 5-186. This reflection is available because of the air gap in the prism system. In one embodiment, the light beam 5-184 and the light beam 5-186 can both be directed to separate detection systems 5-185 and 5-187, respectively. For instance, the detection system 5-185 may collect data signals, and the detection system 5-187 may collect control signals (e.g., focus and tracking servo information).

As explained above, the embodiment described is substantially achromatic within a typical range of wavelength changes from a conventional laser light source. Accordingly, shifts in the wavelength of the incident light do not significantly affect the resulting lateral position of the focussed beam on the optical media 5-190.

5

10

15

Calculations simulating the performance of the prism system 5-170 for variations in wavelength from 780 nm to 785 nm are shown in the chart below. Phi is the incidence angle on the correcting prism (i.e., 35° 26' in the present embodiment) and its variation is estimated as ± 0.5°. The wavelength shift is indicated in one column and the corresponding shift in the focussed spot from the prism system is indicated in the columns for incidence angles of Phi ± 0.5°. For instance, as seen in the first line of the table, for a wavelength shift of the incident light beam of 780 nm - 781.5 nm, the focussed spot shifts by -0.2 nm at the incident angle of Phi, by 2.6 nm for an incidence angle of Phi -0.5°, and by -2.9 nm for a incidence angle of Phi +0.5°.

20	Wavelength Shift	Phi - 0.5°	Phi	Phi + 0.5°
	780-781.5 nm	2.6 nm	-0.2 nm	-2.9 nm
	780-783 nm	5.2 nm	-0.2 nm	-5.6 nm
	780-785 nm	9.0 nm	-0.1 nm	-9.0 nm

As can be seen from the above table, the lateral displacement at the incidence angle, Phi, varies by less than 1

nm for a wavelength shift from 780 to 783 nm, with an incidence angle of Phi. This is contrasted with a lateral displacement of approximately 200 nm for a wavelength shift of 3 nm in an embodiment similar to that described above but without the chromatic correction. This indicates a substantially achromatic system.

Fig. 73 depicts a prism system 5-339 as an alternative embodiment of the present invention. This embodiment has the correcting prism 5-340, a plate prism 5-342, and a quadrilateral prism 5-344. The correcting prism 5-340 and the plate prism 5-342 are both substantially the same as the correcting prism 5-176 and the plate prism 5-172, respectively, of the prism system 5-170 depicted in Fig. 69. The quadrilateral prism 5-344 differs from the trapezoidal prism 5-174.

The quadrilateral prism 5-344 depicted in Fig. 73 is depicted in more detail in FIGS. 74, 74a and 74b. The quadrilateral prism 5-344 has a surface S13 5-346, a surface S14 5-348, a surface S15 5-350, and a surface S16 5-352. The surface S13 5-346, the surface S14 5-348, the surface S15 5-350, and the surface S16 5-352 are configured similarly but not identical to the surface S6 5-240, the surface S7 5-242, the surface S8 5-244, the surface S9 5-246 of the trapezoidal prism 5-174. The surface S13 5-346 and the surface S14 5-348 intersect at an edge 5-353 at an angle referenced as 5-354; the surface S14 5-348 and the surface S15 5-350 intersect at an edge 5-355 at an angle referenced as 5-356; and the surface S15 5-350 and the surface

S16 5-352 intersect at an edge 5-357 at an angle referenced as 5-358, in Fig. 74. Finally, the surface S16 5-352 and the surface S13 5-346 intersect at an edge 5-359. In one embodiment, the angle 5-354 is 49° 40', the angle 5-356 is 135° and the angle 5-358 is 50° 21'. The distance between the edge 5-353 and the edge 5-355, measured perpendicular to the surface S15 5-350 is referenced as 5-360 in Fig. 74. In one embodiment, the distance 5-360 is 8.0 mm. Additionally, the distance from the edge 5-353 to the edge 5-359 is referenced as 5-362 in Fig. 74. In one embodiment, the distance 5-362 is 8.9 mm measured parallel to the surface S15 5-350. Finally, the distance between the edge 5-353 and the edge 5-355, measured along a plane parallel with the surface S15 5-350, is referenced as 5-364 in Fig. 74. In one embodiment, the distance 5-364 is preferably 8.0 mm.

FIG. 74a is a plan view of the surface S13 5-346 and also depicts the surface S16 5-352. FIG. 74a depicts the thickness of the prism 5-344 referenced as 5-368. In one embodiment, the thickness 5-368 is 8.0 mm. Advantageously, the prism 5-344 has a clear aperture 5-370 defined along the surface S13 5-346, and a clear aperture 5-372 defined along the surface S16 5-352, as depicted in FIG. 74a. In the present embodiment, the clear aperture 5-370 is a circular aperture centered across the surface and a distance 5-374 from the edge 5-353. In one embodiment, the clear aperture 5-370 is a circular aperture with a minimum diameter of 6.5 mm and the distance 5-374 is 4.0 mm.

Advantageously, the surface S16 5-352 also has a clear aperture

5-372 centered on the surface. In one embodiment, the clear aperture 5-372 is a 6.5 mm by 8.5 mm oval aperture centered on the surface S16 5-352 as depicted in FIG. 74a.

5

10

15

20

25

FIG. 74b is a plan view of the surface S14 5-348 and also illustrates the surface S15 5-350. The overall length of the prism 5-344 from the edge 5-353 to the edge 5-357 measured along a plane parallel to the surface S15 5-350 is referenced as 5-380 in FIG. 74b. In one embodiment, the length 5-380 is 16.13 mm. As seen in FIG. 74b, the surface S14 5-348 has a clear aperture 5-382 centered on the surface, and the surface S15 5-350 also has a clear aperture 5-384 centered on the surface. In one embodiment, the clear aperture 5-382 is a 6.5 mm by 9.2 mm oval, and the clear aperture 5-384 is a 6.5 mm by 6.7 mm oval.

Advantageously, the quadrilateral prism 5-344 also has coatings on some of its optical surfaces. In one embodiment, the surface S13 5-346 has a coating with reflectance <=0.2% at 4° 40° \pm 5° angle of incidence with respect to the normal for internally incident light. In the same embodiment, the surface S15 5-350 has a coating with reflectance <=0.5% at 10.7° \pm 0.5° angle of incidence with respect to the normal, for internally incident light. Finally, the surface S16 5-352 advantageously has a thin film coating with $R_{\rm s} >$ 90%, $R_{\rm p}$ =12.5% \pm 2.5% at 39° 39° \pm .5° angle of incidence with respect to the normal. Preferably, this thin film coating also has less than 8° phase shift for all operating and optical conditions.

With the configuration shown in Fig. 74, the deviation angle

of the entrance beam to the exit beam totals, advantageously, 90°. This facilitates manufacturing because mounting components for 90° deviations are easier to fabricate than for 87° deviations, as in the embodiment of Fig. 69. For the dimensions and coatings specified for the embodiment of Fig. 73, the prism is not perfectly achromatic. However, the prism system illustrated in Fig. 73 is substantially achromatic over an acceptable range of operating wavelengths around the design wavelength.

5

Calculations simulating the performance of the prism system 5-339 of Fig. 73 for variations in the wavelength from 780 nm to 785 nm are shown in the chart below. Again, Phi is 35° 26' in this embodiment.

15	Wavelength Shift	Phi - 0.5°	Phi	Phi + 0.5°
	780-781.5 nm	12.5 nm	9.8 nm	7.1 nm
	780-783 nm	25.1 nm	19.6 nm	14.3 nm
	780-785 nm	42.0 nm	32.9 nm	24.0 nm

As can be seen, the design shown in Fig. 73 is not as achromatic as the design shown in Fig. 69, however for a wavelength shift of 780 to 783 nm, the lateral displacement of the focussed spot from the light exiting the prism is only 19.6 nm. Again, this should be contrasted with a lateral displacement of approximately 200 nm for a wavelength shift of 3 nm in an embodiment similar to the embodiment described above but without

the chromatic correction.

5

10

15

20

25

Data Retrieval - Transition Detection.

A detailed system for storing and retrieving data from a magneto-optical device is provided in related application Serial No. 07/964,518 filed January 25, 1993, which application is incorporated by reference as if fully set forth herein.

A block diagram of an exemplary magneto-optical system is shown in Fig. 75. The system may have a read mode and a write mode. During the write mode, a data source 6-10 transmits data to an encoder 6-12. The encoder 6-12 converts the data into binary code bits. The binary code bits are transmitted to a laser pulse generator 6-14, where the code bits may be converted to energizing pulses for turning a laser 6-16 on an off. In one embodiment, for example, a code bit of "1" indicates that the laser will be pulsed on for a fixed duration independent of the code bit pattern, while a code bit of "0" indicates that the laser will not be pulsed at that interval. Depending on the particular laser and type of optical medium being used, performance may be enhanced by adjusting the relative occurrence of the laser pulse or extending the otherwise uniform pulse In response to being pulsed, the laser 6-16 heats localized areas of an optical medium 6-18, thereby exposing the localized areas of the optical medium 6-18 to a magnetic flux that fixes the polarity of the magnetic material on the optical medium 6-18. The localized areas, commonly called "pits", store the encoded data in magnetic form until erased.

During the read mode, a laser beam or other light source is reflected off the surface of the optical medium 6-18. The reflected laser beam has a polarization dependent upon the polarity of the magnetic surface of the optical medium 6-18. The reflected laser beam is provided to an optical reader 6-20, which sends an input signal or read signal to a waveform processor 6-22 for conditioning the input signal and recovering the encoded data. The output of the waveform processor 6-22 may be provided to a decoder 6-24. The decoder 6-24 translates the encoded data back to its original form and sends the decoded data to a data output port 6-26 for transmission or other processing as desired.

10.

Figure 76 depicts in more detail the process of data storage and retrieval using a GCR 8/9 code format. For a GCR 8/9 code, a cell 6-28 is defined as one channel bit. Each clock period 6-42 corresponds to a channel bit; thus, cells 6-30 through 6-41 each correspond to one clock period 6-42 of clock waveform 6-45. As an example of clock speeds, for a 3½" optical disc rotating at 2,400 revolutions per minute with a storage capacity of 256 Mbytes, clock period 6-42 will typically be 63 nanoseconds or a clock frequency of 15.879 MHz. GCR input waveform 6-47 is the encoded data output from the encoder 6-12 (see Fig. 75). The GCR input waveform 6-47 corresponds to a representative channel sequence "010001110101". The laser pulse generator 6-14 uses the GCR data waveform 6-47 to derive the pulse GCR waveform 6-65 (which in Figure 76 has not been adjusted in time or duration to reflect performance enhancement for specific data patterns).

Generally, the GCR pulses 6-67 through 6-78 occur at clock periods when the GCR data waveform 6-47 is high. The pulse GCR waveform 6-65 is provided to the laser 6-16. The magnetization of the previously erased optical medium reverses polarity when in the presence of an external magnetic field of opposite polarity to the erased medium and when the laser is pulsed on with sufficient energy to exceed the curie temperature of the media. The laser pulses resulting from GCR pulses 6-68, 6-69, 6-70, etc., create a pattern of recorded pits 6-80 on optical medium 6-18. Thus, recorded pits 6-82 through 6-88 correspond to pulses 6-68, 6-69, 6-70, 6-71, 6-73, 6-76, and 6-77, respectively.

5

10

15

20

25

Successive recorded pits 6-82 through 6-85 may merge together to effectively create an elongated pit. The elongated pit has a leading edge corresponding to the leading edge of the first recorded pit 6-82 and a trailing edge corresponding to the trailing edge of last recorded pit 6-85.

Reading the recorded pits with an optical device such as a laser results in the generation of a playback signal 6-90. The playback signal 6-90 is low in the absence of any recorded pits. At the leading edge of a pit 6-86, playback signal 6-90 will rise and remain high until the trailing edge of the pit 6-86 is reached, at which point the playback signal 6-90 will decay and remain low until the next pit 6-87.

The above described process may be referred to as pulse width modulation ("PWM") because the width of the pulses in playback signal 6-90 indicate the distance between 1-bits. Thus,

the edges of the recorded pits 6-80 which define the length of the pulses in playback signal 6-90 contain the pertinent data information. If the playback signal is differentiated, the signal peaks 6-111 through 6-116 of the first derivative signal 6-110 will correspond to the edges of the recorded pits 6-80. (The signal peaks of the first derivative playback signal 6-110 in Fig. 76 are shown slightly offset from the edges of the recorded pits 6-80 because an ideal playback signal 6-90 is shown). In order to recover the pit edge information from the first derivative signal 6-110, it is necessary to detect the signal peaks 6-111 through 6-116. Such a process is described in detail further herein.

In contrast, most if not all existing RLL 2/7 code systems are used in conjunction with pulse position modulation ("PPM"). In PPM systems, each pit represents a "1" while the absence of a pit represents a "0". The distance between pits represents the distance between 1-bits. The center of each pit corresponds to the location of the data. In order to find the pit centers, the playback signal is differentiated and the zero-crossings of the first derivative are detected. Such a technique may be contrasted with PWM systems, described above, in which the signal peaks of the first derivative contain the pertinent pulse width information.

It is nevertheless possible to utilize PWM instead of PPM with an RLL system such as an RLL 2/7 code system. Each channel bit may correspond to a clock period of a clock waveform. As

with the GCR system described earlier using PWM, a "1" may be represented by a transition in the input waveform. Thus, the RLL 2/7 input waveform may remain in the same state while a "0" occurs, but changes from high-to-low or low-to-high when a "1" occurs.

5

10

15

20

25

In both RLL and GCR codes, as well as other codes, when data patterns are read, the input signal generated from the optical reader 6-20 is often not symmetrical. When an unsymmetrical signal is AC-coupled between circuits, the average DC value shifts away from the peak-to-peak midpoint. The unintended shifting away from the midpoint may result in a shift in the apparent position of the data, adversely affect the ability to determine accurately the locations of data, and reduce timing margins or render the recorded data unrecoverable.

This phenomenon may be explained with reference to Figs. 77A and 77B. These figures show an ideal input signal S_1 derived from a symmetrical data pattern. Normally, transitions between 1's and 0's in the data are detected at the midpoint between high and low peaks of the input signal. It may be observed in Fig. 77A that the areas A_1 and A_2 above and below the peak-to-peak midpoint M_{P1} of the input signal S_1 are equal, and the transitions between 1's and 0's correspond precisely (in an ideal system) to the crossings of the input signal S_1 and the peak-to-peak midpoint M_{P1} .

Figure 77B, in contrast, shows an input signal S_2 derived from an unsymmetrical data pattern. It may be observed that the

area A_1 ' above the peak-to-peak midpoint M_{P2} is greater than the are A_2 ' below the graph. The input signal S_2 therefore has a DC component that shifts the DC baseline DC_{BASE} above the peak-to-peak midpoint M_{P2} . When an attempt is made to locate transitions between 1's and 0's by determining the zero-crossings of the AC coupled input signal S_2 , errors may be made because the DC level is not identical to the peak-to-peak midpoint M_{P2} . The DC level does not stay constant but rises and falls depending on the nature of the input signal. The larger the DC buildup, the more the detected transitions will stray from the true transition points. Thus, DC buildup can cause timing margins to shrink or the data to be unrecoverable.

5

10

15

20

25

Fig. 78 is a block diagram of a read channel 6-200 in accordance with one embodiment of the present invention for mitigating the effects of DC buildup. The read channel 6-200 roughly corresponds to the waveform processor 6-22 of Fig. 75. The read channel 6-200 comprises a preamplification stage 6-202, a differentiation stage 6-204, an equalization stage 6-206, a partial integration stage 6-208, and a data generation stage 6-210. The operation of the read channel 6-200 will be explained with reference to a more detailed block diagram shown in Fig. 79, the waveform diagrams shown in Figs. 84A-84D, and various other figures as will be referenced from time to time herein.

When the optical medium is scanned for data, the preamplification stage 6-202 amplifies the input signal to an appropriate level. The pre-amplification stage 6-202 may comprise a pre-amplifier 6-203 as is well known in the art. The pre-amplifier 6-203 may alternatively be located elsewhere such as within the optical reader 6-20. An exemplary amplified playback signal 6-220 is depicted in Fig. 84A.

The output of the preamplification stage 6-202, as shown in Fig. 79, is provided to the differentiation stage 6-204. The differentiation stage 6-204 may comprise a differential amplifier 6-212 such as a video differential amplifier configured with a capacitor 6-213 in a manner well known in the art. A representative frequency response diagram of the differentiation stage 6-204 is shown in Fig. 80A. The differentiation stage 6-204 effectively increases the relative magnitudes of the high frequency components of the amplified playback signal 6-202. An exemplary waveform of the output of the differentiation stage 6-204 is shown in Fig. 84B.

The differentiation stage 6-204 is followed by an equalization stage 6-206 as shown in Fig. 79. The equalization stage 6-206 provides additional filtering so as to modify the overall channel transfer function and provide more reliable data detection. The equalization stage 6-206 shapes the differentiated input signal so as to even out the amplitudes of high and low frequency components and generate a smoother signal for later processing. Equalizing filters often modify the noise spectrum as well as the signal. Thus, an improvement in the shape of the differentiated input signal (i.e., a reduction in distortion) is usually accompanied by a degradation in the

signal-to-noise ratio. Consequently, design of the equalization stage 6-206 involves a compromise between attempting to minimize noise and providing a distortion-free signal at an acceptable hardware cost. In general, equalizer design depends on the amount of intersymbol interference to be compensated, the modulation code, the data recovery technique to be used, the signal-to-noise ratio, and the noise spectrum shape.

5

10

15

20

25

channel as well.

A substantial portion of linear intersymbol interference when reading stored data in a magneto-optical recording system is caused by limited bandwidth of the analog read channel and roll-off of input signal amplitude with increased storage density. Accordingly, the equalization stage 6-206 may comprise one or more linear filters which modify the read channel transfer function so as to provide more reliable data detection.

Normally, the equalization stage is implemented as part of the read channel, but, under certain conditions, part of the equalization filtering can be implemented as part of the write

For purposes of analysis, the playback signal can be considered as a series of bipolar rectangular pulses having unit amplitude and a duration T. Alternatively, the playback signal may be considered as a series of bidirectional step functions at each flux reversal location, where the step amplitude matches the pulse amplitude. When an input signal is applied to the equalization stage 6-206, clocking information as well as pulse polarity for each clock cell or binit may be derived from the

output signal of the equalization stage 6-206. The clocking and polarity information may be derived, in theory, by use of an ideal waveform restoration equalizer, which produces an output signal having mid-binit and binit boundary values similar to those of the input signal. The zero crossings of the output signal occur at binit boundaries in order to regenerate a clock accurately. If the zero-crossing time and direction are known, both clock and data can be extracted from the signal zero crossings.

In one embodiment, the equalization stage 6-206 comprises an equalizer selected from a class of waveform restoration equalizers. Generally, a waveform restoration equalizer generates a signal comprising a binary sequence resembling the input or playback waveform. The corners of the otherwise rectangular pulses of the resultant signal are rounded because signal harmonics are attenuated in the channel. The resultant signal may also exhibit some output signal amplitude variation.

An equalizer which produces a minimum bandwidth output signal is an ideal low pass filter with response of unity to the minimum cutoff frequency and no response at higher frequencies. Although such an ideal low pass filter is not physically realizable, the Nyquist theorem on vestigial symmetry suggests that the sharp cutoff minimum bandwidth filter can be modified and still retain output pulse zero crossing at all mid-binit cell times. To achieve this result, the high frequency roll-off of the equalized channel is preferably symmetrical and locates the

half-amplitude point at the minimum bandwidth filter cutoff frequency.

One type of roll-off characteristic that may be exhibited by a filter in the equalization stage 6-206 is a raised cosine rolloff, leading to the name raised cosine equalizer. A raised cosine roll-off transfer function is approximately realizable, and has an improved response over the minimum bandwidth filter. The output pulses have a zero value at times nT, but the sidelobe damped oscillation amplitude is reduced. The output zero crossings of the raised cosine filter are more consistent than those of the minimum bandwidth filter, and linear phase characteristics are more easily achieved with a gradual roll-off, such as with the relatively gradual roll-off of the raised cosine These advantages, however, are typically obtained at the expense of increased bandwidth. The ratio of bandwidth extension to the minimum bandwidth, fm, is sometimes referred to as the " α " of the raised cosine channel. Thus, in the case of a modulation code with d=0, $\alpha=0$ is the minimum bandwidth but represents an unrealizable rectangular transfer function, while $\alpha = 1$ represents a filter using twice the minimum bandwidth.

The impulse transfer function of the raised cosine equalization channel (including the analog channel plus equalizer, but excluding the input filter) may be given as follows:

25

5

10

15

20

$$H(f) = 1$$
, for $0 < f < (1 - \alpha) * fm$

$$H(f) = 1/2 \{1 + \cos [(f - (1 - \alpha) * fm)/(2 * \alpha * fm)]\},$$

$$for (1 - \alpha) * fm < f < (1 + \alpha) * fm$$

$$H(f) = 0$$
, for $f > (1 + \alpha) * fm$

5

10

where $\Phi(f) = k * f$ is the phase, and k is a constant. The above family may be referred to as α waveform restoration equalizers. The α = 1 channel has the property of having nulls at half-binit intervals as well as at full binit intervals. Such a channel results in a signal having no intersymbol interference at midbinit or binit boundary times, which are signal zero crossing and sample times, thus allowing accurate clock and data recovery. For such a full bandwidth equalizer, the roll-off starts at zero frequency and extends to the cutoff frequency f.

Raised cosine equalizers are capable of correcting extensive 15 amounts of linear intersymbol interference given adequate signal-20

25

to-noise ratio. A large amount of high frequency boost may be required to compensate for MO-media and optical system resolution. An equalizer bandwidth equal to at least twice the minimum bandwidth is preferred for elimination of linear intersymbol interference, assuming a physically realizable channel operating on a modulation code with d = 0. A bandwidth of such a width generally results in reduction of the signal-to-The equalizer bandwidth is selected so as to achieve the optimum compromise between interference distortion and noise. In some instances, it may be desirable to narrow the bandwidth by using an α < 1 transfer function in order to $improve\ noise\ at\ the\ expense\ of\ added\ distortion\ in\ the\ form\ of\ clock\ jitter.$

Another waveform-restoration equalizer is known as the cosine β response equalizer. The impulse transfer function of a full bandwidth β channel is as follows:

$$H(f) - \cos^{\beta} (\pi * f/(2 * f_c))$$
 for $0 < f < f_c$

10
$$H(f) = 0$$
 for $f > f_c$

5

15

20

25

Like the α equalizer family, there are numerous β equalizers. Full bandwidth β equalizers have a cutoff frequency of f_c , and consequently reduce clock jitter due to the relatively small amount of interference at binit boundaries. Techniques are known in the art for optimizing these types of equalizing filters to achieve the minimum probability of error in various types of noise conditions.

Use of α equalizers generally results in a narrower bandwidth, thereby reducing noise at the expense of clock jitter or horizontal eye opening. Use of a β equalizer generally results in signal-to-noise ratio improvement by reducing high frequency boost without reducing the bandwidth. The choice of β equalizer may reduce the vertical eye opening or an effective amplitude reduction. The α = 1 and β = 2 equalizer channels are identical from the standpoint of eye pattern, both types of

channels having a relatively wide open eye pattern.

A preferred equalizer channel bandwidth for codes with d > 0 does not necessarily depend on the minimum recorded pulse width, Tr, as might be expected, but rather on the binit width, Tm. This is because the data-recovery circuits are generally required to distinguish between pulses that differ by as little as one binit width, and time resolution is a function of signal bandwidth. The (0,k) codes (where k represents the maximum number of contiguous binits without flux reversals) require a nominal bandwidth $BW_{NOM} = 1/Tm = f_c$ so as to eliminate interference at the center and edge of each binit, provided that intersymbol interference at binit boundaries is absent.

For codes with d > 0, interference can be essentially eliminated at binit edges with a reduced bandwidth of BW = $1/(2*Tm) = f_c/2$. In such a case, all binit read pulses then have unit amplitude at a flux reversal, and the read-pulse tails cross zero at flux transitions. The narrower bandwidth BW results in output signal zero crossings at a point of no interference, without considering binit centers, but the bandwidth reduction is typically obtained with an increase in detection ambiguity in the presence of channel impairments. The narrower bandwidth BW may also result in a reduction of the signal zero-crossing slope, leading to a potential increase in detection sensitivity with respect to noise, disc speed variations, analog channel differences, or improper equalization. For example, a half-bandwidth β = 2 equalization channel with a (1,k)2/3 rate

modulation code may result in a signal having no intersymbol interference at the signal zero crossings, but some amplitude variation between zero crossings. The bandwidth is less than the bandwidth for non-return to zero ("NRZI") modulation, even though more information is recorded than with NRZI modulation (e.g., bandwidth = 0.75 and bit rate = 1.33 relative to NRZI). The reduced bandwidth makes up for the modulation code rate loss.

5

10

15

20

25

The α = 1 and β waveform restoration equalizers may permit output zero crossings to occur at the equivalent of input pulse edges. Data detection can then be obtained by hard-limiting the equalized signal, generally resulting in an output signal resembling the original playback signal. However, this result occurs only if the equalizer response extends to DC, which is typically not the case for a magneto-optical channel. Disc birefringence in the MO channel causes drift up and down of the DC baseline, resulting in output binits which are lengthened or shortened according to the degree of amplitude offset at zerocrossing detector. This problem can be reduced by the use of DC restoration as described herein. In order to achieve the desired low frequency response for a waveform-restoration equalizer, the low frequency signals may have to be amplified significantly, which can seriously degrade signal-to-noise ratio under some conditions. If low frequency noise is present in significant amounts, waveform-restoration equalization techniques may not be very satisfactory unless a modulation code with no DC and little low-frequency content or DC restoration circuits are used.

In a preferred embodiment, the equalization stage 6-206 may comprise a programmable filter and equalizer 6-207 located on an integrated chip. Such integrated chips are presently available from various manufacturers. The filter and equalizer 6-207 may be of an equi-ripple variety and have relatively constant group delay up to a frequency equal to about twice the cutoff frequency. A representative frequency response diagram of the equalization stage 6-206 is shown in Fig. 80B, and an exemplary output waveform is shown in Fig. 84C.

After the signal has been processed by the equalization stage 6-206, the signal peaks of the waveform in Fig. 84C contain accurate information regarding the position of the read data. The signal peaks can be detected by taking another derivative, but doing so may be detrimental to the system's signal-to-noise ratio and will likely cause undesired jitter. A preferred embodiment of the invention described herein provides an accurate means for detecting the signal peaks without taking a second derivative, by using partial integration and a novel data generation circuit.

After the signal has been processed by the equalization stage 6-206, it is provided to a partial integrator stage 6-208 for further shaping of the waveform. As illustrated in Fig. 79, the partial integrator stage 6-208 may comprise an amplifier stage 6-229, a bandpass filter stage 6-230, an integrator and low pass filter stage 6-232, and a subtractor and low pass filter stage 6-234. The amplifier stage 6-229 receives the output of

the equalization stage 6-206 and provides a signal to the bandpass filter stage 6-230 and the integrator and low pass filter stage 6-232. The integrator and low pass filter stage 6-232 preferably attenuates a selected range of high frequency components. A representative frequency response 6-260 of the integrator and low pass filter stage 6-232 and a representative frequency response 6-261 of the bandpass filter stage 6-230 are depicted in Fig. 80C.

5

10

15

20

25

The output of the bandpass filter stage 6-230 is thereafter subtracted from the output of the integrator and low pass filter stage 6-232 and filtered by the low pass filter stage 6-234. A graph of the total frequency response of the partial integrator stage 6-208, including the low pass filter 6-234, is shown in Fig. 80D. An exemplary output waveform of the partial integrator stage 6-208 is shown in Fig. 84D.

A detailed circuit diagram of a particular embodiment of a partial integrator stage is illustrated in Fig. 79B. In Fig. 79B, a differential input 6-238, 6-239 is received, such as from the equalization stage 6-206. The differential input 6-238, 6-239 is provided to differential amplifier 6-240, configured as shown, which differentially sums its inputs. Differential amplifier 6-240 essentially corresponds to amplifier stage 6-229 shown in Fig. 79.

An output 6-249 from the differential amplifier 6-240 is connected to a pair of current generators 6-241 and 6-242. The first current generator 6-241 comprises a resistor R77 and a PNP

transistor Q61, configured as shown in Fig. 79B. The second current generator 6-242 also comprises a resistor R78 and a PNP transistor Q11, configured as shown in Fig. 79B.

An output from current generator 6-241 is connected to a bandpass filter 6-243. The bandpass filter 6-243 comprises an inductor L3, a capacitor C72 and a resistor R10, configured in parallel as shown in Fig. 79B. The bandpass filter 6-243 essentially corresponds to bandpass filter stage 6-230 of Fig. 79. An output from the other current generator 6-242 is connected to an integrator 6-244. The integrator 6-244 comprises a capacitor C81 and a resistor R66, configured in parallel as shown in Fig. 79B.

An output from the integrator 6-244 is connected through a resistor R55 to a NPN transistor Q31. Transistor Q31 is configured as an emitter-follower, providing isolation with respect to the output of the integrator 6-244, and acting as a voltage source. The emitter of transistor Q31 is connected to a low pass filter 6-245. The low pass filter 6-245 comprises an inductor L6, a capacitor C66 and a resistor R49, configured as shown in Fig. 79B. The integrator 6-244, emitter-follower including transistor Q31, and low pass filter 6-245 essentially correspond to the integrator and low pass filter stage 6-232 shown in Fig. 79. The frequency response of the integrator 6-244 essentially corresponds to the frequency response 6-260 shown in Fig. 80C, while the frequency response of the band pass filter 6-243 essentially corresponds to the frequency response 6-261

shown in Fig. 80C.

5

10

15

20

25

An output from the low pass filter 6-245 and an output from the bandpass filter 6-243 are coupled to a differential amplifier 6-246, configured as shown in Fig. 79B. Differential amplifier 6-246 differentially sums its inputs, and provides a differential output to another low pass filter 6-247. The differential amplifier 6-246 and low pass filter 6-247 correspond essentially to the subtractor and low pass filter stage 6-234 shown in Fig. 79.

Exemplary waveforms for the circuit of Fig. 79B are shown in Fig. 80G. Figure 80G shows first an exemplary input waveform 6-256 as may be provided to differential amplifier 6-240 from, e.g., equalizer 6-206. The next waveform 6-257 in Fig. 80G corresponds to an output from the bandpass filter 6-243 in response to the Fig. 79B circuit receiving input waveform 6-256. The next waveform 6-258 in Fig. 80G corresponds to an output from the low pass filter 6-245 in response to the Fig. 79B circuit receiving input waveform 6-256. Waveform 6-258 shows the effect of operation of the integrator 6-244. The function of low pass filter 6-245 is essentially to provide a delay so as to align the output of the bandpass filter 6-243 and the integrator 6-244 in time at the input of differential amplifier 6-246. Low pass filter 6-245 thereby matches the delays along each input leg of the differential amplifier 6-246 prior to differential summing.

The final waveform 6-259 in Fig. 80G corresponds to an output from the second low pass filter 6-247, after the signals

output from the bandpass filter 6-243 and low pass filter 6-245 have been combined and filtered. Waveform 6-259 typically exhibits considerably improved resolution over the original playback signal read from the magnetic medium.

It should be noted that the partial integration functions described with respect to Figs. 79 and 79B are carried out using differential amplifiers (e.g., differential amplifiers 6-240 and 6-246), thereby providing common mode rejection or, equivalently, rejection of the DC component of the input signal 6-238, 6-239. Another feature of the embodiments shown in Figs. 79 and 79B is the relatively favorable frequency response characteristics exhibited by the partial integration stage. In particular, by combining an integrated signal with a high pass filtered signal (e.g., at subtractor and low pass filter block 6-214 or differential amplifier 6-246), noise is removed from the differentiated and equalized playback signal, but while maintaining relatively rapid response time due in part to the high pass frequency boost provided by the bandpass filter.

A primary function of the combination of the differentiation stage 6-204, the equalization stage 6-206, and the partial integration stage 6-208 is to shape the playback signal 6-220 in an appropriate manner for facilitating data recovery. As can be seen by comparing Figs. 84A and 84D, the resultant signal shown in Fig. 84D is similar to the playback signal 6-220 of Fig. 84A (from which it was derived) but differs therefrom in that the amplitudes of its high and low frequency components have been

equalized and sharp noise-like characteristics removed. A graph of the total frequency response for the combination of the differentiation stage 6-204, the equalization stage 6-206, and the partial integration stage 6-208 is shown in Fig. 80E. A graph of the total group delay response for the same chain of elements is shown in Fig. 80F.

It may be noted that tape drive systems presently exist utilizing equalization and integration of a playback signal in order to facilitate data recovery. However, to a large degree such systems do not suffer from the problems of DC buildup because they typically utilize DC-free codes. As mentioned previously, DC-free codes have the disadvantage of being relatively low in density ratio and hence inefficient. The present invention in various embodiments allows for the use of more efficient coding systems by providing means for eliminating the effects of DC buildup without necessarily using a DC-free code.

The output of the partial integrator stage 6-208 (e.g., the waveform in Fig. 84D) is provided to a data generation stage 6-210 of Fig. 79. A block diagram of the data generation stage 6-210 is shown in Fig. 81. The data generation stage 6-210 comprises a positive peak detector 6-300, a negative peak detector 6-302, a voltage divider 6-304, a comparator 6-306, and a dual edge circuit 6-308. The operation of the circuit show in Fig. 81 may be explained with reference to Fig. 83. In Fig. 83, it is assumed that a recorded bit sequence 6-320 has been read

and eventually caused to be generated, in the manner as previously described, a preprocessed signal 6-322 from the partial integrator stage 6-208. It should be noted that the preprocessed signal 6-322 and various other waveforms described herein have been idealized somewhat for purposes of illustration, and those skilled in the art will appreciate that the actual waveforms may vary in shape and size from those depicted in Fig. 83 and elsewhere.

5

10

15

20

25

The preprocessed signal 6-322 is fed to the positive peak detector 6-300 and the negative peak detector 6-302 which measure and track the positive and negative peaks, respectively, of the preprocessed signal 6-322. The positive peak output signal 6-330 of the positive peak detector 6-300 and the negative peak output signal 6-332 of the negative peak detector 6-302 are depicted in Fig. 83. The positive peak output signal 6-330 and the negative peak output signal 6-332 are averaged by a voltage divider 6-304, which is comprised of a pair of resistors 6-340 and 6-341. output of voltage divider 6-304 is utilized as a threshold signal 6-334 and represents the approximate peak-to-peak midpoint of the preprocessed signal 6-322. The output of the voltage divider 6-304 is provided to a comparator 6-306 which compares the divided voltage with the preprocessed signal 6-322. comparator 6-306 changes states when the preprocessed signal 6-322 crosses the threshold signal 6-334, indicating a transition in the read data from a 1 to 0 or a 0 to 1. The output of comparator 6-306 is shown as output data waveform 6-362 in Fig.

83. As explained in more detail below, the output data waveform 6-362 is fed back to the positive peak detector 6-300 and negative peak detector 6-302 to allow tracking of the DC envelope. The output of the comparator 6-306 is also provided to a dual edge circuit 6-350 which generates a unipolar pulse of fixed duration each time the comparator 6-306 changes states.

The output of the dual edge circuit 6-350 provides clocking and data information from which recovery of the recorded data may be had in a straightforward manner. For example, in a pulse-width modulation ("PWM") technique such as the GCR 8/9 modulation code described previously, each data pulse output from the dual edge circuit 6-350 represents a transition in flux (i.e., a recorded 1-bit), while the lack of data pulse at clock intervals would represent the lack of transition in flux (i.e., a recorded 0-bit). The sequence of recorded bits can thereafter be decoded by decoder 6-24 (shown in Fig. 75) by methods well known in the art to determine the original data.

In order to properly track the envelope caused by the DC portion of the preprocessed signal 6-322, a preferred embodiment feeds back duty cycle information from the output signal 6-362 to the peak detectors. Thus, the output of the comparator 6-306 is fed back to the positive peak detector 6-300 and the negative peak detector 6-302. This process may be explained further by reference to Fig. 82 which depicts a more detailed circuit diagram of the data generator stage 6-210. As shown in Fig. 82, the preprocessed signal 6-322 is provided to the base of

transistors Q2 and Q5. Transistor Q2 is associated with the positive peak detector 6-300, and transistor Q5 is associated with the negative peak detector 6-302. Because the positive peak detector 6-300 and negative peak detector 6-302 operate in an analogous fashion, the duty cycle feedback operation will be explained only with reference to the positive peak detector 6-300, while those skilled in the art will understand by perusal of Fig. 82 and the description below the analogous operation of negative peak detector 6-302.

5

10

15

20

25

Transistor Q2 charges a capacitor C1 when the amplitude of the preprocessed signal 6-322 exceeds the stored voltage of the capacitor C1 (plus the forward bias voltage of the transistor In Fig. 83, it can be seen that the positive peak output signal 6-330 charges rapidly to the peak of the signal 6-322. The output signal 6-362, through feedback, maintains the positive charge on the capacitor C1 when the output signal 6-362 is high and allows the capacitor C1 to discharge when the output signal 6-362 is low. Thus, if the output signal 6-362 is high, the positive charge on capacitor C1 is maintained by transistor Q1 through resistor R2. Preferably, resistors R1 and R2 are selected to be the same value so that charge is added to the capacitor through resistor R2 at the same rate that it is discharged through resistor R1, thus maintaining as constant the net charge on capacitor C1. If, on the other hand, the output signal 6-362 is low, then transistor Q1 is turned off and capacitor C1 is allowed to discharge though resistor R1.

values of capacitor C1 and resistor R1 are preferably selected such that the time constant is slightly faster than the speed of expected of DC buildup so that the capacitor C1 can track the change in DC level as it occurs.

5

10

15

20

25

The output of capacitor C1 is provided to the base of transistor Q3. The voltage level of the emitter of Q3 is a bias voltage level above the output of capacitor C1. Current is drawn through resistor R3 which allows the emitter of transistor Q3 to follow the voltage of the capacitor C1 (offset by the emitter-base bias voltage). Thus, the emitter of transistor Q3 yields positive peak output signal 6-330. It should be noted that transistors Q1 and Q2 are NPN type transistors while Q3 is a PNP type transistor. Thus, the NPN-PNP configuration largely cancels out adverse thermal effects that may be experienced with transistors Q1, Q2 and Q3 and also cancels out the bias voltages associated with their operation.

The negative peak detector 6-302 operates in an analogous fashion to the positive peak detector 6-300 and is therefore not explained in greater detail. The emitter of transistor Q6 yields negative peak output signal 6-332.

As described previously, positive peak output signal 6-330 and negative peak output signal 6-332 are averaged by a voltage divider 6-304 comprised of pair of resistors R4 as shown in Fig. 82 to form threshold signal 6-334. The threshold signal 6-334 therefore constitutes the approximate midpoint of the peak-to-peak value of the preprocessed signal 6-322 and tracks the DC

envelope of the preprocessed signal 6-322 through duty cycle feedback compensation.

Although the duty cycle feedback has been shown in the preferred embodiment as originating from the output of the comparator 6-306, it may be observed that other feedback paths may also be utilized. For example, a similar feedback path may be taken from the output of dual edge circuit 6-308 if a flip/flop or other memory element is placed at the output of the dual edge circuit 6-308. Also, other means for measuring duty cycle and adjusting the threshold signal to track the DC envelope may be utilized.

A preferred technique such as described generally in Figs. 78 and 79 includes the step of differentiation of the playback signal prior to partial integration, followed thereafter by the step of DC tracking. The preferred method is particularly suitable for systems having a playback signal with relatively poor resolution, and may be advantageously applied, for example, to reading information stored in a GCR format. In one aspect of the preferred method, the initial step of differentiation reduces the low frequency component from the incoming playback signal. In another aspect of the preferred method, the partial integration stage results in restoration or partial restoration of the playback signal while providing rapid response due to the high pass boost (e.g., from the bandpass filter stage). The preferred method may be contrasted with a method in which integration of the playback signal is carried out initially

(i.e., prior to differentiation), which may lead to an increased size of DC component and a correspondingly more difficult time in tracking the DC component.

It will be appreciated that the various circuits and methods described herein are not limited to magneto-optical systems but may also be useful in systems for reading data on stored tapes and other types of disks as well and, in a more general sense, in any system (whether or not a data storage system) for processing electrical signals in which it is desired to mitigate the effects of DC buildup.

Data Storage and Other Aspects of Data Retrieval

5

10

15

20

25

In Fig. 85, during the write mode, a data source 7-10 transmits data to an encoder 7-12. The encoder 7-12 converts the binary data into binary code bits. The code bits are then transmitted to a laser pulse generator 7-14, where the code bits are converted to energizing pulses for turning a laser 7-16 on and off. In the preferred embodiment, a code bit "1" indicates that the laser will be pulsed on for a fixed duration independent of the code bit pattern. However, depending on the laser and optical medium being used, performance may be enhanced by adjusting the occurrence of the laser pulse or by extending the otherwise uniform pulse duration. The output of laser 7-16 heats localized areas of an optical medium 7-18, which is being exposed to a magnetic flux that sets the polarity of the magnetic material on the optical medium 7-18. During reads of the optical medium, a laser beam is impinged on the surface of the medium.

The polarization of the reflected laser beam will be dependent upon the polarity of the magnetic surface of the optical medium.

During the read mode, the reflected laser beam will be inputted into an optical reader 7-20, where the read code output will be sent to the waveform processor 7-22. The processed read code will be sent to a decoder 7-24, where output data will be transmitted to a data output port 7-26 for transmission.

5

10

15

20

25

Fig. 86 depicts the differences between the laser pulsing in GCR 8/9 and RLL 2,7 code formats. In GCR 8/9, a cell 7-28 is defined as a code bit. For GCR 8/9, nine cells or code bits are equal to eight data bits. Thus, cells 7-30 through 7-41 each correspond to one clock period 7-42 of clock waveform 7-45. For a 3½" optical disc rotating at 2,400 revolutions per minute (RPM) with a storage capacity of 256 Mbytes, clock period 7-42 will typically be 63 nanoseconds or a clock frequency of 15.879 MHz. GCR data waveform 7-47 is the encoded data output from the encoder 7-12. A representative data sequence is depicted in FIG. 86. The code data sequence "010001110101" is shown in GCR data 7-50 through 7-61, where GCR data 7-50 is low. GCR data 7-51 is high. GCR data 7-52 is high and so forth for GCR data 7-53 through 7-61. Pulse GCR waveform 7-65 is the output from laser pulse generator 7-14 and inputted into laser 7-16. In practicing the invention, a non-return-to-zero driving signal is utilized to energize the magnetic recording head. Thus, the magnetization of the previously erased optical medium reverses polarity when, in the presence of an external magnetic field of opposite polarity

to the erased medium, the laser is pulsed on with sufficient energy to exceed the Curie temperature of the medium. Pulse GCR waveform 7-65 as shown has not been adjusted in time or duration to reflect performance enhancement for specific data patterns. Pulse GCR 7-67 through 7-78 reflect no pulse when the corresponding GCR data 7-47 is low and reflect a pulse when GCR data 7-47 is high. For example, pulse GCR 7-67 has no pulse because GCR data 7-50 is low. Conversely, pulse GCR 7-68, 7-69, 7-70, and 7-71 show a laser pulse because GCR data 7-51 through 7-54 are each high, respectively, and similarly for pulse GCR 7-72 through 7-78. Under the depicted uniform scenario, pulse GCR pulse width 7-65 is uniform for pulse GCR 7-68, 7-69, 7-70, 7-71, 7-73, 7-76, and 7-77. For the preferred embodiment, this pulse width is 28 nanoseconds. Each laser pulse corresponding to pulse GCR waveform 7-65 creates a recorded pit on optical medium 7-18. Recorded pit 7-82 corresponds to pulse GCR 7-68. Recorded pit 7-83 corresponds to pulse GCR 7-69. Similarly, recorded pits 7-84 through 7-88 correspond to pulse GCR 7-70, 7-71, 7-73, 7-76, and 7-77, respectively.

5

10

15

20

25

Because of thermal dissipation and spot size on the optical medium 7-18, the recorded pits 7-80 are wider in time than pulse GCR 7-65. Successive recorded pits 7-80 merge together to effectively create a larger recorded pit. Thus, the elongated recorded pit has a leading edge, corresponding to the first recorded pit, and a trailing edge, corresponding to the last recorded pit. For example, the pit created by recorded pits 7-82

through 7-85 has a leading edge from recorded pit 7-82 and a trailing edge from pit 7-85. Under the GCR 8/9 data format, a leading edge corresponds to GCR data 7-47 going high, and a trailing edge corresponds to GCR data 7-47 going low. Hence, for data pattern "10001" as shown by GCR data 7-51 through 7-55, a leading edge occurs for the first "1" (GCR data 7-47 going high) as shown by recorded pit 7-82; and, at the end of the GCR data 7-54, a trailing edge occurs as shown by recorded pit 7-85, because GCR data 7-55 is low.

5

10

15

20

25

Playback signal 7-90 will be low when recorded pits 7-80 shows no pits. At the leading edge of a pit, playback signal 7-90 will rise and remain high until the trailing edge of the pit is reached. The signal will go low and remain low until the next pit. For example, playback signal 7-91 is low because GCR data 7-50, which is low, did not create a pit. At the front edge of recorded pit 7-82, playback signal 7-90 has a leading edge as shown in playback signal 7-92. Playback signal 7-90 will then remain unchanged until a trailing edge occurs on a recorded pit. For example, because recorded pits 7-83 and 7-84 show no trailing edge, playback signals 7-93 and 7-94 remain high. The signal remains high during playback signal 7-95 because of recorded pit 7-85. However, because GCR data 7-55 is low, recorded pit 7-85 creates a trailing edge. Thus, playback signal 7-96 decays. The signal will decay to "O" until a recorded pit occurs, creating a leading edge. Thus, with the occurrence of recorded pit 7-86, which corresponds to GCR data 7-56 being high, playback signal

7-97 rises. Because there is no immediate successor to recorded pit 7-86 when GCR data 7-57 is low, playback signal 7-98 decays. Playback signal 7-99 remains low because there is no recorded pit when GCR data 7-58 is low. With GCR data 7-59 and 7-60 being high, recorded pits 7-87 and 7-88 overlap creating one larger pit. Thus, playback signal 7-100 rises and playback signal 7-101 remains high. Playback signal 7-102 falls at the trailing edge of recorded pit 7-88 when GCR data 7-61 is low.

For RLL 2,7 a cell consists of two data bits, which corresponds to two clock periods 7-121 of 2F clock waveform 7-120. For a 256 Mbyte disc, an RLL 2,7 encoding format will require a 2F clock pulse width 7-121 of 35.4 nanoseconds or a clock frequency of 28.23 MHz. The calculation of this value is straightforward. In order to maintain the same disc density, the GCR 8/9 and RLL 2,7 encoding formats must contain the same amount of information in the same recording time. Because two code bits are required per data bit in the RLL 2,7 format, it requires a clock frequency of 2 * (8/9) that of the GCR data format. The GCR data format records nine bits of code bits per eight bits of data. Thus, the GCR data bit clock is nine- eighths of the clock period 7-42. Thus, for a GCR clock period 7-42 of 63 nanoseconds, the RLL 2,7 pulse width 7-121 must be 35.4 nanoseconds in order to maintain the same disc density.

The RLL 2,7 data waveform 7-122 reflects two code bits per cell. For example, RLL 2,7 data 7-124 shows a data pattern "00" while RLL 2,7 data 7-125 shows a data pattern "10". In this data

format, a "1" represents a transition in data. Thus, RLL 2,7 data 7-125 goes high when the "1" occurs in the data pattern. Similarly, RLL 2,7 data 7-126 goes low when the "1" occurs in the data pattern. While a "O" occurs, RLL 2,7 data 7-122 remains in the same state. Pulsed 2,7 waveform 7-137 reflects the pulsing of laser 7-16 corresponding to RLL 2,7 data 7-122. Thus, for RLL 2,7 data 7-125 and 7-126, during the period when that signal is high, pulsed 2,7 waveform 7-140 and 7-141 is high. Because of the thermal elongation of the pit, pulsed 2,7 waveform 7-141 goes low prior in time to RLL 2,7 data 7-126. For longer data patterns of "O", the pulsing must remain on. For example, during the data pattern "10001" as shown in RLL 2,7 data 7-128 and 7-129, pulsed 2,7 waveform 7-143 and 7-144 remains high longer than pulsed 2,7 waveform 7-140 and 7-141. For data patterns of successive "O", the pulsed 2,7 waveform 7-137 can be pulsed as separate pulses. For example, for the data pattern "1000001", RLL 2,7 data 7-132, 7-133, and 7-134 can be pulsed in two separate pulses as shown in pulsed 2,7 7-147, 7-148, and 7-149.

5

10

15

20

25

As with the GCR 8/9 format, recorded pits 7-160 show thermal elongation. For example, recorded pit 7-162 is wider in time than the pulse from pulsed 2,7 waveform 7-140 and 7-141; a similar result may be seen for recorded pit 7-163. Again, playback signal 7-167, depicted by playback signal 7-168 through 7-174, goes high on leading edges of recorded pits 7-160, decays on trailing edges of recorded pits 7-160, and remains constant during the presence or absence of pits.

The pulsed GCR code can be improved by correcting predictable position shifts. Fig. 87 shows the timing diagram for the write compensation of the laser pulse generator 7-14. Experimental testing showed that recording early when the laser 7-16 is off for two bits or greater enhances performance. Clock waveform 7-176 is the code bit clock used for clocking data 7-177, 7-203, and 7-229, which show the worst case data patterns for enhancement. Other patterns can be corrected, but will suffer in signal amplitude. Data 7-180 through 7-184 correspond to the data sequence "10100". The uncompensated pulse waveforms 7-188 through 7-192 correspond to this data pattern without write compensation. Uncompensated pulse waveforms 7-189 and 7-191 occur in the second half of the clock period. After write compensation, the output of laser pulse generator 7-14 corresponds to compensated pulse waveform 7-195, where compensated pulse waveforms 7-197 and 7-198 remain unchanged, and a shortened off-period for compensated pulse waveform 7-199 provides an earlier compensated pulse waveform 7-200. During compensated pulse 7-201, laser 7-16 remains off for a longer duration than uncompensated pulse 7-192. Similarly, for data 7-206 through 7-209, corresponding to data pattern "1100", uncompensated pulse waveform 7-211 would be off for uncompensated pulse waveform 7-213 followed by two pulses, i.e., uncompensated pulse waveforms 7-214 and 7-216. Again, the write compensation circuit adjusts compensated pulse waveform 7-220 so that compensated pulse waveform 7-225 will occur closer in time to compensated pulse

5

10

15

20

25

waveform 7-223 so that compensated pulse waveform 7-224 is shorter than uncompensated pulse waveform 7-215. Finally, data 7-231 through 7-235, corresponding to the data pattern "00100", have uncompensated pulse waveform 7-237 occurring at uncompensated pulse waveform 7-240. Write compensation would move compensated pulse waveform 7-243 earlier in time to compensated pulse waveform 7-246.

5

10

15

20

25

Fig. 88 shows the schematic diagram of the write compensation circuit, which comprises data pattern monitor 7-248, write compensation pattern detector 7-249, and delay circuit 7-269. Data pattern monitor 7-248 is a serial shift register that sequentially clocks encoded data from encoding means 7-12. The last five clocked in data bits are sent to write compensation pattern detector 7-249, where they are analyzed for determining whether to pulse the laser earlier than normal.

Data pattern monitor 7-248 consists of data sequence D flip-flops 7-250 through 7-256. Encoded data is input into the D port of data sequence D flip-flop 7-250, whose Q output WD1 becomes the input of the D port of data sequence D flip-flop 7-251. This clocking continues through data sequence D flip-flops 7-252 through 7-256, whose Q output WD7 is the data sequence delayed by seven clock periods from when it was first input into data pattern monitor 7-248. The Q outputs WD1, WD2, WD3, WD4, and WD5 of data sequence D flip-flops 7-250 through 7-254, respectively, represent the last five of the last seven data bits

inputted into a data pattern monitor 7-248. These five bits are

sent to a write compensation pattern detector 7-249, where they are compared to predetermined data patterns; and, if they match, an enable write signal is sent to a delay circuit 7-269 to indicate that the laser pulse is to occur earlier than normal.

5

10

15

20

25

The first data pattern is detected by inverting the Q data WD1, WD2, WD4, and WD5 from data sequence D flip-flops 7-250, 7-251, 7-253, and 7-254, respectively, through data inverters 7-260, 7-261, 7-262, and 7-263, respectively. The outputs of these inverters are AND'ed with the output from data sequence D flip-flop 7-252 in detect AND gate 7-264. Thus, when a sequence "00100" occurs, the output of detect AND gate 7-264 goes high, indicating that a detect of the data pattern occurred. Similarly, the second data pattern is detected by inverting the Q outputs WD1, WD2, and WD4 from data sequence D flip-flops 7-250, 7-251, and 7-253, respectively, through the data inverters 7-282, 7-283, and 7-284, respectively, and AND'ing these inverted outputs with the outputs WD3 and WD5 of data sequence D flip-flops 7-252 and 7-254 in detect AND gate 7-286. Thus, a data pattern of "10100" will trigger a high from detect AND gate 7-286, indicating a detect. The third data sequence is detected by inverting the Q outputs WD1 and WD2 from data sequence D flip-flops 7-250 and 7-251, respectively, through data inverters 7-287 and 7-288 and AND'ing these inverted outputs with the Q outputs WD3 and WD4 from data sequence D flip-flops 7-252 and 7-253, respectively, in data detect AND gate 7-289. Thus, the data pattern of "1100" will trigger a detect from detect AND gate 7-289, indicating the

presence of the data. The data pattern detect outputs of detect AND gates 7-264, 7-286, and 7-289 are OR'ed in detected pattern OR gate 7-266, whose output goes high when one of the three data patterns is detected. The detected pattern output is clocked in enable write D flip- flop 7-268, whose Q output, the enable write signal, is then sent to delay circuit 7-269.

5

10

15

20

25

Delay circuit 7-269 takes the clocked data output WD4 of data sequence D flip-flop 7-253 and simultaneously inputs it into delay circuit 7-276 and not-delay-select AND gate 7-274. The delayed output of delay circuit 7-276 is inputted into delay-select AND gate 7-272. The enable write signal from write compensation pattern detector 7-249 will enable either delay-select AND gate 7-272 or not-delay-select AND gate 7-274. When the enable write signal is low, which indicates that one of the three data patterns has not occurred, it is inverted by enable write inverter 7-270. This allows the delayed data from delay circuit 7-276 to be clocked. on the other hand, if enable write is high, which indicates that one of the three data patterns has occurred, then the not-delay-select AND gate 7-274 allows the transmission of the data from data sequence D flip-flop 7-253, which is undelayed. The outputs from delay-select AND 7-272 and not-delay-select AND gate 7-274 are OR'ed in data OR gate 7-278, where it is outputted from delay circuit 7-269. Although prior discussions about the write compensation circuit or timing indicated that for the three data patterns, the write pulse would occur 7-10 nanoseconds earlier,

in actual implementation, data is delayed 7-10 nanoseconds for all data but the three data patterns. The delay of delay circuit 7-276 is set between 7 to 12 nanoseconds for the frequency of the preferred embodiment.

When recording lower frequency data patterns, the resultant magneto-optical signal has a slower rise time than fall time. This causes the final output from the waveform processor 7-22 to have degraded amplitude on positive peaks, which can be corrected by recording with higher effective power at the leading edge of the data pattern. For the preferred embodiment, the data pattern "000111" will trigger a wide-write signal during the second "1" of the data pattern, thereby pulsing the laser during its normal off period.

In Fig. 89, clock waveform 7-301 clocks data waveform 7-303 through the laser pulse generator 7-14 for the data pattern "000111". As depicted by data 7-305 through 7-310, the laser pulse generator 7-14 generates pulse waveform 7-312 with pulses 7-314, 7-315, and 7-316 when data waveform 7-303 is a "1". During the second "1" of this data pattern, the laser pulse generator 7-14 will turn on for the increase power waveform 7-318 and generate a pulse 7-320. The output laser pulse waveform 7-322 results from the OR of pulse 7-312 and the increase power waveform 7-318 that creates laser pulses 7-323, 7-324, and 7-325. Under normal operations, laser pulse 7-324 would be off during the first half of the clock period. However, under this particular data pattern, keeping the laser on for the laser

pulses 7-323 and 7-324, effectively increases the power fifty percent during this time period.

5

10

15

20

25

In Fig. 90, amplitude asymmetry correction circuit 7-291 generates the write-wide pulse 7-292 (corresponds to increase power waveform 7-318 in Fig. 89), which will be OR'ed with the laser pulse output from delay circuit 7-269 (corresponds to pulse waveform 7-312 in Fig. 89) in laser pulse OR gate 7-280 (Fig. 88), resulting in output laser pulse waveform 7-322. The data pattern monitor 7-248 operates as shown in Fig. 88. The Q outputs WD2, WD3, WD4, WD5, WD6, and WD7 of data sequence D flip-flops 7-251 through 7-256, respectively, are 5 inputted into the amplitude asymmetry correction circuit 7-291, where the outputs WD5, WD6, and WD7 of data sequence D flip-flops 7-254, 7-255, and 7-256, respectively, are inverted in data inverters 7-293, 7-294, and 7-295, respectively. The outputs of data inverters 7-293, 7-294, and 7-295 and data sequence D flip-flops 7-251, 7-252, and 7-253 are AND'ed in detect AND gate 7-296. The output of detect AND gate 7-296 indicates a detected pattern form "000111", which will be clocked out of write-wide D flip-flop 7-297 at the next clock 7-301.

The waveform output of the optical reader 7-20 will be degraded as a function of frequency and data pattern. Amplitude and timing can be enhanced by processing the signal through the waveform processor 7-22. The asymmetry of the rise and fall times of an isolated pulse can be improved by summing an equalized, differentiated signal with its derivative. In Fig. 91,

magneto-optical signal 7-327 is differentiated by a differential amplifier 7-329. The differentiated signal is inputted into an equalizer 7-331, where it is equalized by 5 dB in the preferred embodiment, and the amplitude is equalized as a function of frequency. The derivative of the equalized signal is taken by a derivative processor 7-333 and summed with the equalized signal in an adder 7-335. The output of the adder 7-335 is the read signal 7-337.

5

10

15

20

25

Fig. 92 shows the timing diagram for the dynamic threshold circuit shown in Fig. 93.

Read signal 7-337 will contain an overshoot produced by the pulse slimming. Because this overshoot is predictable, the threshold for the read circuitry can be increased during the overshoot to prevent false data reads during positive peaks 7-339, 7-340, 7-341, and 7-342, and during negative peaks 7-343, 7-344, and 7-345 of read signal 7-337. Threshold waveform 7-348 is switched high during positive peaks. Threshold waveforms 7-349, 7-350, and 7-351 are high during positive peaks 7-339, 7-340, and 7-341, respectively. Threshold waveforms 7-352, 7-353, and 7-354 are low during negative peaks 7-343, 7-344, and 7-345, respectively. Each peak, whether positive or negative, of the read signal 7-337 generates peak waveform 7-356, which is a short clocking pulse that occurs shortly after the read signal 7-337 peaks. Peaks 7-339, 7-343, 7-340, 7-344, 7-341, 7-345, and 7-342 of the read signal 7-337 generate peak waveforms 7-358 through 7-364, respectively.

As shown in Fig. 93, threshold waveform 7-348 is inputted into the D port of threshold delay D flip-flop 7-366. Peak waveform 7-356 clocks threshold waveform 7-348 through this flip-flop. Delayed threshold waveform 7-368 is the Q output of threshold delay D flip-flop 7-366, which is exclusively OR'ed with threshold waveform 7-348 in threshold-exclusive OR gate 7-370. The EXOR signal 7-372 is the output of thresholdexclusive OR gate 7-370. The EXOR signal 7-372 has twice the frequency of the original threshold waveform 7-348. The EXOR signal 7-372 is inputted into the D port of EXOR D flip-flop 7-374, where it is clocked at read clock 7-375. Fl waveform 7-376 is the Q output of EXOR D flip-flop 7-374. Read clock waveform 7-375 has a leading edge during high pulses of EXOR signal 7-372, except when EXOR signal 7-372 is low for more than one read clock waveform 7-375. Thus, the Fl waveform 7-376 is high except for the time between the first read clock 7-375 pulse after the EXOR signal 7-372 is low for more than one read clock 7-375 and the next EXOR signal 7-372 pulse.

5

10

15

20

25

Fl waveform 7-376 is OR'ed with the EXOR signal 7-372 in envelope OR gate 7-378. The output of envelope OR gate 7-378 is high except for the time from the first read clock 7-375 after the EXOR signal 7-372 has been low for more than one clock period until the signal 7-372 goes high again. The output of envelope OR gate 7-378 is clocked through the D input of envelope D flip-flop 7-379, which is clocked by read clock 7-375. The Q output of the envelope D flip-flop 7-379 is F2 waveform 7-381. The F2 waveform

7-381 is high except from the second read clock 7-375 period after the EXOR signal 7-372 goes low until the next read clock 7-375 clocks a high for the EXOR signal 7-372. The F2 waveform 7-381 is inverted through the F2 inverter 7-383 and NOR ed with the EXOR signal 7-372 in dynamic threshold NOR gate 7-385 to produce the dynamic threshold waveform 7-387. The dynamic threshold waveform 7-387 is high any time the EXOR signal 7-372 is low, except when the F2 waveform 7-381 is low. Thus, the dynamic threshold waveform 7-387 has an on-time less than a half read clock 7-375 period except when the EXOR signal 7-372 is low on the next read clock 7-375 period. For this exception, the dynamic threshold waveform 7-387 stays high from the end of the EXOR signal 7-372 until the second read clock 7-375 pulse.

The dynamic threshold waveform 7-387 is used to forward or reverse bias a biasing diode 7-389. When dynamic threshold 7-387 is high, biasing diode 7-389 is reverse biased. Conversely, when the dynamic threshold waveform 7-387 is low, the biasing diode 7-389 is forward biased.

When the dynamic threshold waveform 7-387 forward biases the biasing diode 7-389 (i.e., is low), the potential of the filter bias signal 7-390 is higher by the junction voltage of the biasing diode 7-389. This potential is 0.6 volts for standard devices. The 5-volt supply voltage drops across the limiting resistor 7-393 to the potential of the filter bias signal 7-390, because the voltage across the charging capacitor 7-394 is the difference between the filter bias signal 7-390 and ground. The

charging capacitor 7-394 charges up to this potential, which is also the base voltage of a transistor 7-395. This turns on the transistor 7-395, causing the voltage on the emitter of transistor 7-395 to be 1.4 volts. Because the emitters of the transistors 7-395 and 7-396 are connected, the emitter voltage of the transistor 7-396 is less than the 2.5-volt base voltage of the transistor 7-396. Accordingly, the transistor 7-396 is off so that the collector voltage across the collector resistor 7-397 produces an increase threshold waveform 7-399 which is 0 volts (ground). The increase threshold waveform 7-399 is the signal that increases the threshold of the read signal 7-377 detector during periods of overshoot.

When the dynamic threshold waveform 7-387 is high, the biasing diode 7-389 is reversed biased, thereby no longer taking the base of the transistor 7-395 to 6 volts. When the dynamic threshold waveform 7-387 goes high, the charging capacitor 7-394 starts charging, creating a potential at the base of the transistor 7-395 that will rise exponentially up to the supply voltage, 5 volts. As the filter bias signal 7-390 rises in voltage, the voltage at the emitter of the transistor 7-395 increases, which equally increases the emitter voltage of the transistor 7-396. When this emitter voltage exceeds the base voltage by the junction potential across the emitter-to-base junction of the transistor 7-396, the transistor 7-396 is turned on. Turning on the transistor 7-396 causes the increase threshold waveform 7-399 to go high.

Under normal operations, the dynamic threshold waveform 7-387 is pulsed as described above. During normal read signals, the dynamic threshold 7-387 is on for a period equivalent to the on-period of read clock 7-375. The charge time for the voltage across the charging capacitor 7-394 to exceed the base voltage of 2.5 volts is longer than this half clock period of time. Thus, under normal circumstances, the increase threshold waveform 7-399 remains low. However, during periods of overshoot, the dynamic threshold waveform 7-399 is on for a longer period of time, thereby allowing the charging capacitor 7-394 to charge to a voltage that exceeds 2.5 volts, thereby triggering the increase threshold waveform 7-399 to go high.

In Fig. 94, a host computer 7-410, which serves as a source and utilizer of digital data, is coupled by interface electronics 7-412 to a data bus 7-414. As host computer 7-410 processes data, and it wants to access external memory from time to time, a connection is established through interface electronics 7-412 to data bus 7-414. Data bus 7-414 is coupled to the input of a write encoder 7-416 and the input of a write encoder 7-418. Preferably, write encoder 7-416 encodes data from bus 7-414 in a low-density (i.e., ANSI) format; and write encoder 7-418 encodes data from data bus 7-414 in a higher density format. The Draft Proposal for 90MM Rewritable Optical Disc Cartridges for Information Interchange, dated 1 January 1991, which describes the ANSI format, is incorporated herein by reference. The outputs of write encoders 7-416 and 7-418 are coupled alternatively through a

switch 7-422 to the write input of a magneto-optical read/write head 7-420. The read output of head 7-420 is coupled alternatively through a switch 7-424 to the inputs of a read decoder 7-426 and a read decoder 7-428. Read decoder 7-426 decodes data in the same format, i.e., ANSI, as write encoder 7-416; and read decoder 7-428 decodes data in the same format as write encoder 7-418. Preferably, the encoding and decoding technique disclosed above is employed to implement write encoder 7-418 and read decoder 7-428. The outputs of decoders 7-426 and 7-428 are connected to data bus 7-414.

Responsive to a mode-selection signal, switch-control electronics 7-430 set the states of switches 7-422 and 7-424 into either a first mode or a second mode. In the first mode, write encoder 7-418 and read decoder 7-428 are connected between data bus 7-414 and read/write head 7-420. In the second mode, write encoder 7-416 and read decoder 7-426 are connected between data bus 7-414 and read/write head 7-420. Read/write head 7-420 reads encoded data from and writes encoded data to a 90 millimeter optical disc received by a replaceable optical disc drive 7-432, which is controlled by disk-drive electronics 7-434. Read/write head 7-420 is transported radially across the surface of the disc received by disc drive 7-432 by position-control electronics 7-436.

When a 90 millimeter disc in a high-density format is received by disc drive 7-432, a mode-selection signal sets the system in the first mode. As a result, data from host computer

7-410, to be stored on the disc, is organized by interface electronics 7-412 and encoded by write encoder 7-418; data read from the disc is decoded by read decoder 7-428, reorganized by interface electronics 7-412, and transmitted to host computer 7-410 for processing.

When a 90 millimeter disc in the low-density, ANSI format is received by disc drive 7-432, a mode-selection signal sets the system in the second mode. As a result, data from host computer 7-410, to be stored on the disc, is organized by interface electronics 7-412 and encoded by write encoder 7-416; data read from the disc is decoded by read decoder 7-426, reorganized by interface electronics 7-412, and transmitted to host computer 7-410 for processing.

Preferably, irrespective of the format used to store data, the mode-selection signal is stored on each and every disc in one format, e.g., the low-density, ANSI format, and the system defaults to the corresponding mode, e.g., the second mode. The mode-selection signal could be recorded in the control track zone in ANSI format. When a disc is installed in disc drive 7-432, disk-drive electronics 7-434 initially controls position-control electronics 7-436 to read the area of the disc on which the mode-selection signal is stored. Read decoder 7-426 reproduces the mode-selection signal, which is applied to switch-control electronics 7-430. If the installed disc has the low-density, ANSI format, then the system remains in the second mode when the mode-selection signal is read. If the installed disc has the

high-density format, then the system switches to the first mode when the mode-selection signal is read.

In certain cases, it may be desirable to modify the laser for the first and second modes. For example, different laser frequencies could be used or different laser-focussing lens systems could be used for the different modes. In such case, the mode-selection signal is also coupled to read/write head 7-420 to control the conversion between frequencies or optical-lens focussing systems, as the case may be.

5

10

15

20

25

It is preferable to organize the data stored in both formats to have the same number of bytes per sector, i.e., in the case of ANSI, 512 bytes. In such case, the same interface electronics 7-412 can be used to organize the data stored on and retrieved from the disks in both formats.

In accordance with the invention, the same read/write head 7-420, position-control electronics 7-436, optical disc drive 7-432, disk-drive electronics 7-434, interface electronics 7-412, and data bus 7-414 can be employed to store data on and retrieve data from optical disks in different formats. As a result, downward compatibility from higher- density formats that are being developed as the state of the art advances, to the industry standard ANSI format can be realized using the same equipment.

With reference to FIGS. 95, 96, and 98, the preferred format of the high-density optical disc will now be described. There are ten thousand tracks, namely tracks 0 to 9999, arranged in 21 zones. Each track is divided into a plurality of sectors. There

are a different number of sectors in each zone, increasing in number moving outwardly on the disc. The frequency of the data recorded in each zone is also different, increasing in frequency moving outwardly on the disc. (See FIGS. 95 and 98 for a description of the number of tracks in each zone, the number of sectors in each zone, and the recording frequency in each zone.) In contrast to the low-density disks, the format markings are erasably recorded on the disc using the same recording technique as is used for the data, preferably magneto-optical (MO). These format markings comprise sector fields, header fields for each sector, and control tracks. In contrast to the header fields and the data, the sector fields for all the zones are recorded at the same frequency. A description of the preferred embodiment of the sector format follows.

15 Sector Layout.

5

10

20

25

A sector comprises a sector mark, a header, And a recording field in which 512 user data bytes can be recorded. The recording field can be empty or user-written. The total length of a sector is 721 bytes (one byte is equivalent to nine channel bits) of header and recording fields at a frequency that varies from zone to zone, plus 80 channel bits of sector mark at a fixed frequency, i.e., the same frequency for each zone. Tolerances are taken up by the buffer, i.e., the last field of the sector. The length of the header field is 48 bytes. The length of the recording field is 673 bytes.

Sector Mark (SM)

The sector mark consists of a pattern that does not occur in data, and is intended to enable the drive to identify the start of the sector without recourse to a phase-locked loop. The sector marks are recorded with a fixed frequency of 11.6 MHz for all zones. The length of the sector mark is 80 channel bits. The following diagram shows the pattern in the NRZI format.

1111 1111 1100 0000

1111 1100 0000 0000

0000 1111 1100 0000

1111 1100 0000 1111

1111 1100 1001 0010

VFO Fields.

5

10

15

There are four fields designated either, VFO1, one of two VFO2, or VFO3 to give the voltage-controlled oscillator of the phase locked loop of the read channel a signal on which to phase lock. The information in VFO fields, VFO1 and VFO3 is identical in pattern and has the same length of 108 bits. The two fields designated VFO2 each have a length of 72 bits.

Address Mark (AM).

The address mark consists of a pattern that does not occur in data. The field is intended to give the disc drive the drive-byte synchronization for the following ID field. It has a length of 9 bits with the following pattern:

110000101

25 ID Fields.

The three ID fields each contain the address of the sector,

i.e., the track number and the sector number of the sector, and CRC bytes. Each field consists of five bytes with the following contents:

1st byte - Track MSByte

2nd byte - Track LSByte

3rd byte -

5

10

20

bit 7 and 6

00 - ID Field 0

01 - ID Field 1

10 - ID Field 2

11 - not allowed

bit 5 - zero.

bit 4 through bit 0 - binary sector number

4th and 5th bytes - CRC field

The CRC bytes contain CRC information computed over the first three bytes according to FIG. 99.

Postambles (PA)

The postamble fields are equal in length, both having

9 bits. There is a postamble following ID3 and a postamble

following the data field. A postamble allows closure of the last

byte of the preceding CRC or data field. The postambles (PA) have

9 bits of the following pattern:

10 00100 01

Gaps.

25 GAP 1 is a field with a nominal length of 9 channel bits, and GAP 2 is of 54 channel bits. GAP 1 shall be zeroes and GAP 2

not specified. GAP 2 is the first field of the recording field, and gives the disc drive some time for processing after it has finished reading the header and before it has to write or read the VFO3 field.

5 Sync.

The sync field allows the drive to obtain byte synchronization for the following data field. It has a length of 27 bits and is-recorded with the bit pattern:

101000111 110110001 111000111

10 Data Field.

15

25

The data field is used to record user data. It has a length of 639 bytes (one byte = 9 channel bits) and comprises:

512 bytes of user data;

- 4 bytes the contents of which are not specified by his standard and shall be ignored in interchange;
 - 4 bytes of CRC parity;
 - 80 bytes of ECC parity; and
 - 39 bytes for resynchronization.

User Data Bytes.

The user data bytes are at the disposal of the user for recording information.

CRC and ECC Bytes.

The Cyclic Redundancy Check (CRC) bytes and Error Correction Code (ECC) bytes are used by the error detection and correction system to rectify erroneous data. The ECC is a Reed-Solomon code of degree 16.

Resync Bytes.

5

10

15

20

25

The resync bytes enable a drive to regain byte synchronization after a large defect in the data field. It has a length of 9 bits with the following pattern:

100010001

Their content and location in the data field is as follows The resync field is inserted between bytes A15n and A15n+l, where $1 \le n \le 39$.

Buffer Field.

The buffer field has a length of 108 channel bits.

The 8-bit bytes in the three address fields and in the data field, except for the resync bytes, are converted to channel bits on the disc according to FIGS. 100a and 100b. All other fields in a sector are as defined above in terms of channel bits. The recording code used to record all data in the information regions on the disc is Group-Code (GCR 8/9).

In Fig. 97, the write data is decoded by the RLL 2,7 encoder/decoder (ENDEC) 7-502 for the low-capacity, 128 Mbyte (low-density) mode. The GCR encoder/decoder (ENDEC) 7-504 is used in the high-capacity, 256 Mbyte (high-density) mode. The write pulse generator 7-506 produces a pulse width of 86 nsec with write power level varying from 7.0 mW to 8.5 mW from the inner to the outer zones for the low-capacity mode. For the high-capacity mode, the write pulse generator 7-507 decreases the pulse width to 28 nsec, but the write power is increased to a level that varies from 9.0 mW to 10.0 mW from the inner to the outer zones.

The select circuit 7-509 alternatively couples pulse generator 7-506 or 7-507 to the laser diode driver of the magneto-optical read/write head depending upon the state of an applied control bit HC. Control bit HC equals zero in the low- capacity mode and equals one in the high-capacity mode. The appropriate output is selected to drive the laser diode driver. The write clock is generated by the frequency synthesizer in the data separator 7-508. The frequency is set to 11.6 MHz for the low-capacity mode and 10.59 MHz to 15.95 MHz from inner to outer zones for the high-capacity mode.

During the playback, the preamplifier 7-510, which is fed by the photodiodes in the magneto-optical read/write head, can be selected for the sum mode (A+B) or the difference mode (A-B). For the sum mode, the preamplifier 7-510 reads the reflectance change due to the preformatted pits. These pits are stamped in the RLL 2,7 code and identify the sector mark, VFO fields, and track sector data. There are 512 user bytes of data recorded in each preformatted sector. There are 10,000 tracks, segmented into 25 sectors, which totals 128 Mbytes of data for the low-capacity mode. In the high-capacity mode, the disc is formatted with GCR code. There are 40 sectors at the inner zone (i.e., zone 1), and the number of sectors gradually increases to 60 sectors at the outer zone (i.e., zone 21). Again, 512 bytes of user data are recorded in each sector, which totals 256 Mbytes of data.

The writing of data in the RLL 2,7 mode is also pit-type recording. When these pits are read in the difference mode (A-B),

the waveform appearing at the output of the preamplifier is identical to the preformatted pits when read in the sum mode (A+B). This signal only needs to be differentiated once by the dv/dt amplifier 7-512. A pulse corresponding to approximately the center of each pit is generated by digitizing the nominal output (VNOM P, VNOM N) from the programmable filter. The filter cutoff frequency is set to 5.4 MHz for the low-capacity mode responsive to the HC control bit. The filtered signal is digitized and passed through the deglitching logic circuit 7-518. The resulting signal called HYSTOUT (Hysteresis) is fed to the data separator 7-508. The signal is also coupled to the system controller to detect the sector marks. Responsive to the HC control bit, the PLO divider of the frequency synthesizer in data separator 7-508 is set to 3, and the synthesizer is set to 11.6 MHz. The sync data is identical to the original data encoded by the RLL ENDEC 7-502. This is coupled to the RLL ENDEC 7-502 for decoding purposes and then to the data bus to be utilized.

5

10

15

20

25

In the high-capacity mode, the difference mode of preamplifier 7-510 is selected. The playback signal appearing at the output of the preamplifier is in the NRZ (non-return-to-zero) form and requires detection of both edges. This is accomplished by double differentiation by the dv/dt amplifier and the differentiator in the programmable filter chip 7-514 after passage through the AGC amplifier 7-516. The differentiator, a high-frequency filter cutoff, and an equalizer on chip 7-514 are activated by the HC control bit. The filter cutoff is adjusted

depending upon zone-identification bits applied to chip 7-514. (The differentiator and equalizer in chip 7-514 are not used in the low-capacity mode.) The output signal (VDIFF P, VDIFF N) from chip 7-514 is digitized and deglitched in the deglitching logic circuit 7-518. This circuit suppresses low signal level noise. The threshold level is set by a HYST control signal applied to deglitching logic circuit 7-518. The DATA P output is fed to the data separator. Responsive to the HC control bit, the PLO divider is set to 2, and the synthesizer is set to the appropriate frequency as determined by the applied zone number bits from the system controller. The cutoff frequency of the programmable filter is also dependent on the zone bits, but only in the high-capacity mode. The sync data is identical to the original GCR encoded data. This is coupled to the GCR ENDEC 7-504 for decoding purposes and then to the data bus to be utilized. The entire read function is shared between the low- and high-capacity modes.

5

10

15

20

25

The RLL 2,7 ENDEC 7-502 and write pulse generator 7-506 are represented by write encoder 7-416 and read decoder 7-426 in Fig. 94. The GCR ENDEC 7-504 and write pulse generator 7-507 are represented by write encoder 7-418 and read decoder 7-428 in Fig. 94. Select circuit 7-509 is represented by - switch 7-422 in Fig. 94. The internal control of ENDECs 7-502 and 7-504, which alternately activates them depending on the HC control bit, is represented by switch 7-424 in Fig. 94. Preamplifier 7-510, amplifier 7-512, AGC amplifier 7-516, chip 7-514, deglitching

logic circuit 7-518, and data separator 7-508 are employed in both the high-capacity and low-capacity modes. Thus, they are represented in part by both read decoder 7-426 and read decoder 7-428.

Mechanical Isolator

5

10

15

20

25

Referring to Figures 120 and 121, there is shown a mechanical isolator 9-10 and 9-12. The mechanical isolator is ideally suited for use in an optical drive such as a compact disc, laser disc, or magneto-optical player/recorder. However, the mechanical isolator will also be useful in any similar system. Two embodiments of the invention are envisioned -- the first embodiment of the mechanical isolator 9-10 is shown in Figure 120 and the second embodiment mechanical isolator 9-12 is shown in Figure 121. The mechanical isolator 9-12 has compression ribs 9-14. These function to absorb compression of the invention. The mechanical isolators 9-10 and 9-12 may be fitted to the end of a pole piece assembly 9-16. A crash stop 9-18 is designed to prevent a moving, optical carriage from crashing into solid metal. The shoe 9-20 fits over the end of the pole piece 9-16 and assists in providing vibration isolation and helps accommodate thermal expansion.

The mechanical isolators 9-10 and 9-12 should be made of a material that exhibits minimum creep. As such a silicon rubber, polyurethane or injection molded plastic may be used. In this case the material MS40G14H-4RED was selected.

Firmware.

5

10

15

20

25

Appendix 1-1 contains the hexadecimal executable code contained in the firmware. Appendices 1-2 through 1-5 provide a functional and structural definition of the hexadecimal code contained in Appendix 1-1. As described in these appendices, the 80C188 firmware handles the SCSI interface to and from the host. The firmware contains the necessary code to be able to initiate and complete reads, writes, and seeks through an interface with the digital signal processor, and also contains a drive command module which interfaces directly with many of the hardware features.

The firmware includes a kernel and a SCSI monitor task module. The kernel and SCSI monitor task module receive SCSI commands from the host. For functions not requiring media access, the SCSI monitor task module either performs the functions or directs a low-level task module to perform the functions. For all other functions, the SCSI monitor forwards the function request to a drive task layer for execution, and awaits a response from the drive task layer to indicate that the function has been completed.

The drive task layer, in turn, directs any of several modules to perform the requested function. These modules include the drive command module, the drive attention module and the format module. These modules interact with each other, with a defect management module, with an exception handling module, and with a digital signal processor to perform these functions.

The drive command module directs the digital signal processor, or directs the hardware devices themselves, to control the movement of the hardware devices. The format module directs the drive command module to format the media. Any defects in the media discovered during this process are stored in the defect management module, which may be located in random access memory.

Feedback from the digital signal processor and the hardware devices occurs in the form of command complete signals and interrupts passed to the drive attention module. In addition, the drive attention module allows other modules to register attentions, so that when an interrupt occurs, the registering module receives notice of the interrupt.

when a drive attention interrupt signals a fault or exception, the drive attention module retrieves from the drive command module information concerning the status of the media and drive, and the exception handler module uses this information to attempt to recover from the fault. Without passing a failure status back to the drive task layer and SCSI interface with the host, the exception handling module may direct the drive control module or format module to attempt the function again. The drive attention module may direct many retries before aborting the function and returning a failure status to the drive task layer. This exception handling process may occur for any drive function, such as seek, eject, magnetic bias, and temperature. In addition to the failure status, a sense code qualifier is passed to the drive task layer. The sense code qualifier specifies exactly

which failure occurred, allowing the SCSI interface to specify that information to the host. It will be obvious to one skilled in the art that the exception handling module may be contained within the drive attention module.

5

10

15

20

25

In operation with respect to magnetic bias, the bias magnet is turned on, and the bias is monitored through a serial analog-to-digital converter. The bias is monitored until it comes within the desired range, or until 5 milliseconds have passed, in which case a failure status is passed to the drive task layer.

In operation the temperature of the main board is monitored. Characteristics of the media may change as the temperature increases. At high information densities, a constant-intensity writing beam might cause overlap in the information recorded as temperature changes and media characteristics change. Therefore, by monitoring the ambient temperature within the housing, the firmware can adjust the power to the writing beam in response to the temperature-sensitive characteristics of the media, or can perform a recalibration.

Characteristics of the writing beam are also changed in response to position on the media. The media is divided into concentric zones. The number of zones is determined by the density of the information recorded on the media. For double density recording, the media is divided into 16 zones. For quadruple density recording, the media is divided into either 32 or 34 zones. The power of the writing beam differs approximately linearly between zones.

Additionally, characteristics of the writing beam and reading beam change in response to the media itself. Different media made by different manufacturers may have different optical characteristics. When the media is at the desired rotational speed, an identification code is read from the media. Optical characteristic information concerning the media is loaded into non-volatile random access memory (NVRAM) at the time the drive is manufactured, and the information corresponding to the present media is loaded into the digital signal processor when the identification code is read. If the identification code is unreadable, the power of the reading beam is set to a low power, and is slowly raised until the identification code becomes readable.

In monitoring and changing the power of the reading beam or writing beam, a plurality of digital-to-analog converters may be used. The monitoring and changing of the power may include one or more of the digital-to-analog converters.

When the spindle motor is spinning up from a rest or slower rotational state, the drive command module writes into the digital signal processor an upper limit for rotational speed. This upper limit is slower than the desired speed. When the spindle speed exceeds this upper limit, the digital signal processor generates an interrupt. The acceleration of the spindle motor speed may be decreased at this point. Then, the drive command module writes another upper limit into the digital signal processor. This new upper limit is the lower acceptable

limit for normal operation. When the spindle speed exceeds this new upper limit, a final upper limit and lower limit is written into the digital signal processor. These final limits define the operational range for spindle speed, and may be on the order of 1% apart.

When the spindle motor is spinning down from a faster rotational state, the drive command module writes into the digital signal processor a lower limit for rotational speed. This lower limit is faster than the desired speed. When the spindle speed passes this lower limit, the digital signal processor generates an interrupt. The rate of change of the spindle motor speed may be decreased at this point. Then, the drive command module writes another lower limit into the digital signal processor. This new lower limit is the upper acceptable limit for normal operation. When the spindle speed passes this new lower limit, a final upper limit and lower limit is written into the digital signal processor. These final limits define the operational range for spindle speed, and may be on the order of 1% apart.

The algorithm for spinning up or spinning down a spindle motor, although disclosed with respect to a magneto-optical drive, is equally applicable to optical drives including but not limited to CD-ROM drives, CD-R drives, Mini-Disc drives, Write-Once Read Many (WORM) drives, Video Disc drives, and CD-Audio drives. Additionally, the algorithm is applicable to magnetic drives, both fixed disk drives and removable disk drives.

At the initial spinning up process, the media is first spun to the lowest speed for normal operation of the drive, according to the above-described process. At this point, an identification code is read. If the identification code is unreadable, the media is spun at the next highest speed for normal operation, and the identification code is attempted to be read again. This process is repeated until either the identification code is unreadable at the highest speed for normal operation, in which case a failure status occurs, or the identification code is successfully read.

There may be several types of memory storage in the drive. First, there may be flash electrically erasable programmable read only memory (EEPROM). Implementations of the invention may include 256 kilobytes of flash EEPROM. Second, there may be static random access memory, and implementations of the invention may include 256 kilobytes of static random access memory. Finally, there may be NVRAM, and implementations of the invention may include 2 kilobytes of NVRAM.

Portions of the information in Appendices 1-2 through 1-5 are represented as "TBD," indicating either that the implementation of the modules had yet to be determined, that certain parameters related to optimization or environment, but not critical to design, had yet to be agreed upon, or that certain modules became unnecessary based on the implementation of other modules as represented in the executable code in Appendix 1-1, and as described in Appendices 1-2 through 1-5. The modules

whose implementation had yet to be determined may be implemented as follows.

The defect management module will create a defect table while the media is being formatted, and will write the defect table to a portion of the media. When a previously-formatted media is loaded into the drive, the defect management module will read the defect table from the media and load it into the memory. The defect management module can then consult the defect table to ensure that the digital signal processor or the hardware devices directly do not attempt to access a defective portion of the media.

5

10

15

20

25

The commands SEEK_COMP_ON and SEEK_COMP_OFF activate and deactivate, respectively, an algorithm which optimizes seek time to a certain point on the media. The commands may invoke the algorithm directly, may set a flag indicating to another module to invoke the algorithm, or may generate an interrupt directing another module to invoke the algorithm. In addition, other implementations will be obvious to one skilled in the art.

The commands NORMAL_PLL_BWIDTH, HGH_PLL_BWIDTH, AND VHGH_PLL_BWIDTH may read values from memory and store values into the read chip memory. In addition, the commands may calculate values and store values into the read chip memory.

The Write Power Calibration for 2x and Write Power
Calibration for 4x may have a similar implementation. During
manufacturing, values from a digital-to-analog converter control
the write power for the radiant energy source. The write power

may be measured for different digital-to-analog converter values, and sense values may be determined. These sense values may be stored in the memory of the drive. During use of the drive, values from a digital-to-analog converter control the write power for the radiant energy source, and sense values may be measured. These sense values are compared against the stored sense values until they are equal within tolerable limits. This process may use more than one digital-to-analog converter. In addition, the process may also calibrate the write power according to temperature, as described above.

5

10.

15

25

Recalibration is performed as described above based on temperature, media type, and other factors. Additionally, recalibration of the servos may be performed by directing the digital signal processor to set the servos based on certain variable factors.

Manufacturing Requirements dictate that the information described above that is determined at time of manufacture of the drive be recorded and stored in memory associated with the drive.

The Front Panel Eject Request function generates a drive attention interrupt. The Front Panel Eject Request function may determine the drive status and, based on that information, allow the current command to complete or stop that command.

Firmware Performance issues are optimization issues. In particular, movement of the carriage assembly requires power. Power requirements are related to the speed of movement of the carriage, and heat is generated relative to the power

requirements. The firmware seeks to minimize the speed of movement of the carriage assembly without affecting access time for a given command.

5

10

15

20

25

When a command is queued within the firmware, modules within the firmware determine the initial radial position of the carriage assembly relative to the storage medium, the initial circumferential position of the carriage assembly relative to the storage medium, and the initial circumferential velocity of the storage medium. Modules within the firmware also determine the target radial position of the carriage assembly relative to the storage medium and the target circumferential position of the carriage assembly relative to the storage medium. The firmware then calculates a velocity trajectory for the carriage assembly. The velocity trajectory is related to the initial radial position, the initial circumferential position, the target radial position, the target circumferential position, and the initial circumferential velocity. The velocity trajectory is calculated such that, if the carriage assembly is moved from the initial position to the target position at the velocity trajectory, the carriage assembly will arrive radially and circumferentially at the target position at substantially the same time.

The firmware directs the carriage assembly to move from the initial position to the target position substantially at the velocity trajectory. The carriage assembly may begin moving from the initial position to the target position at a predetermined speed before the firmware has calculated the velocity trajectory.

Instead of calculating the velocity trajectory relative to the initial radial and circumferential position, the velocity trajectory will be calculated relative to an intermediate radial and circumferential position. The intermediate radial and circumferential position correspond to the radial and circumferential position of the carriage assembly at the time when the firmware finishes calculating the velocity trajectory.

Additionally, the firmware may determine a target circumferential velocity of the storage medium. In this case, the velocity trajectory is further related to the target circumferential velocity as well. The carriage assembly moves from the initial position to the target position substantially at the velocity trajectory, and the rate of rotation of the storage medium is changed from the initial circumferential velocity to the target circumferential velocity. In this case, the carriage assembly will arrive radially and circumferentially at the target position substantially at the same time. The storage medium may arrive at the target circumferential velocity either before, at the same time, or after the carriage assembly arrives at the target position.

The Firmware Performance optimization algorithm, although disclosed with respect to a magneto-optical drive, is equally applicable to optical drives including but not limited to CD-ROM drives, CD-R drives, Mini-Disc drives, Write-Once Read Many (WORM) drives, Video Disc drives, and CD-Audio drives.

Additionally, the algorithm is applicable to magnetic drives,

both fixed disk drives and removable disk drives.

The SCSI Eject Command may be disabled by an option switch.

The option switch may be implemented in the form of DIP switches.

The External ENDEC Test and the Glue Logic Test, performed as part of the Power-On Self Test, comprise reading and writing information under certain conditions to ensure proper functioning of the External ENDEC and the Glue Logic.

Electronics.

5

10

15

20

25

The drive electronics consist of three circuit assemblies: an integrated spindle motor circuit shown in figure 101, a flex circuit with pre-amps shown in figures 102, 103, 104 and 105, and a main circuit board containing a majority of the drive functions shown in figures 106 through 119.

The Integrated Spindle Motor Board.

The spindle motor board has three functions. One function is to receive the actuator signals on connector J2 and pass them to the main board through connector J1. Other functions on the board are a brushless spindle motor driver and a coarse position sensor preamp. These features are described in detail below.

Referring to figure 101, the circuit shown drives the spindle motor. This spindle driver circuit contains U1, which is a brushless motor driver, and miscellaneous components for stabilizing the spindle motor (motor not shown). U1 is programmable and uses a 1 MHz clock which is supplied from the main board. U1 sends a tack pulse on the FCOM signal to the main board so the main board can monitor the spindle speed.

The circuit shown in figure 101 also functions to generate a coarse position error. Operational amps U2 and U3 generate the error signal. U2 and U3 use a 12 volt supply and a +5 volt supply. The +5 volt supply is used as a reference. A reference signal propagates through a ferrite bead into inputs pins 3 and 5 of U3, which have 487K feedback resistors R18 and R19 with 47 picofarad capacitors C19 and C20 in parallel. Two transimpedance amplifiers U3A and U3B receive an inputs from a position sensitive detector located on the actuator (not shown). The detector is similar to a split detector photodiode. Amplifier U2A differentially amplifies the outputs from U3A and U3B with a gain of 2. The output of U2A is sent to the main circuit board as a course position error.

The other operational amp U2B has a reference level on input pin 6 generated by resistors R23 and R17. That reference level requires that the summed output of the transimpedance amplifiers U3A and U3B, the sum of those two as seen at node 5 of U2B, will be the same as what is seen on node 6 from the resistor divider R23 and R17. A capacitor C21 in the feedback causes U2B to act as an integrator thereby driving the transistor Q3 through resistor R21. Q3 drives an LED which shines light on the photodiode (not shown). This is basically a closed loop system guaranteeing that certain levels of voltage out of transimpedance amplifiers U3A and U3B.

Referring again to figure 101, the other function on this board is the motor eject driver. The motor driver is a

Darlington Q1, current limited by transistor Q2 as determined by resistor R7. Diode D1 and C11 are noise suppression for the motor (not shown). The position of the cartridge eject mechanism is detected through hall effect sensor U4 and functions to determine the position of the gear train until the cartridge is ejected. There are also three switches WP-SW, CP-SW, and FP-SW on the board to detect whether the cartridge is write protected, whether there is a cartridge present and whether the front panel switch requests that the main processor eject a cartridge.

10 Pre-amplifiers.

5

15

20

25

Described here are two embodiments of pre-amplifiers.

Common elements are shown in figures 102 and 103. Differing elements between the two embodiments are shown in figures 104 and 105.

The optics module flex lead, shown in figures 102 - 105, has three main functions. One is a servo transimpedance amplifier section; a second is the read channel read pre-amplifier; and, the third is the laser driver.

In figure 102 is shown the connector J4 and the signals coming out of U1 are the transimpedance signals. TD and RD are two quad detectors for the servo signals. During initial alignment, X1 is not connected to X2 so that the individual quads can be aligned. After that, X1 pin 1 is connected to X2 pin 1, X1 pin 2 to X2 pin 2, etc. The sums the currents of the two quads which are then transimpedance amplified through amplifier U1A through U1D. Four quad signals create the servo signals on

the main board. The transimpedance amplification U1A-U1D is done with 100k ohm resistors RP1A, RP1B, RP1C, and RP1D with 1 picofarad capacitors C101-C104 in parallel.

A photodiode FS is a forward sense diode. The forward sense current is an indication of the power coming out of the laser, and is communicated to the main board via connector J4 on pin 15.

5

10

15

20

25

Still referring to figure 102, in the lower left hand corner is U106, which is connected to J103. J103 is another quad detector of which two of the four quads are used to generate the differential MO (magneto optics) signal and the sum signal. The VM8101, U106, is a pre-amp specifically made for MO drives and is also a transimpedance amplifier. The read +/- signals from U106 can be switched between a difference and sum signal by the preformat signal coming in from the connector J103, pin 6.

Figure 103 shows the level translators U7B, U7C, and U7D for the write level. U7B, U7C, and U7D are three differential operational amps that are also compensated to be stable with large capacitive loads. The resistors and capacitors around U7B, U7C, and U7D preform the stabilization. The differential amplifiers U7B, U7C, and U7D have a gain of 1/2 to set up write levels for transistor bases Q301, Q302, Q303, Q304, Q305 and Q306 which are shown on figure 104. There are three write levels: write level 1; write level 2; and write level 3 which allows the invention to have different write levels for different pulses in the pulse train that will write the MO signals.

The fourth operational amplifier U7A, shown in figure 103,

sets the read current level. U7A drives Q12 and the current is mirrored in transistors Q7, Q8, and Q9. The mirrored current in Q7 and Q8 is the actual read current going to the laser.

5

10

15

20

25

Figure 104 shows the actual pulse drivers and the enable to turn the laser LD1 on. The laser is actually protected with CMOS gates U301 and U302A to guarantee that as the voltage levels are rising, the laser is not actually affected by any current spikes. U302A guarantees logic low coming in on Laser On signal and U302A will keep the current mirror, see figure 103, from being enabled until read enable bar, pins 1, 2, and 3 of U302A, is enabled with a high logic level on U302A pins 20, 21, 22, and 23. It also provides a signal which will enable the write pulses to drive the laser only after the laser is activated. The activation is performed at pin 4 of U302A, which controls the inputs of 301A, 301B and 302B.

The enable pins, pins 13 and 24 of U302 and U301, and pin 24 of U301A are the individual write signals corresponding to write strobe 1, write strobe 2, and write strobe 3. Turning on the current sources generated by individual transistors Q301 through Q306 allows three levels of writing. Ferrite beads 301 and 302 act to isolate the read current from the write current and also keeps the RF modulation from being emitted back out the cables for EMI purposes.

Referring to figure 105, U303 is an IDZ3 from Hewlett

Packard, a custom integrated circuit, which performs a function

of generating about 460 MHz current. This current is conducted

into the laser for RF modulation to reduce laser noise. Its output is coupled through C307. There is an enable pin, pin 1 on U303 to turn modulation on and off.

In figure 104, the second embodiment uses a Colpitts oscillator built around a single transistor Q400, a split capacitor design C403, and C402 with an inductor L400. This circuit is biased with 12 volts with a 2k resistive load R400 to ensure that write pulses coming in through ferrite bead FB301 will not have any ringing generated by the oscillator circuit. If a disable is needed, the disable for the oscillator would be provided through the base signal by shorting R402 to ground.

Previous designs of the Colpitts oscillator include a 5 volt supply and an inductor in place of R400. This other design provided sufficient amplitude modulation into the laser to reduce noise. However, this previous design would ring every time a write pulse was supplied. The write pulse no longer induces ringing in the oscillator circuit because the inductor was replaced with a resistor R400. In order to eliminate ringing and still maintain enough peak to peak current in the RF modulation, it required changing the supply for the oscillator from 5 volts to 12 volts and then revising all resistors appropriately.

Main Circuit Board

5

10

15

20

25

Figures 106 through 119 depict the main circuit board. The main circuit board contains the functions of the drive not contained on the spindle motor board, or pre-amplifiers, including a SCSI controller, encoders/decoders for the reading

and writing, the read channel, servos, power amplifiers and servo error generation.

Figure 106 shows the connection from the pre-amplifier flex circuit J1. Pin 15 of pre-amplifier flex circuit J1 is the forward sense current from the pre-amplifier flex circuit board, as shown in figure 102. Resistor R2 references the sense output to the minus reference voltage. Operational amplifier U23B buffers this signal, which is measured with ADC U11 (Fig. 110).

5

10

15 ·

20

Two resistors R58, R59 perform the function of a resistor divider to obtain finer resolution on the laser read current level. Outputs from the Digital to Analog converter U3 shown in figure 110 set the laser read current. The DSP U4, shown in figure 110, controls the converters.

Figure 106 shows the Eval connector J6, also known as the test connector. The Eval connector J6 provides a serial communication link in a test mode to the processor U38 (Fig. 109) through I/O ports of U43 shown in figure 108. Comparator U29A generates the SCSI reset signal for the processor.

Power monitor U45 monitors the system power and holds the system in reset until such time as the 5 volt supply is within tolerance and the 12 volt supply is within tolerance.

Connector J3A connects the main circuit board to the main power. Power filters F1, F2 provide filtering for the main circuit board.

25 Capacitively coupled chassis mounts MT1, MT2, shown on figure 106 capacitively ground the main circuit board to the

chassis, providing AC grounding to the chassis.

5

10

15

20

25

Figure 107 U32 is the SCSI buffer manager/controller circuit. U32 performs the buffering function and command handling for the SCSI bus. U19A stretches the length of the ID found signal from figure 108 U43. In Figure 107 U41, U42, and U44 are a 1 Mb x 9 buffer RAM for the SCSI buffer. Figure 107 shows an eight position dip switch S2. Switch S2 is a general purpose DIP switch for selecting SCSI bus parameters such as reset and termination.

Figure 108 shows an encode/decode circuit U43, which is part of the SCSI controller. Encode/decode circuit U43 performs a RLL 2,7 encode/decode of data and provides all the signals necessary, as well as decoding the sector format for ISO standard disc formats for the 1x and 2x 5-1/4 inch discs. There is also general purpose input/output, which performs miscellaneous functions including communication with various serial devices, enabling the bias coil driver and determining the polarity of the bias coil.

A small non-volatile RAM U34, shown in figure 108, stores drive-specific parameters. These parameters are set during drive calibration at drive manufacture time.

SCSI active termination packages U50, U51, shown in figure 108, may be enabled by the switch S2, shown in figure 107.

The encode/decode circuit U43 in figure 108 has a special mode that is used in the drive where an NRZ bit pattern can be enabled for input and output. When enabled, a custom GLENDEC

U100 on figure 115 can be used for RLL 1,7 encode/decode for the 4X disc. In this mode of the encode/decode, circuit U43 can enable the use of many other encode/decode systems for other disc specifications.

5

10

15

20

25

Figure 109 shows an 80C188 system control processor U38.

The 80C188 system control processor U38 operates at 20 megahertz, with 256k bytes of program memory U35, U36 and 256k bytes RAM U39, U40. The 80C188 system control processor U38 controls function of the drive. The 80C188 system control processor U38 is a general purpose processor and can be programmed to handle different formats and different customer requirements. Different disc formats can be handled with the appropriate support equipment and encode/decode systems.

Figure 110 shows a TI TMS320C50 DSP servo controller U4, a multi-input analog to digital converter U11 for converting the servo error signals, and an 8 channel/8 bit digital to analog converter U3 for providing servo drive signals and level setting. The DSP servo controller U4 accepts signals from the analog to digital converter U11 and outputs signals to digital to analog converter U3.

The DSP servo controller U4 controls functions such as monitoring the spindle speed via an index signal on pin 40 of the DSP servo controller U4. The DSP servo controller U4 determines whether the drive is writing or reading via a control signal on pin 45. The DSP servo controller U4 communicates with the system control processor U38 via the GLENDEC U100, shown on figure 115.

The DSP servo controller U4 performs the fine tracking servo, coarse tracking servo, focus servo, laser read power control, and the cartridge eject control. The DSP servo controller U4 also monitors spindle speed to verify that the disc is rotating within speed tolerances. The analog to digital converter U11 performs conversions on the focus, tracking and coarse position signals. Focus and tracking conversions are done using a +/-reference from pins 17 and 18 of the analog to digital converter U11, generated from a quad sum signal. The quad sum signal is the sum of the servo signals. A normalization of the error signals is performed by using the +/- quad sum as the reference. The coarse position, the quad sum signal, and the forward sense are converted using a +/- voltage reference.

The digital to analog converter U3 has outputs including a fine drive signal, a coarse drive signal, a focus drive, LS and MS signals. These signals are servo signals functioning to drive the power amplifier (U9 and U10 of Fig. 111, and U8 of Fig. 112) and to close the servo loops. The focus has a FOCUSDRYLS and FOCUSDRYMS drive signals. The FOCUSDRYLS signal allows fine stepping of the focus motor in an open loop sense to acquire the disc by stepping in very fine steps. The FOCUSDRYMS signal is used as the servo loop driver. Pin 7 of the digital to analog converter U3 contains a signal READLEVELMS. Pin 9 of the digital to analog converter U3 contains a signal READLEVELLS. These signals from pins 7, 9 of the digital to analog converter U3 are used for controlling the laser read power. Pin 3 of the digital

to analog converter U3 is a threshold offset that is used in 4x read channel error recovery, enabling an offset to be injected into the read channel for error recovery.

Figure 110 also shows a 2.5 volt reference U24, which is amplified by a factor of 2 by amplifier U23D, yielding a 5 volt reference. The 2.5 volt reference U24 is used by a comparator U29. The comparator U29 compares the AC component of the tracking error signal to zero volts to determine zero track crossings. The track error signal is digitized and sent to the GLENDEC U100, shown in figure 115, for determining track crossings which are used during seek operation.

The analog to digital converter U11 uses a quad sum signal for performing conversions for the focus and tracking error. By using the quad sum for a reference on pins 17 and 18 of the analog to digital converter U11 the error signals are automatically normalized to the quad sum signal. The analog to digital converter U11 divides the error by the sum signal and gives a normalized error signal for input into the servo loop. The advantage is that the servo loop deals with a reduced number of variations. This normalization function can be performed externally with analog dividers. Analog dividers have inherent precision and speed problems. This function can also be performed by the DSP servo controller U4 by doing a digital division of the error signal by the quad sum signal. A division in the DSP servo controller U4 requires a significant amount of time. At a sample rate of 50 kilohertz, there may not be time to

do the divisions and process the error signals digitally inside the servo loops. Since the quad sum is used as the reference, division is not necessary and the error signals are automatically normalized.

5

10

15

20

25

Referring to figures 110 and 113, the analog to digital reference signals on pins 17, 18 of analog to digital converter Ull, originate from operational amplifiers Ul7A, Ul7B. Operational amplifiers U17A, U17B generate the reference +/voltages. Switches U27A, U27B select the input reference for the operational amplifiers U17A, U17B. The operational amplifiers U17A, U17B function to generate a 1 volt reference and a 4 volt reference (2.5 volt +/- 1.5 volt reference) when switch U27B is activated, or a reference from the quad sum when switch U27A is activated. The switches U27A and U27B are switched at the servo sample rate of 50 kilohertz. This enables focus and tracking samples to used Quad Sum in every servo sample and Quad Sum, forward sense and coarse position will be taken with the 2.5 volt +/- 1.5 volts as a reference. By multiplexing the reference, the automatic normalization of the servo errors is achieved in the single analog-to-digital conversion.

In summary, the switching system shown in figure 113 multiplexes two different reference levels. The switching system enables a true reference level analog to digital conversion for laser power and amount of detected signals from the disc, as well as the normalization of servo error signals when using the quad sum reference. The conversion can be done in real time on

signals such as the laser power, the quad sum level, the error signals focus, and tracking by switching between both reference levels at a 50 kilohertz rate.

Figure 111 shows a circuit with focus power amplifier U9 and fine drive power amplifiers U10. The power amplifiers U9, U10 have digital enable lines, on pins 10, that are controlled by the processor. One advantage of microprocessor control is that the power amplifiers are inactive during drive power up, preventing damage and uncontrolled movement of the associated focus and drive assemblies. Both of the power amplifiers U9, U10 have a 2.5 volt reference used as an analog reference and are powered by a 5 volt supply. The power amplifiers U9, U10 have digital to analog inputs from the DSP servo controller U4 to control the current outputs. The focus power amp can drive +/- 250 milliamps current and the fine power amp can drive +/- 200 milliamps

Figure 112 shows a circuit having power amplifiers U30 and U8 for the MO bias coil drive and the coarse drive. The power amplifiers U30, U8 are powered by the 12 volt supply to allow higher voltage range across the motors. The bias coil (not shown) is digitally controlled to be enabled and set to either erase polarity or write polarity. Power amplifier U30 will output 1/3 of an amp into a 20 ohm coil. The coarse motor power amplifier U8 is designed to supply up to 0.45 amps into a 13-1/2 ohm load. Power amplifier U8 has a level translator U23A at an input, so that the voltage drive is referenced to 5 volts instead

of 2.5 volts.

5

10

15

20

25

The power amplifiers U9, U10, U30, U8, as shown in figures 111 and 112, are configured similarly and compensated to yield bandwidths of greater than 30 kilohertz. Clamping diodes CR1, CR2, CR4, CR5 on the coarse power amplifier U8 keep the voltage on the output of the power amplifier U8 from exceeding the rails when the direction the coarse motor is reversed due to the back EMF of the motor. The clamping diodes CR1, CR2, CR4, CR5 will keep the power amplifier U8 from going into saturation for extended periods of time and thereby making seeks difficult.

The output of amplifier U26A and resistor divider R28/R30 feed the bias current back into the analog to digital converter U5, shown on figure 114. This enables the processor U38 (Fig. 109) to ensure that the bias coil is at the desired level before writing is attempted.

Referring to Fig. 113, the quad sum reference translator is realized as circuits U27A, U27B, U17A, and U17B, as previously discussed with reference to Fig. 110. Spindle motor connector J2 transmits signals to other circuit elements.

A differential amplifier U23C translates the course position error to a 2.5 volt reference. The coarse position error from the spindle motor board (J2) is referenced to $V_{\rm cc}$. Transistor Q14 is a driver for the front panel LED, LED1.

Referring now to Fig. 114, U6 is a serial A to D convertor, which converts a signal from a temperature sensor U20.

Recalibration of the drive occurs responsive to measured

temperature changes. This is an important feature of the invention, particularly in the case of 4x writing, where the write power is critical, and may be required to vary as a function of the system temperature.

5

10

15

20

25

Signals at pin 2 (PWCAL) and pin 6 of the analog-to-digital converter U6 are servo differential amplifier signals originating from the 84910 (Fig. 117). These signals may be used to sample the read channel signals and are controlled by digital signals at pins 27 - 30 of the 84910. In the present embodiment pins 27 - 30 are grounded, but those skilled in the art will appreciate that these pins could be driven by a variety of different signals, and would allow various signals to be sampled for purposes of calibration.

Pin 3 of U6 is the AGC level, which is buffered by U21B, and then resistively divided to scale it for input into the A to D converter. The AGC level will be sampled in a known written sector. The resulting value will be written out on pin 19 of U16 as a fixed AGC level. The fixed AGC level is then input into the 84910. The 84910 then sets the AGC level that inhibits the amplifiers from operating at maximum gain while a sector is being evaluated to determine if it is a blank sector.

The bias current, which has been discussed with reference to Fig. 112, is monitored on pin 4 of analog to digital converter U6 as a further safeguard during write and erase operations in order to determine that it has correct amplitude and polarity.

Signals PWCALLF and PWCALHF appear on pins 7 and 8 of U6 at

A6 and A7 respectively. These signals are derived from sample and hold circuits (see Fig. 118), and can be controlled by the glue logic encoder/decoder (GLENDEC) by signals WTLF or WTHF, as shown in Fig. 118. They are employed within a sector in order to sample a high frequency written pattern, and the average DC component of a low frequency written pattern. The average values can be compared to obtain an offset that can be used to optimize 4x write powers.

Pin 11 of U6 (A9) is coupled through U21A, a differential amplifier having inputs INTD+ and INTD-. These signals are the DC level of the data relative to the DC level of the restore signal in the 4x read channel. The difference signal determines the threshold level for the comparator in the 4x read channel. Using the D-to-A converter, DSP threshold, at U3, pin 3 (Fig. 110) this DC offset can be canceled. Additionally, for error recovery an offset could be injected to attempt to recover data that may be otherwise unrecoverable. Thus a 4x read channel recovery and calibration function is provided.

Signal ReadDIFF appears at Pin 12 of U6, A10, as the output of a differential amplifier U15B. ReadDIFF is the DC component of the MO preamplifier, or the pre-format preamplifier. Thus the DC value of the read signal can be determined, and can be used to measure the DC value of an erased track in a first direction, and an erased track in a second direction in order to provide a difference value for the peak-to-peak MO signal. Also the written data can be averaged to yield an average DC value that

provides a measure of the writing that is occurring. This value is also used for a 4x write power calibration.

U16 is a D-to-A converter which is controlled by the 80C188 (Fig. 109; U38) processor. The outputs of U16 are voltages that control the current levels for the three write power levels; WR1-V, WR2-V, and WR3-V. These signals determine the power of the individual pulses. The fourth output is the above noted fixed AGC level.

5

10

15

20

25

The GLENDEC is shown in Fig. 115 as U100. The Glue Logic ENcode/DECode essentially combines a number of different functions in a gate array. The ENcode/DECode portion is an RLL 1, 7 encode/decode function. The ENcode function's input is the NRZ of U43 (Fig. 108), pin 70, and its output is encoded to RLL 1, 7, which is then written to the disc by pin 36, 37 and 38 of U100 (WR1, WR2, WR3). The DECode function accepts RLL 1, 7-encoded data from the disc, which is decoded and returned to the NRZ for transmission to U43 (Fig. 108). U16 also contains the 4x sector format which is used for timing. Of course U16 is programmable, so that different sector formats can be defined therein.

Other functions conducted by the GLENDEC U100 include the communication interface between the DSP (U4, Fig. 110) and the host processor, the 80Cl88 (U38; Fig. 109). Counters for track crossing, and timers for measuring time between track crossings are also provided, which are used by the DSP for seek functions.

Fig 116 shows the servo error generation circuitry. Signals

QUADA, QUADB, QUADC, AND QUADD represent the output of the servo transimpedance amplifiers which are located on the preamp board (Fig. 102, U1A - U1D). These signals are added and subtracted as appropriate in operational amplifiers U22A and U22B in order to generate tracking and focus error signals TE and FE, respectively, on J4. U22C sums QUADA, QUADB, QUADC, AND QUADD as quad sum signal QS.

5

10

15

20

25

The switches, U28A, U28B, U28C, U28D, U27C and U27D, are enabled during writing to lower the circuit gain because of increased quad currents during writes. During a write QUADA, QUADB, QUADC, AND QUADD are all attenuated by approximately a factor of 4.

The read channel is now discussed with reference to Fig. 118. The read signals RFD+, RFD- originate on the preamplifier board (Fig. 102, U106), and propagate through gain switches U48A, U48B for normalizing the relative levels of the preformatted signal and the MO signal. The gain switches are controlled by U25B, which switches between preformatted and MO areas of the disk.

During write operations U48C and U48D are open, so that the read signals do not saturate the inputs of the read channel.

During read operations, both of these switches are closed, and the read signal fed through to the differentiator U47. U47 is compensated for minimum group delay errors, and can operate out to 20 MHz. The output of U47 is AC coupled through C36 and C37 to SSI filter U1 and to the 84910 (Fig. 117) through FRONTOUT+

and FRONTOUT-. Signals are resistively attenuated by R75 and R48, as shown in Fig. 117, so that acceptable signal levels are seen by the 84910. FRONTOUT+ and FRONTOUT- are then AC coupled to the 84910 through C34 and C33 respectively.

5

10

15

Several functions are included in the 84910 in order that the read channel can function properly. These include the read channel AGC, read channel phase lock loop, data detector, data separator, frequency synthesizer. Servo error generators, which are typical Winchester servo error generator functions, also are part of the 84910; however these are not used in the present embodiment.

The output of the data separated signal of the 84910 (U13) comes out on pins 14 and 15 and is then connected to the SM330, U43 (Fig. 108). These signals are used for the 1x and 2x read channel modes.

The pre-format signal controls pin 31 of the 84910 so that there are actually two separate AGC signals. One is used for reading the header or pre-formatted data and the other for MO data.

In the case of the 4x read channel, signals SSIFP and SSIFN

(Fig. 118) enter U49, a buffer amplifier (Fig. 119). The output

of U49 is conducted to Q3, Q4 and Q5, which function as an

integrator with boost. U5 is a buffer amplifier for the

integrated and boosted signal. The 4x read channel thus involves

an SSI filter, equalization, differentiation, and integration.

The output of U5 is buffered by amplifier U12, and is

coupled to a circuit that determines the midpoint between the peak-to-peak levels, also known as a restore circuit. As a result of the restoration, the signals INTD+ and INTD- are input to a comparator whose output provides the threshold level signal used in data separation. Signals INT+, INT-, INTD+ and INTD- are then input to U14, an MRC1 (Fig. 118), where they are compared, and read data is separated. The output of U14 is returned to the GLENDEC U100 (Fig. 115) for encode/decode operation.

The digital signal processor firmware is disclosed in Appendix 1-6.

Digital Lead/Lag Compensation Circuit.

5

10

15

20

25

It is well known in the art that there are particular concerns with position control systems that use a motor having a drive signal proportional to acceleration (e.g., the drive signal is a current). These position control systems require lead/lag compensation to substantially eliminate oscillation to stabilize the position control system or servo system.

The circuit of the present invention is a digital lead/lag compensation circuit that not only substantially eliminates oscillation, but also provides a notch filter frequency of one half the digital sampling frequency. Referring now to appendix 2-1 there are listed the transfer functions of a digital lead/lag circuit of the present invention, which is a single lead, complex lag compensation. Also listed for comparison are a few prior art digital lead/lag compensations circuits and one analog lead/lag compensation circuit. From appendix 2-1, the transfer function

of the invention is seen to be $H(s) = (s + w6) \times square (w7)$ divided by (square (s) + 2 zeta7 w7s + square(w7)) w6.

5

10

15

20

25

Also listed in the appendix 2-1 is the s-domain formulation of the transfer function, a formulation suitable for display on a Bode plot. From the Bode plot one can see that the compensation circuit of the present invention has a minimal impact on phase.

While the prior art compensation circuits also can be seen to have minimum phase impact, only the compensation circuit of the present invention has a notch filter at a frequency of one half the digital sampling frequency. With proper choice of sampling frequency, this notch filter can be used to notch parasitic mechanical resonance frequencies, such as those of the servo motor being compensated. In drive 10 (Fig. 1) the single lead complex lag compensation circuit is used to suppress mechanical decoupling resonance of the fine and focus servo motors as shown in appendix 2-2.

To the extent not already disclosed, the following U.S.

Patents are herein incorporated by reference: Grove et al., U.S.

Pat. No. 5,155,633; Prikryl et al., U.S. Pat. No. 5,245,174;

Grassens, U.S. Pat. No. 5,177,640.

Although the preferred embodiment of the present invention has been described and illustrated above, those skilled in the art will appreciate that various changes and modifications can be made to the present invention without departing from its spirit. Accordingly, the scope of the present invention is limited only by the scope of the following appended claims.